THE ROLE OF CARBOXYLESTERASES IN THE BIOTRANSFORMATION OF A RADIONUCLIDE DECORPORATION AGENT DTPA PENTA-ETHYL ESTER PRODRUG

Jing Fu

A dissertation submitted to the faculty of the University of North Carolina at Chapel Hill in partial fulfillment of the requirements for the degree of Doctor of Philosophy in the Eshelman School of Pharmacy.

Chapel Hill
2016

Approved by:

Michael Jay

Xiao Xiao

Zhi Liu

Dhiren Thakker

Shawn D Hingtgen

ABSTRACT

Jing Fu: The Role of Carboxylesterases in the Biotransformation of a Radionuclide Decorporation Agent DTPA Penta-ethyl Ester Prodrug
(Under the direction of Michael Jay)

A penta-ethyl ester prodrug of diethylenetriaminepentaacetic acid (C2E5) was developed for radionuclide decorporation. Previous studies of C2E5 delivered by oral and transdermal routes in rats suggested that the prodrug is metabolized to C2E2, and not the active drug DTPA. Although it was later determined that C2E2 is an active drug, it is unknown if C2E5 is converted into C2E2 and/or DTPA in humans, and whether C2E5 metabolic mechanisms affect its delivery. Therefore, the objectives of this study were to investigate the hepatic, intestinal and plasma hydrolysis of C2E5 hydrolysis in preclinical species and humans, identify the human CESs (CESs) isoforms that hydrolyze C2E5, evaluate the biotransformation of C2E5 by CESs in human skin, and determine the effect of excipients on transdermal C2E5 hydrolysis.

Hydrolysis of C2E5 was assessed using S9 fractions from human, dog and rat tissues, and human recombinant CESs in the absence or presence of an esterase inhibitor. The data revealed interspecies differences in C2E5 metabolism caused by differences in CES expression profiles, and demonstrated that C2E5 metabolism in dog and rat is not representative of its metabolism in humans. Therefore, further studies were conducted using S9 fractions from human keratinocyte cell lines and CES-specific inhibitor to determine the contributions of individual CESs to C2E5

metabolism in human skin. Data analysis by LC/MS/MS revealed that C2E5 is hydrolyzed by CESs in human keratinocytes, with a primary metabolic role for CES1.

Since cutaneous metabolism contributes to C2E5 transdermal delivery, 12 common excipients used in transdermal formulations were analyzed for their potential to alter C2E5 hydrolysis by human skin. Significant inhibition of C2E5 metabolism was observed with Miglyol 840, Eudragit RLPO, Crodamol EO-LQ-(MH), Brij 72, sodium lauryl sulfate and Tween 20, at concentrations of 100 μg/ml, whereas Eudragit RSPO enhanced C2E5 hydrolysis.

Overall, this research project provides important insights into C2E5 metabolism through oral and transdermal delivery routes in humans that could impact multiester-based prodrug development.

ACKNOWLEDGEMENTS

I would like to express my appreciation to my advisor, Dr. Michael Jay, for his support, generosity, and mentorship during my graduate training. In addition, I would like to thank my committee members, Drs. Dhiren Thakker, Xiao Xiao, Zhi Liu, Shawn D Hingtgen for their time and advice. Their wisdom has guided me towards the right direction. In addition, thank to Dr. Philip Smith for his scientific suggestions. I would like to acknowledge all previous and current members of the Jay laboratory for their attentive scientific inputs to my study, especially Erik, James, Matt and Lesley.

Fortunately, Dr. Jay has sponsored me to attend three American Associations Pharmaceutical Science and one Gordon Research Conferences in Drug Metabolism to present my scientific works. Thanks for providing me those opportunities for professional growth. Meanwhile, thanks to Dr. Dhiren Thakker for choosing me to work with him as an advanced teaching assistant for graduate course, drug metabolism. I learned to work with professors, students and instructors to teach course that provided the best experience for students. Thanks to UNC pharmacy school for choosing me to represent UNC to attend GPEN meeting in Finland at 2014. I was able to communicate my work to graduate students in pharmaceutical sciences over the world.

I would like to express my gratitude to Dr. Ruth Everett, who cared me with great love, as well as to my Christian friends. Thank to my aunt, Dr. Cindy Xia, for her wise guidance at "crisis" in life. Thanks to my parents, younger brother and cousin for their support at the other

side of the global. Thanks to the peers from MOPH and DPET for growing professionally with me. Thanks to work with Tojan and other students to form Cross-Culture Leadership Development program together.

Thanks to UNC Eshelman School of Pharmacy to give me this opportunity to pursue Ph.D. study.

DEDICATION

To God for giving me tremendous opportunities to grow scientifically and personally.

May this work make a positive influence on people's lives.

TABLE OF CONTENTS

LIST OF TABLES

LIST OF FIGURES

LIST OF ABBREVIATIONS

A431	Human epidermoid carcinoma cell line
ACN	Acetonitrile
ADME	Absorption Distribution Metabolism Excretion
Am	Americium
ANOVA	Analysis of Variance
BCS	Biopharmaceutics Classification System
BNPP	Bis(4-nitrophenyl)phosphate
C2E1	DTPA Mono-ethyl Ester
C2E2	DTPA Di-ethyl Ester
C2E3	DTPA Tri-ethyl Ester
C2E4	DTPA Tetra-ethyl Ester
C2E5	DTPA Penta-ethyl Ester
C2Ex	C2E5 metabolites
CESs	Carboxylesterases
Confgen	A conformational search method for efficient generation of bioactive conformers
DNA	Deoxyribonucleic Acid
DTPA	Diethylene Triamine Pentaacetic Acid
EDTA	Ethylenediaminetetracetic Acid
FDA	US Food and Drug Administration
FSA	Flow Scintillation Analyzer
HaCaT	Immortalized Human Keratinocytes

hEGF	Human Epidermal Growth Factor
HEKa	Human Epidermal Keratinocytes, adult
HEKn	Human Epidermal Keratinocytes, neonatal
HPLC	High Performance Liquid Chromatography
Hu Skin	Human Skin
IND	Investigational New Drug
IPA	Isopropyl Alcohol
IV	Intravenous
LC/MS/MS	Liquid Chromatography-Mass Spectrometry
mg	Milligram
min	Minute
ml	Milliliter
mSv	Millisievert
NDA	New Drug Application
4-NP	4-nitrophenol
4-NPV	4-nitrophenyl Valerate
PBS	Phosphate Buffered Saline
PNPA	4-Nitrophenyl Acetate
RNA	Ribonucleic Acid
RT-qPCR	Quantitative real-time Polymerase Chain Reaction
S9	Subcellular Fractions after Centrifugation at 9000g
SD	Standard Deviation
SE	Standard Error of the Mean

SLS	Sodium Lauryl Sulfate
Tween 20	Polysorbate 20
µg	Microgram
µl	Microliter
UNC	University of North Carolina
UV	Ultraviolet

CHAPTER 1: INTRODUCTION

1.1 General Introduction

The development of prodrugs started in the early 20th century, with prodrugs expanding into multiple aspects of medicinal therapy: chemotherapy, ACE inhibitors, diabetic therapy and antibiotics. The use of prodrugs is a common strategy applied to improve absorption, disposition, metabolism and excretion (ADME) properties of therapeutic medicines: for example, adding a new moiety to obtain the balance of the lipophilic-hydrophilic properties of drug. Hydrophobic drugs usually need to be structurally modified by adding a hydrophilic moiety. For example, fenofibric acids, used in clinics to reduce fatty acids in the blood, are covalently conjugated to symmetrically branched oligoglycerols (BGL), resulting in increased water solubility by two thousand fold compared to applying fenofibric acid alone. This BGL conjugated fenofibric acid prodrug has displayed improved pharmacological efficacy and pharmacokinetic properties but with increased toxicity [1] . In contrast, ester or amide groups can be used to mask polar ionized groups to improve the drug absorption. For example, pivaloyloxymethyl phosphoric acid ester of adefovir has four times greater bioavailability than adefovir [2] . Among all the ester-based prodrugs, carboxylic acid ester prodrug strategy is widely used to significantly improve water-solubility, cell membrane permeability, and bioavailability.

Prodrugs are pharmacologically inactive and thus need to be converted to active drugs by endogenous enzymes for treatment. Consequently, prodrug designs are strategically tailored to be biotransformed by metabolic enzymes, for example, cytochrome P450 reductase, cytochromes

P450, hydrolase and glutathion S-transferase [3] . It is necessary to study metabolic enzyme-mediate activation of prodrug to verify the effectiveness of prodrug design.

Prodrug development requires strict compliance with FDA regulatory guidance. Drugs are tested in pre-clinical animal models before clinical trials; however, careful consideration is needed for selection of the appropriate animal model required for the first-dose calculation in human trials. Especially, interspecies differences exist in-between animals and human. Metabolic studies should be carried out in one rodent and one non-rodent. The study results from the representative animal model for a specific compound are important indicator for the prediction to human. Metabolic enzyme isoform differences in expression are associated with interspecies difference in drug metabolism. For example, the species-specific isoforms of CYP1A, 2C, 2D and 3A exhibit interspecies differences in catalytic activity and some adjustments are necessary in order to extrapolate data from animal models to humans [4] .

Currently, drug metabolism is investigated in major metabolic sites (liver, intestine, and plasma). Fewer published reports have examined metabolism through the skin. Small molecular weight drugs have been reported to be bio-transformed in the epidermal layer of the skin. For example, theophylline that is used as a treatment for respiratory disease was metabolized in skin, which resulted in enhanced absorption and improved the therapeutic effect [5] . Phase I and II metabolic enzymes that are also responsible for prodrugs activation presented in skin. Their role in metabolism by transdermal delivery varies, which dictates ADME properties of the administered compounds. Different approaches can be applied to assess skin metabolism. Reconstructed skin models, for example, Graftskin™ LSE™ (living skin equivalent) and the Skinethic™ HRE (human reconstructed epidermis), are commonly used [6] . Even thought skin of pig has been considered as one of the most appropriate models for human, the species differences

in cutaneous metabolism still impact the predictability of the dermal absorption of drug from pig to human. [7,8] . Therefore, the characterization of the enzyme expression and activity in human skin tissue and human cell models are considered as a necessary approach.

Excipients are crucial component for transdermal drug delivery formulation. Non-ionic excipients are usually used in cream or gel formulation. They can be easily mixed with active pharmaceutical ingredients (API) or prodrugs to obtain a zero-order release rate. On the contrary, their non-ionic properties can sometime resulted in difficulty in bio-degradation. The complex chemical structure can interact with biological components easily, for example, enzymes. The unpredicted interaction between excipients and metabolic enzymes could alter release and clearance pathways of prodrugs. Therefore, it is important to understand the effects of excipients on transdermal delivered drug's efficacy and toxicity. Those discussions set an initial platform for this dissertation work illustrated in the subsequent chapters.

1.2. Decorporation of Radionuclide Contamination

Radiation hazards usually are known as ionizing radiation, produced by nuclear reaction, nuclear reactor industry waste and nuclear weapons from terrorists. Examples include lethal effects to individuals, large radioactive release to the environment or reactor core melt. Nuclear-related accidents have been reported worldwide. The major radiation incidents reported in history include accidents of nuclear power plants and radionuclides such as, Fukushima Daiichi (2011) [9] , Goiania accident (1987) [10] , and Chemobyl (1986) [11] . These incidents resulted in exposure to large populations and resulted in a variety of medical needs and the demand of urgent and effective treatment.

Ionizing radiation emits particles that pass human body that push electrons out of the orbit around the atom or nucleus from DNA or other vital molecules in tissues to cause damage.

On the other hand, radiation can also create free radicals by ionizing water molecules in body fluids. The free radicals mutate DNA and disrupt cell reproduction, which can lead to cancer. If the damage occurs in germ cells, it usually results in hereditary disease to the unborn children [12] .

The greatest concerns are transuranic elements that are chemical elements with atomic numbers greater than uranium (92), which are unstable and radioactive. The development of Americium (Am), plutonium (Pu), and curium (Cm) for the use in nuclear plant, weapon, and wastes are the sources of the threats.

The possible spread of radioactive material over a populated area has made the development of medical countermeasures against these threats a national security priority. The National Institute of Health has been leading an effort to identify innovative therapies that can be included in the US Strategic National Stockpile for distribution to populations affected by an act of nuclear terrorism. Among them, Am, Pu and Cm have been ubiquitously applied to nuclear power plants and other usages. In the history of the United States, a number of people who have worked in the plutonium industry since the Manhattan project had higher chance of radiation exposure or contamination. Radioactive elements can enter the human body by a few different routes, for example, inhalation, skin absorption, minor cuts and abrasion. After a radioactive element enters into the blood, the element is predominantly deposited in the liver and skeleton, where retention appears to be prolonged. The current methods of removing accidental intakes of actinides from the body are moderately successful. If insoluble materials are inhaled, bronchopulmonary lavage is the effective treatment. If the actinides are localized, the removal of damaged tissue is recommended.

The chelating agent, DTPA (Fig 1.1), approved by FDA, is used for the treatment to eliminate soluble forms of plutonium, americium and curium for internal contamination. The

intravenous (IV) injection of either Ca-DTPA or Zn-DTPA (Fig 1.2) effectively clears actinides from the blood and extracellular fluids where they are finally removed via urination [13] .

Other than IV injection treatment, inhalation therapy of Ca-DTPA was developed by Yutaka Jin. He managed to deliver 26% of Ca-DTPA by aerosol route to trachea and lung. A 50 mg inhalation of DTPA is a recommendable safe dosage. However, DTPA should be still administered once the dose of actinide is greater than 20mSv [14] . Gervelas reported to the development of lung delivery of a dry powder formulation of DTPA [15] . In addition, Ca-DTPA and Zn-DTPA have been formulated in minicapsules at Lawrence Livermore National Laboratory [16] . The FDA suggests that Ca-DTPA should be used as a first dose, following Zn-DTPA as a preferred treatment for maintenance because Ca-DTPA can cause essential mineral loss.

The working mechanism of chelation is based on coordination chemistry. Chelating agents are organic or inorganic compounds that are competent in binding to metal ions to form complex ring-like structures as 'chelates'. Atoms like sulfur (S), nitrogen (N), and oxygen (O) function as ligand atoms in the form of chemical groups like –SH, -S-S, -NH2, =NH, -OH, -OP3H, or >C=O [17] . Chemical properties of ideal chelators include: high affinity and minimal toxicity, ability to penetrate cell membranes, rapid elimination, high water solubility, resistance to other biotransformation, ability to reach the sites of metal storage, retain chelating ability at the pH of body fluids and have the ability to form metal complexes that are less toxic than the free metal ion [17] . Ethylenediaminetetraacetic acid (EDTA) can be used in chelation, however DTPA has better affinity to metals because DTPA has five carboxylic acids in comparison to four for EDTA. The carboxylic acid groups act as claws to binds to metal ions by forming eight

coordinate bonds. The stronger the binding, the better the sequestration of the ions for elimination.

1.3 Oral Formulation of Prodrug C2E5

C2E5 (MW=533.61232 (g/mol), Log P=3.3) was developed for oral formulation in our lab previously. The orally available route is natural, easy and safe. It is convenient for patients and can be self-applied. The strategy to develop DTPA prodrug (C2E5) improved the undesirable low lipophilicity of DTPA to high lipophilicity and improved the pharmacokinetic properties (rapid excretion) of DTPA. It is known that esterases are expressed in the liver, intestine and plasma and they can readily cleavage prodrugs in the metabolic organs help to sustain the long-term effect of the activated prodrugs. Sueda's result has shown that oral delivery of C2E5 produces a higher pharmacological effect on rats [18] . The maximum tolerated dose study demonstrated that the adverse effects were only observed in animals at ten times of the effective dose of C2E5. Oral delivery of C2E5 is 66% as effective as an equivalent i.v. delivery of DTPA in decorporating ^{241}Am when C2E5 is administered at 30 mins right after contamination [19] . Therefore, oral treatment is much preferred even if it is not as effective as i.v. DTPA. However, the partially effective delivery using oral route is still advantageous to FDA approved formulation due to its self-administered nature.

1.4 Transdermal Formulation of Prodrug C2E5

C2E5 was developed for transdermal delivery in our lab previously. The C2E5 non-aqueous gels that are comprised of 40% C2E5, 40-45% Miglyol 840 and 15-20% ethyl cellulose and prepared by solvent evaporation method proved to be effective by the evaluation of mass balance study and in vivo decorporation study in rodents [20] . The pharmacokinetic data in rat from Zhang's studies demonstrated that non-aqueous gel transdermal delivery of C2E5 resulted

in a higher systemic exposure to C2E3 and C2E2, (metabolites of C2E5), compared to oil formulation. Advantageously, C2E5 was metabolized into a newly discovered active drug C2E2 in rat [21,22] .

1.5 The Role of Metabolism Studies in Prodrug C2E5 Development

In order to find out whether a prodrug strategy works, it is necessary to investigate metabolism, pharmacokinetics, safety and toxicity which are necessary prior to human clinical trials. In most of the cases, the outcomes of this research help to evaluate the efficacy of prodrugs, identify potential toxic metabolites, and estimate a safe starting dose of the drug for human. As C2E5 would be used for radionuclide decorporation, it cannot be tested in humans due to ethical limitations. Therefore, metabolism studies (metabolism kinetics, mechanisms and drug-excipient interactions) provide important information. Meanwhile, the discovered metabolic information can be used for prodrug candidate optimization.

1.6 Interspecies Differences in Drug Development

In drug development, animal models are used in the preclinical development of new drugs to predict the metabolic behavior, toxicity, exposure, response, and first-time dose in human trials. Appropriate surrogate species need to be utilized for different purposes respectively.

Humans are different from animals at anatomically and molecularly. The isoforms of the enzyme's composition, expression and catalytic activities tend to be different among all the species. This leads to different metabolic or toxicological profiles in animals compared to humans. For example, paclitaxel, a drug used to treat cancer, was evaluated in rats and humans. However, results indicated that different metabolites were formed in the rat and human [23] . The metabolites found in rats which caused drug-drug interactions did not exist in human metabolism

pathways, and paclitaxel, was subsequently developed and approved for cancer treatment Another example is zidovudine. Rapid glucuronidation in humans produced a much shorter half-life than expected from studies in animals. As a result, the drug was excreted at different rates in humans and animals, which leads to different drug exposure in species [23] . Iododeoxydoxorubicin is another example. The parent molecule predominates in mice, in contrast to metabolites of iododeoxydoxorubicin predominates in human [23] . If the interspecies differences had not been investigated, in the above examples, then scientists would misleadingly extrapolate experimental results in animals to human. Numbers of different factors are necessary to be examined while studying species differences in drug metabolism. These factors include tissues binding affinity or plasma components, types and amount of drug-metabolizing enzymes present in each species, and the volume of distribution.

Therefore, the study of interspecies differences in drug metabolism will help to accurately elucidate drug action in human from those obtained from animal data alone. Common experimental approach is to use S9 fractions for physiological disposition and metabolic fate of a compound in multiple species over short amount of duration. Another approach is to use specific inhibitors and inducers to decrease or increase the metabolic enzyme activity in different animals that normalize the metabolic patterns to that of humans. The third way to examine potential interspecies differences is to use humanized mice [24] , which are commonly used as small animal models in biological and medical research for human therapeutics. Immunodeficient mice (SCID mice) are often used as the animal for incorporating human cells or tissues to create humanized animal models. Mainly, those mice produce minimum immune response to heterologous cells due to the fact that they are lack of immunity.

1.7 CESs Isoform in Drug Metabolism

CESs (Fig 1.3) are members of the serine hydrolases, that have five subfamilies (CES1-CES5) according to the Hosokawa classification [25] . CESs are ubiquitously expressed and distributed abundantly in the liver, kidney, small intestine, brain, nasal and mucosal passages, lungs, testicles, and saliva [26] . The catalytic triad (Ser-Glu-His) assists cleavage using a two-step process, which involves the formation and degradation of an acyl-enzyme, intermediate [27-29] .

CESs work to break down endogenous lipids and cholesterol, hydrolyze biochemicals, such as acylcarnitine, palmitoyl-CoA, mono and diacylglycerols, and chaperone and carry proteins in the endoplasmic reticulum. The most important isoforms involved in phase I drug metabolism are CES1 and CES2. CES1 is expressed the highest in the liver, while CES2 is highly expressed in the small intestine [30-32] . The expression and activity of CES1 and CES2 affect the ADME of the ester-based or amide-based prodrugs, which consequently influence the pharmacological efficacy and toxicological profiles of the drugs in patients.

CES1 and CES2 exhibit 48% sequence identify. However, different substrate preferences have been reported in the literature. CES1 prefers substrates with large acyl and small alcohol moieties, while CES2 prefers substrates with smaller acyl and bulky alcohol moieties [31,33] . Interestingly, substrates for CES2 can also be substrates for CES1, in contrast substrates for CES1 are not necessary a substrate for CES2. Thus, CES1 metabolizes a wider range of substrates compared to CES2.

Ester-based prodrugs are expected to be hydrolyzed very rapidly in tissues where expression of CES is high. Therefore, understanding of the mechanisms behind the metabolism of C2E5 by the liver and skin will help the development of more potent and effective prodrugs.

1.8 Skin Metabolism in Transdermal Delivery

Skin (Fig 1.4) the largest organ in human body, has been used as a target for application of cosmetics and pharmaceutical delivery because its anatomical advantage. Human skin is comprised of the epidermis and dermis. The epidermis has three main types of cells: keratinocytes (skin cells), melanocytes (pigment-producing cells) and Langerhans cells (immune cells). The epidermis layer varies from 50 μm to 1.5 mm thick [34] , depending on the location on the skin. The stratum cornium in the epidermis is the major barrier for transdermal delivery. Keratinocytes make up most of the epidermis, and are also known as highly specialized squamous stratified epithelium. Keratinocytes do not have nerves to go into them; therefore, they need to have a very dynamic enzyme environment to transport nutrition. It is understandable why keratinocytes express considerable amount of a diversified group of metabolic enzymes, as their role is to degrade harmful environmental compounds.

There are two major pathways for dermal absorption: intercellular and transcellular penetration (Fig1.5). Small molecular compounds are usually transported transcellularly by passive diffusion, mainly following Fick's law of diffusion [35] ; Skin permeation of macromolecular is very difficult.

Hydrolysis of topically applied esters is important for the activation of prodrugs. Clark showed that both the epidermal and dermal layers of human skin have the capacity to hydrolyze esters. It has previously been shown that human skin CESs are located at the basal layer of the epidermis [36] . The amount of metabolizing enzymes in the skin is generally lower compared to the major site of metabolism, the liver [37] , nevertheless, esterase and phase II enzymes that are expressed in the skin may influence systemic delivery of transdermal drugs.

Skin has been known to possess a considerable nonspecific esterase activity, which has been exploited for the delivery of ester prodrugs. CESs are located at rat skin cytosol and microsomes. Moreover, much higher amounts of drug metabolizing enzymes were found in keratinocytes. In most studies, the keratinocytes were shown to be the major site of drug metabolism in the skin [38] .

The rate of metabolism is influenced by a balance between the capacity of an enzyme to metabolize the chemical and the accessibility of the drug to the metabolic enzymes. This is the reason that rapidly diffusing drugs are generally less easily metabolized than slowly diffusing drugs. Biological monitoring of urinary metabolites generally reflects the metabolism in the liver rather than skin metabolism even for a dermally absorbed dose [26,37] .

Inhibition studies with loperamide have suggested that hCES2 is expressed in human skin microsomes and cytosol [39,40] . It has been reported that human skin expresses mainly the CES1 isozyme, and to a lesser extent CES2 isozymes. Zhu et al. has reported a higher expression of hCE2 [41] and a weaker expression of hCE1 in human HaCaT keratinocytes. Esterases, including CESs, are rarely investigated in animal skin [42] .

The common approaches for cutaneous metabolism are to use cell models or reconstructed skin model. Monolayer cell cultures are frequently used *in vitro* to evaluate toxic effects. Usually they could overestimate the toxic effects of tested compounds, because cell cultures are lack of physiologically cellular interactions, which make them a less valuable predictor of the clearance of xenobiotic. Both human-cell derived reconstructed human epidermis (RHE) and reconstructed full thickness human skin (RHS) can imitate the native human skin, which could be alternative approaches for human skin metabolism and absorption studies. However, the application of S9 fractions derived from keratinocytes can successfully used to

investigate scientific questions related to keratinocytes specifically. Since keratinocyte process the most metabolic enzymes at epidermis, it is reasonable to investigate cutaneous metabolism from this cell models.

Few keratinocytes cell lines are representatives for study: human keratinocyte cell line HaCaT, HEKn, HEKa and A431 cell lines. Among them, HaCaT cells are derived as spontaneously transformed keratinocyte cell lines from adult human skin, widely used in scientific research. HaCaT cells are utilized for their high capacity to differentiate and proliferate *in vitro*. They have been used as a model system for vitamin D3 metabolism in skin [43] . Human Epidermal Keratinocytes, neonatal (HEKn) are the primary human epidermal keratinocytes isolated from neonatal foreskin from a single donor, which are cryopreserved at the end of the primary cells, with viability (>70%), and it also belongs to adherent cell type, which the cell grows as attached to the bottom of the cell culture flasks. Human Epidermal Keratinocytes (HEKa) are adult primary human epidermal keratinocytes isolated from adult skin. A431 cells are a model human cell line (epidermoid carcinoma) used in biomedical research primarily for the study of cell cycles and cancer related cell signaling pathways.

1.9 The Effect of Excipients in Transdermal Delivery

Drug formulations such as tablets, capsules, or injectable solutions consist of active pharmaceutical ingredients and other "inactive" ingredients that are added for multiple purposes. Excipients are added to preserve the medicine stability and to enhance its absorption for better efficacy. Interactions between the drug and excipients need to be carefully studied to ensure that the drug is stable in the formulation and that the solubility, as well as the dissolution properties in the case of orally administrated drugs, is satisfactory.

Not all the excipients in approved drug formulations are "inactive", some are known to alter drug metabolism and/or transporter activities. Therefore, in the formulation development process, one needs to consider whether the chosen excipients in drug formulation can alter systemic exposure of the drug itself or affect other potentially co-administered therapeutic agents, due to interactions with drug-metabolizing enzymes and/or transporters. For example, it has been shown that Cremophor EL and Tween 80 decrease the intrinsic clearance of midazolam in rat hepatocytes by 30% and 25%, respectively. In another study, Cremophor RH40 inhibited CYP 3A-mediated nifedipine oxidation in human liver microsomes [44] . In addition, Cremophor EL in an oral paclitaxel formulation was found to reduce absorption of paclitaxel from the gut, presumably by micelle entrapment of the drug. Therefore, this study was conducted to examine whether any of the chosen excipients negatively affected the activity of CESs.

1.10 Rationale for Proposed Research and Specific Aims

Even though Ca-DTPA/Zn-DTPA is effective, it is a challenge to arrange for trained medical professionals to administer intravenous medications, especially under emergency conditions. The benefits of developing ester-based prodrugs of DTPA include their ability to be delivered over many convenient routes and might provide an increase in bioavailability. Oral, transdermal and solid dispersion formulations of C2E5 have been developed in our laboratory. During development, concerns about the metabolism of C2E5 to an active drug when given via oral and transdermal routes have been discussed. It was anticipated that C2E5 would be metabolized in a stepwise fashion to DTPA by CESs. However, after both oral and transdermal administration, the primary metabolites detected in plasma were the tri-ethyl (C2E3) and di-ethyl (C2E2) esters of DTPA and thus C2E5 did not fully converted into DTPA. In order to further understand the potential conversion of C2E5 to DTPA *in vivo*, a number of questions arise.

What enzymes are responsible for metabolizing C2E5 and the metabolites of C2E5? Where are the enzymes located? Do the same or different enzymes convert the prodrug to the same extent in rat and human? Can we extrapolate the data from rat to human directly? Would skin metabolism be beneficial in enhancing the drug metabolism into an active compound? Would the addition of an excipient in the transdermal formulation be beneficial?

Therefore, the present study aims to describe the mechanisms by which the prodrug, the penta-ethyl ester of DTPA (referred to as C2E5) is metabolized. Specifically, investigational studies focused on the interspecies differences in C2E5 metabolism, which determined the hydrolytic proficiency of human CESs on C2E5 metabolism, examined different isoforms of CESs expression in human skin tissue obtained from different cell lines to discover the contribution of cutaneous metabolism to C2E5 transdermal formulation. Additional studies were performed to examine whether excipients in transdermal formulations would affect CES-mediated hydrolysis of prodrugs C2E5.

Hypothesis:

(1) Specific enzyme plays a role in C2E5 prodrug activation and metabolism in different species and tissue organs.

(2) Specific enzyme in human skin cells and human S9 fractions metabolizes C2E5, which would enhance C2E5 transdermal delivery.

(3) Excipients in transdermal formulations inhibit the metabolic activity of CESs and impede the hydrolysis of C2E5 in human skin S9 fractions.

The following specific aims were designed to test these hypotheses:

Specific Aim 1: Investigate the interspecies differences in C2E5 hydrolysis and identify which of the CESs isoforms play an important role in C2E5 metabolism.

1A. Evaluate the hydrolysis of C2E5 in liver, intestine, and plasma S9 fractions, from human, dog and rat.

1B. Use CES1b, CES1c, and CES2 recombinant protein to evaluate CESs-mediated C2E5 hydrolysis.

1C. Use inhibitors, bis (4-nitrophenyl)-phosphate (BNPP), to confirm the role of CESs in C2E5 hydrolysis.

Specific Aim 2: Evaluate the biotransformation capacity of carboxylesterases in skin and keratinocytes for C2E5.

2A. Characterize CESs genetic expression in HEKn, HEKa, HaCaT and A431 cell lines by RT-qPCR.

2B. Evaluate CESs protein expression in HEKn, HEKa, HaCaT and A431 by western blot.

2C. Evaluate CESs activity using the PNPA Assay and 4-NPV Assay.

2D. Measure C2E5 hydrolysis in human keratinocyte S9 fractions and human skin S9 fractions by HPLC and LC/MS/MS.

2E. Measure the specific CESs inhibitors effect on CESs-mediated C2E5 hydrolysis in human skin S9 fractions.

Specific Aim 3: Determine if any of the excipients used in transdermal formulations inhibit CES-mediated C2E5 hydrolysis.

Those excipients are Miglyol 840, Miglyol 812, Eudragit RLPO, Eudragit RSPO, Crodamol™ EO-LQ-(MH), Capmul MCM, Capmul MCM EP, Captex® 355, polyoxyethylene tridecyl ether, Brij 72, sodium lauryl sulfate and Tween 20.

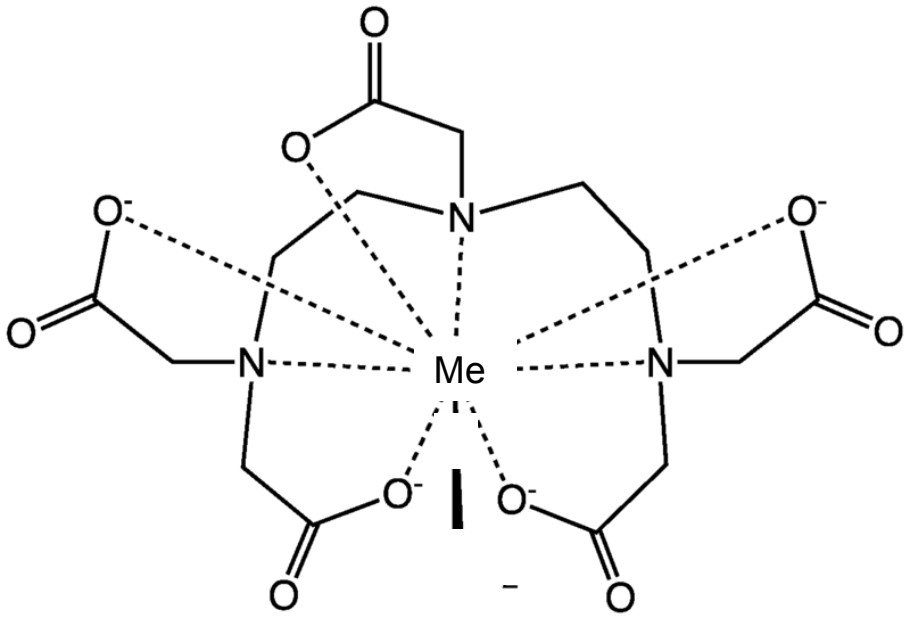

Figure 1.1 Diethylene triamine penta-acetic acid (DTPA).

Figure 1.2. FDA approved treatment (Ca-DTPA / Zn-DTPA) for Plutonium, Americium and Curium contamination.

Figure 1.3. Human CES1 crystal structure downloaded from protein data bank.

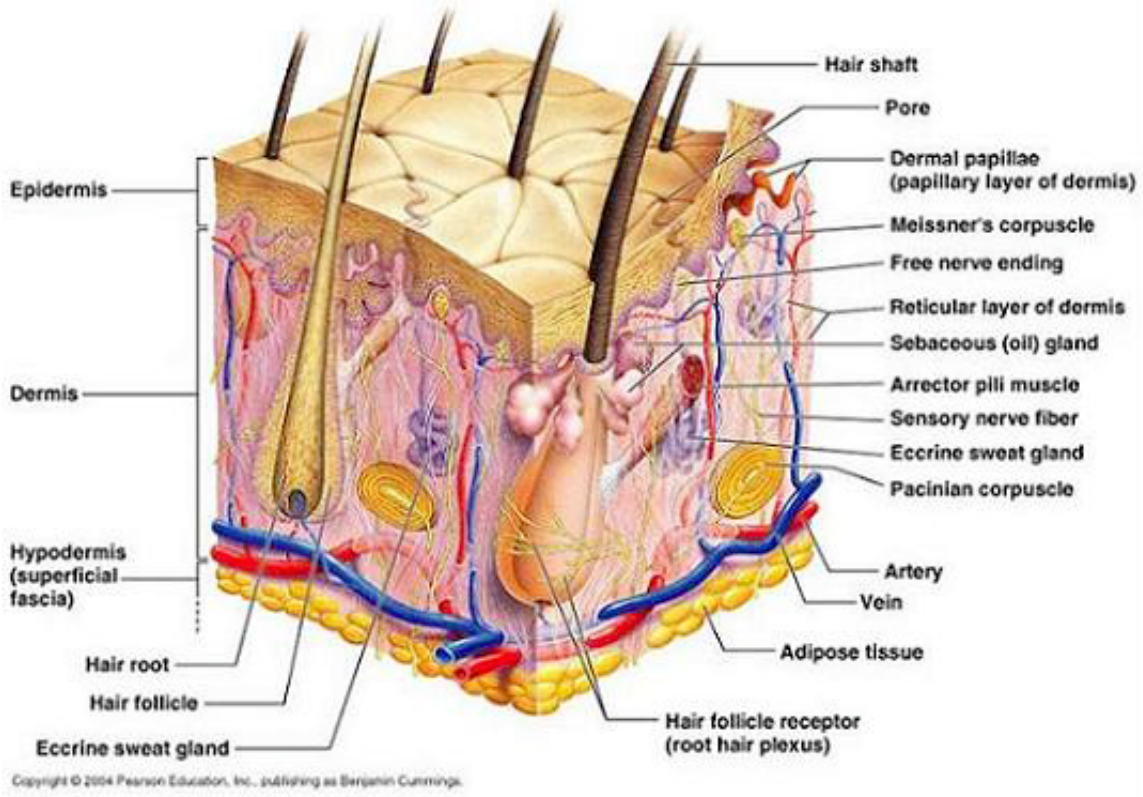

Figure 1.4. Human skin tissue anatomy available on:
http://www.osovo.com/diagram/skindiagram.htm

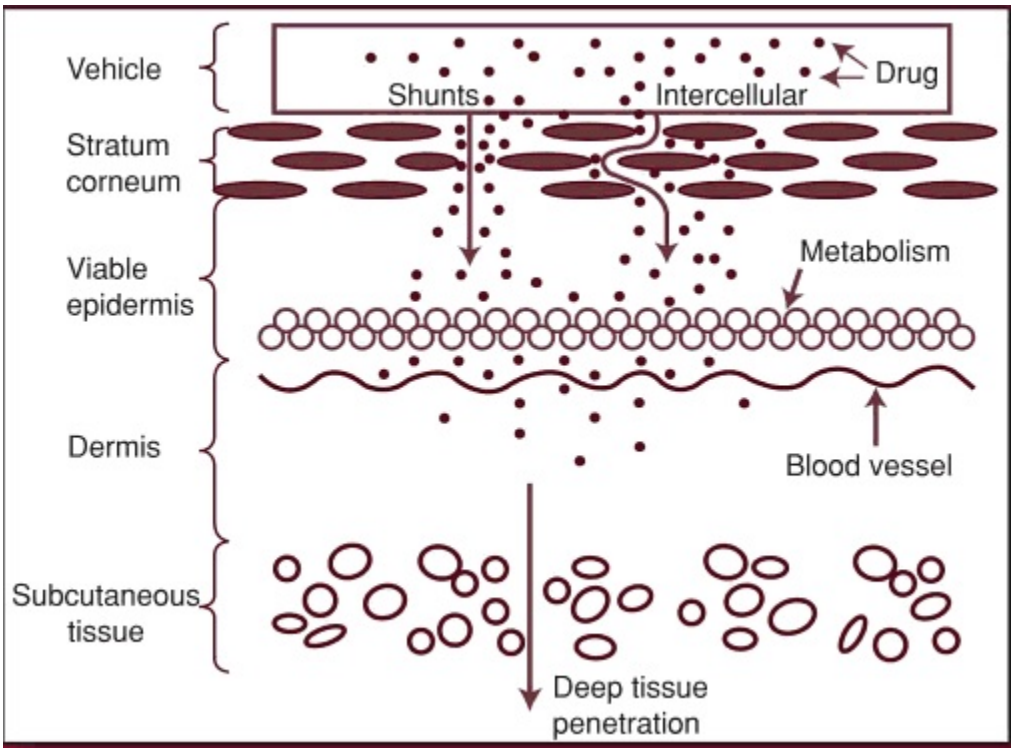

Figure 1.5 Dermal absorption of small molecule.

REFERENCES

1. Miyamoto L, Watanabe M, Taoka C, Kono M, Tomida Y, Matsushita T, Kamiya M, Hattori H, Ishizawa K, Abe S, Nemoto H, Tsuchiya K 2013. A novel prodrug strategy for extremely hydrophobic agents: conjugation to symmetrically branched glycerol trimer improves pharmacological and pharmacokinetic properties of fenofibrate. Mol Pharm 10:2723-2729.

2. Huttunen KM, Raunio H, Rautio J 2011. Prodrugs--from serendipity to rational design. Pharmacol Rev 63:750-771.

3. Rooseboom M, Commandeur JN, Vermeulen NP 2004. Enzyme-catalyzed activation of anticancer prodrugs. Pharmacol Rev 56:53-102.

4. Martignoni M, Groothuis GM, de Kanter R 2006. Species differences between mouse, rat, dog, monkey and human CYP-mediated drug metabolism, inhibition and induction. Expert Opin Drug Metab Toxicol 2:875-894.

5. Ademola JI, Wester RC, Maibach HI 1992. Cutaneous metabolism of theophylline by the human skin. J Invest Dermatol 98:310-314.

6. Schmook FP, Meingassner JG, Billich A 2001. Comparison of human skin or epidermis models with human and animal skin in in-vitro percutaneous absorption. Int J Pharm 215:51-56.

7. Barbero AM, Frasch HF 2009. Pig and guinea pig skin as surrogates for human in vitro penetration studies: a quantitative review. Toxicol In Vitro 23:1-13.

8. Kao J, Carver MP 1990. Cutaneous metabolism of xenobiotics. Drug Metab Rev 22:363-410.

9. Rhodes CJ 2014. The Fukushima Daiichi nuclear accident. Sci Prog 97:72-86.

10. Roberts L 1987. Radiation accident grips Goiania. Science 238:1028-1031.

11. Parkin DM, Clayton D, Black RJ, Masuyer E, Friedl HP, Ivanov E, Sinnaeve J, Tzvetansky CG, Geryk E, Storm HH, Rahu M, Pukkala E, Bernard JL, Carli PM, L'Huilluier MC, Menegoz F, Schaffer P, Schraub S, Kaatsch P, Michaelis J, Apjok E, Schuler D, Crosignani P, Magnani C, Bennett BG 1996. Childhood leukaemia in Europe after Chernobyl: 5 year follow-up. Br J Cancer 73:1006-1012.

12. Khanna KK, Jackson SP 2001. DNA double-strand breaks: signaling, repair and the cancer connection. Nat Genet 27:247-254.

13. Taylor DM 1989. The biodistribution and toxicity of plutonium, americium and neptunium. Sci Total Environ 83:217-225.

14. Jin Y 2008. Diethylene-triamine-penta-acetate administration protocol for radiological emergency medicine in nuclear fuel reprocessing plants. Hemoglobin 32:199-206.

15. Gervelas C, Serandour AL, Geiger S, Grillon G, Fritsch P, Taulelle C, Le Gall B, Benech H, Deverre JR, Fattal E, Tsapis N 2007. Direct lung delivery of a dry powder formulation of DTPA with improved aerosolization properties: effect on lung and systemic decorporation of plutonium. J Control Release 118:78-86.

16. Cassatt DR, Kaminski JM, Hatchett RJ, DiCarlo AL, Benjamin JM, Maidment BW 2008. Medical countermeasures against nuclear threats: radionuclide decorporation agents. Radiat Res 170:540-548.

17. Flora SJ, Pachauri V 2010. Chelation in metal intoxication. Int J Environ Res Public Health 7:2745-2788.

18. Sueda K, Sadgrove MP, Huckle JE, Leed MG, Weber WM, Doyle-Eisele M, Guilmette RA, Jay M 2014. Orally administered DTPA penta-ethyl ester for the decorporation of inhaled (241)Am. J Pharm Sci 103:1563-1571.

19. Nate Hafer 2009. NIH/NIAID Radionuclide Decorporation Agent Development Program GHSI Workshop on Public Health Emergency Medical Countermeasures.

20. Zhang Y, Sadgrove MP, Sueda K, Yang YT, Pacyniak EK, Kagel JR, Braun BA, Zamboni WC, Mumper RJ, Jay M 2013. Nonaqueous gel for the transdermal delivery of a DTPA penta-ethyl ester prodrug. AAPS J 15:523-532.

21. Huckle JE, Sadgrove MP, Mumper RJ, Jay M 2015. Species-dependent chelation of (241)Am by DTPA Di-ethyl ester. Health Phys 108:443-450.

22. Huckle JE, Sadgrove MP, Pacyniak E, Leed MG, Weber WM, Doyle-Eisele M, Guilmette RA, Agha BJ, Susick RL, Mumper RJ, Jay M 2015. Orally administered DTPA di-ethyl ester for decorporation of (241)Am in dogs: Assessment of safety and efficacy in an inhalation-contamination model. Int J Radiat Biol 91:568-575.

23. Collins JM 2001. Inter-species differences in drug properties. Chem Biol Interact 134:237-242.

24. Shultz LD, Ishikawa F, Greiner DL 2007. Humanized mice in translational biomedical research. Nat Rev Immunol 7:118-130.

25. Pindel EV, Kedishvili NY, Abraham TL, Brzezinski MR, Zhang J, Dean RA, Bosron WF 1997. Purification and cloning of a broad substrate specificity human liver carboxylesterase that catalyzes the hydrolysis of cocaine and heroin. J Biol Chem 272:14769-14775.

26. Liederer BM, Borchardt RT 2006. Enzymes involved in the bioconversion of ester-based prodrugs. J Pharm Sci 95:1177-1195.

27. Bencharit S, Morton CL, Xue Y, Potter PM, Redinbo MR 2003. Structural basis of heroin and cocaine metabolism by a promiscuous human drug-processing enzyme. Nat Struct Biol 10:349-356.

28. Hosokawa M 2008. Structure and catalytic properties of carboxylesterase isozymes involved in metabolic activation of prodrugs. Molecules 13:412-431.

29. Hatfield JM, Wierdl M, Wadkins RM, Potter PM 2008. Modifications of human carboxylesterase for improved prodrug activation. Expert Opin Drug Metab Toxicol 4:1153-1165.

30. Sanghani SP, Quinney SK, Fredenburg TB, Davis WI, Murry DJ, Bosron WF 2004. Hydrolysis of irinotecan and its oxidative metabolites, 7-ethyl-10-[4-N-(5-aminopentanoic acid)-1-piperidino] carbonyloxycamptothecin and 7-ethyl-10-[4-(1-piperidino)-1-amino]-carbonyloxycamptothecin, by human carboxylesterases CES1A1, CES2, and a newly expressed carboxylesterase isoenzyme, CES3. Drug Metab Dispos 32:505-511.

31. Satoh T, Taylor P, Bosron WF, Sanghani SP, Hosokawa M, La Du BN 2002. Current progress on esterases: from molecular structure to function. Drug Metab Dispos 30:488-493.

32. Satoh T, Hosokawa M 2006. Structure, function and regulation of carboxylesterases. Chem Biol Interact 162:195-211.

33. Imai T 2006. Human carboxylesterase isozymes: catalytic properties and rational drug design. Drug Metab Pharmacokinet 21:173-185.

34. Simpson CL, Patel DM, Green KJ 2011. Deconstructing the skin: cytoarchitectural determinants of epidermal morphogenesis. Nat Rev Mol Cell Biol 12:565-580.

35. Farahmand S, Tien L, Hui X, Maibach HI 2009. Measuring transepidermal water loss: a comparative in vivo study of condenser-chamber, unventilated-chamber and open-chamber systems. Skin Res Technol 15:392-398.

36. Clark NW, Scott RC, Blain PG, Williams FM 1993. Fate of fluazifop butyl in rat and human skin in vitro. Arch Toxicol 67:44-48.

37. Williams FM 2008. Potential for metabolism locally in the skin of dermally absorbed compounds. Hum Exp Toxicol 27:277-280.

38. Swanson HI 2004. Cytochrome P450 expression in human keratinocytes: an aryl hydrocarbon receptor perspective. Chem Biol Interact 149:69-79.

39. Jewell C, Prusakiewicz JJ, Ackermann C, Payne NA, Fate G, Williams FM 2007. The distribution of esterases in the skin of the minipig. Toxicol Lett 173:118-123.

40. Jewell C, Prusakiewicz JJ, Ackermann C, Payne NA, Fate G, Voorman R, Williams FM 2007. Hydrolysis of a series of parabens by skin microsomes and cytosol from human and minipigs and in whole skin in short-term culture. Toxicol Appl Pharmacol 225:221-228.

41. Zhu QG, Hu JH, Liu JY, Lu SW, Liu YX, Wang J 2007. Stereoselective characteristics and mechanisms of epidermal carboxylesterase metabolism observed in HaCaT keratinocytes. Biol Pharm Bull 30:532-536.

42. Imai T, Takase Y, Iwase H, Hashimoto M 2013. Involvement of Carboxylesterase in Hydrolysis of Propranolol Prodrug during Permeation across Rat Skin. Pharmaceutics 5:371-384.

43. Lehmann B 1997. HaCaT cell line as a model system for vitamin D3 metabolism in human skin. J Invest Dermatol 108:78-82.

44. Mountfield RJ, Senepin S, Schleimer M, Walter I, Bittner B 2000. Potential inhibitory effects of formulation ingredients on intestinal cytochrome P450. Int J Pharm 211:89-92.

CHAPTER 2

INTERSPECIES DIFFERENCES IN THE METABOLISM OF A MULTI-ESTER PRODRUG BY CARBOXYLESTERASES

2.1 Introduction

The development of medical countermeasures is a national security priority due to the diversion of radioactive materials and the threat of nuclear terrorism. A number of potential terrorist threat scenarios have been envisioned, including the deployment of a Radiological Dispersal Device ("dirty bomb") that spreads radioactive material over a large populated area. Of particular concern are isotopes of the transuranic elements americium (Am), plutonium (Pu), and curium (Cm) due to their abundance and availability. The National Institutes of Health has been leading an effort to identify innovative therapies that can be included in the US Strategic National Stockpile for distribution to populations affected by an act of nuclear terrorism. The current strategy to reduce the absorbed radiation dose involves decorporation therapy to accelerate excretion of the contaminating radionuclide [1,2]. Intravenous (i.v.) administration of either the calcium or zinc salts of diethylene triamine pentaacetic acid (Ca-DTPA/Zn-DTPA) has been approved by the US Food and Drug Administration (FDA) for contamination with Am, Pu, or Cm [3]. To improve access to treatment, there is considerable interest in developing orally bioavailable chelators for the actinides. As a Class III compound in the Biopharmaceutics Classification System (high solubility, low permeability), DTPA is not a good candidate for oral delivery and can only be effectively given by i.v. administration.

Introduction of an ester linkage has been shown to enhance the systemic delivery of pharmacologically active compounds with low oral absorption due to high hydrophilicity [4-6]. Therefore, in order to achieve higher oral bioavailability, a penta-ethyl ester DTPA prodrug, designated as C2E5, was synthesized. The five added ester moieties greatly increase the lipophilicity of DTPA, which is measured by increased CLogP. (CLogP of-2.7 for DTPA in contrast to ClogP of 4.7 to C2E5) Studies in rats confirmed that C2E5 shows enhanced oral bioavailability compared to DTPA, with extensive but incomplete metabolism [7] and can elicit effective radionuclide decorporation following oral [8] and transdermal delivery [9]. Together, these findings suggest that this prodrug may be a useful and effective alternative treatment to DTPA. The enzymes responsible for C2E5 metabolism to DTPA have not previously been reported, but promising candidates for metabolism are the Carboxylesterases (CESs), which could sequentially cleave the five ester moieties to form the metabolites C2E4, C2E3, C2E2, C2E1, and DTPA as shown in Figure 1.

Many of the ester-based prodrugs are biotransformed by carboxylesterases (CESs) (EC 3.1.1.1), which are members of the α/β-fold hydrolase superfamily. CESs are grouped in five subfamilies (CES1–CES5) according to the homology of the amino acid sequence [10,11]. The most prolific CESs belong to the CES1 and CES2 families, and are categorized as phase I enzymes important for metabolism of xenobiotics, including drugs and prodrugs. All CESs cleave esters via a two-step process that involves the formation and degradation of an acyl-enzyme intermediate. CESs exhibit ubiquitous tissue expression, but are predominantly expressed within the small intestine and liver consistent with their roles in biotransformation and detoxification. Carboxylesterase expression differs among species and organs within a single species, resulting in differences in substrate specificity [12,13]. For example, rat plasma has high expression of CES

whereas the human and dog are lacking of CES activities [14]. In addition to the differences in expression, species differences exist regarding to CES activity. In general, it has been shown that CES2 has much greater affinity for lipophilic substrates compared to CES1 [13]; meanwhile, CES1 prefers small alcohol group compound and CES2 prefers bigger alcohol group compound. Those characteristics of CESs could have important implications for lipophilic ester prodrugs, such as C2E5.

The increasing threat of nuclear and biological terrorism has led the FDA to expedite the development and approval of new drug and biological products. The Animal Efficacy Rule (21 C.F.R. § 314.610, drugs) [16,17] states, "when efficacy studies in humans are unethical or infeasible, studies in animal models will typically be needed to provide the efficacy data required to support approval, licensure, clearance, or emergency authorization." As new therapies are being developed that utilize these hydrolytic pathways, it is vital to understand the similarities and differences in CES activity between humans and preclinical models of drug disposition [18]. Thus, establishment of a reliable animal model for assessing the efficacy of radionuclide decorporation therapy is critical. The goal of the current study was to identify potential species and tissue differences in the CES-mediated hydrolysis of the multi-ester prodrug C2E5.

2.2 Material and Methods

Chemicals and Materials. [^{14}C]-diethylene triamine pentaacetic acid pentaethyl ester ([^{14}C]-C2E5; 50 mCi/mmol) was purchased from American Radiolabeled Chemicals, Inc. (St. Louis, MO). Sprague-Dawley rat intestinal S9 fractions, isolated from a single male were purchased from Celsis *In Vitro* Technologies (Baltimore, MD). Pooled, mixed gender human (intestinal, hepatic), single male Beagle dog (intestinal, hepatic), and single male Sprague-

Dawley (hepatic) S9 fractions were purchased from Xenotech, LLC (Lenexa, KS). All S9 fractions were prepared in the absence of phenylmethanesulfonylfluoride. Human CES1 and CES2 supersomes were obtained from BD Biosciences (Woburn, MA). Human, Beagle dog, and Sprague-Dawley rat plasma was purchased from Lampire Biological Laboratories, Inc. (Pipersville, PA). Ultima-Flo AP scintillation fluid was obtained from PerkinElmer Life and Analytical Sciences (Waltham, MA). Acetonitrile (ACN) and bis-(*p*-nitrophenyl) phosphate (BNPP) were purchased from Sigma Aldrich (St. Louis, MO).

C2E5 *In Vitro* Metabolism in Human, Dog and Rat Intestinal and Hepatic S9 Fractions and Plasma. [^{14}C]-C2E5 (50μM) was pre-incubated in 0.1 M phosphate buffer (pH 7.4) for 5 min at 37°C. Reactions were initiated by the addition of intestinal or hepatic S9 fractions (1 mg/ml) and were maintained at 37°C. Plasma (250 μl reaction volumes) was pre-incubated for 5 min at 37°C. Reactions were initiated by the addition of 50 μM [^{14}C]-C2E5 and were maintained at 37°C. Equivalent boiled S9 fractions were used as a blank to correct for non-enzymatic C2E5 degradation. The reactions were terminated by addition of an equal volume of ice-cold ACN followed by centrifugation at 14,000 x g for 10 min at 4°C. The supernatant was transferred to HPLC vials for subsequent analysis.

C2E5 Metabolism by Human CES1-b, CES1-c, and CES2. One μM of [^{14}C]-C2E5 was pre-incubated in 0.1 M phosphate buffer (pH 7.4) for 5 min at 37°C. Reactions were initiated by the addition of CES1-b, CES-c and CES2 recombinant supersomes. The final enzyme concentration was 1 mg/ml and maintained at 37°C. In all instances, equivalent boiled S9 fractions were used as blanks to correct for non-enzymatic C2E5 degradation. The reactions were terminated by addition of an equal volume of ice-cold ACN followed by centrifugation at

14,000 x g for 10 min at 4°C. The supernatant was transferred to HPLC vials for subsequent analysis.

Inhibition Studies on C2E5 metabolite formation. Recombinant human supersomes of CES1-b, CES1-c, and CES2 (final concentration of 1 mg/ml) were incubated in the absence and presence of the esterase inhibitor bis (4-nitrophenyl)-phosphate (BNPP) at 100 μM. The final concentration of the organic solvent (methanol) was less than 1%.

HPLC analysis of C2E5 and Metabolites. C2E5 and its metabolites were analyzed using a Shimadzu Prominence HPLC system equipped with a Perkin Elmer Radiomatic 625TR Flow Scintillation Analyzer. Two Chromolith® Fast Gradient columns (RP-18e 50 x 2 mm Sorbent Lot No. UM8507) were used in tandem with an Alltima Alltech HP All-Guard Cartridge (C18, 5 μm particle size, 2.1 x 7.5 mm). Mobile phase A consisted of water with 0.1% TFA and mobile phase B was ACN with 0.1% TFA. Six regions of interest in the radiochromatogram were identified with a linear 14-min gradient with a flow rate of 0.3 ml/min, 5-95% B over 8 min before returning to 5% B for the remaining six min. Each sample (10 μl) was injected in quadruplicate. The activity in each region that met the threshold criteria (peak height greater than 60 cpm) was determined and expressed as a percentage of the total activity in all regions. The regions of interest were as follows: DTPA, 1.20-2.30 min; C2E1, 3.60-4.90 min; C2E2, 4.90-5.60 min; C2E3, 5.60-6.50 min; C2E4, 6.50-7.30 min; and C2E5, 7.30-9.00 min.

DATA ANALYSIS

All assays were performed in triplicate and expressed as the mean ± S.D. Data were analyzed with one-way ANOVA test by using GraphPad Prism 5 software. (***) is designated for $P<0.001$.

2.3 Results

C2E5 Hydrolysis Catalyzed by Human, Dog and Rat Intestinal S9 Fractions. As shown in Fig. 2A, C2E5 hydrolysis was minimal in human intestinal S9 fractions, with approximately 84% C2E5 remaining over the 2 h incubation, whereas no hydrolysis occurred in the dog intestinal fractions. Rat intestinal fractions metabolized 85% of the C2E5. The C2E5 metabolic profile of human, dog and rat fractions was determined by a radiomatic HPLC assay and is shown in Figs. 2.2B-2.2D. In human intestinal fractions, no metabolites were detected at the early time points; however, at 2 h, a modest amount (16%) of the activity had been converted to the tetraethyl ester (C2E4) metabolite (Fig. 2.2B). The rapid disappearance of C2E5 in rat intestinal fractions coincided with time-dependent C2E4 formation as early as 10 min (Fig 2.2D). A minor amount of the triethyl ester (C2E3) was observed at later time points.

C2E5 Hydrolysis Catalyzed by Human, Dog and Rat Liver S9 Fractions. As shown in Fig. 2.3A, C2E5 is rapidly metabolized in liver S9 fractions from all tested species. Human and dog S9 fractions hydrolyze approximately 85% of C2E5 within the first 30 min. No further metabolism was observed over the remainder of the 2 h incubation period. Similarly, rat S9 fractions efficiently metabolized greater than 95% of C2E5 over the same incubation period. Interestingly, in all three species C2E5 hydrolysis correlated with primarily an increase in C2E4. In the case of human and dog fractions (Fig. 2.3B and 2.3C), C2E4 formation peaked at nearly 80% of the detected activity by 60 min, before a slight decrease at the 120 min time point, due to minor increases in C2E3 and the diethyl ester (C2E2). In rat fractions, C2E4 formation was complete at 10 min and C2E3 became the predominant metabolite, accounting for nearly 80% of the detected activity, from 15 min through the duration of the assay (Fig. 2.3D).

C2E5 Hydrolysis Catalyzed by Human, Dog and Rat Plasma. Species differences are clearly evident when C2E5 was incubated in plasma of human, dog and rat (Fig. 2.4A). Moderate (~30%) and no C2E5 hydrolysis were observed in human and dog plasma respectively (Fig. 2.4A). Human plasma generated only C2E4 as a metabolite after 2 h of incubation, comprising approximately 30% of the total activity, while dog plasma did not show any detectable metabolites within this time period (Fig. 2.4B and 2.4C). In contrast, C2E5 was rapidly hydrolyzed in rat plasma and yielded a strikingly different metabolic profile, in which C2E4 was the primary metabolite in the first min of incubation (Fig. 2.4D and 2.4E). The principle metabolite identified within the first 60 min was C2E3 which accounted for ~60% of the activity. At the 2 h time point, there are equivalent amounts of C2E3, C2E2 and the mono-ethyl ester (C2E1) each accounting for ~30% of the activity. The remaining activity was attributed to C2E4 and DTPA (Fig. 2.4E).

C2E5 Hydrolysis Catalyzed by Recombinant Human CES1-b, CES1-c and CES2. Incubation of 1μM [^{14}C]-C2E5 with human CES1 or CES2 supersomes are presented in Figure 2.5. These data show that C2E5 was hydrolyzed (~15%) over 60 min**.** CES1-b, CES1-c and CES2 all contribute to the hydrolysis of C2E5.

Inhibition Studies of C2E5 Metabolism. The inhibition effects of BNPP on C2E5 metabolite formation were investigated (Fig. 2.6). In the presence of the esterase inhibitor BNPP, C2E5 metabolism was significantly reduced in recombinant human CES1-b and CES1-c and human liver S9 fractions.

2.4 Discussion

The path to FDA approval for treatments against bio- and nuclear-terrorism agents is unique. Instead of relying on human studies, the FDA Animal Rule allows approval of drugs that have been shown to be effective in animal models in the absence of clinical trials. However, the predictive human efficacy obtained in experimental animals is confounded by interspecies variations in metabolism. The inhibition effects of the specific esterase inhibitor, BNPP, confirmed that C2E5 was mainly cleaved by esterase. Our results provide direct evidence that C2E5 is metabolized in a species and tissue dependent manner. Additionally, C2E5 metabolism observed in the presence of recombinant human CES isoforms (CES1-b, CES1-c and CES2) further supports the role of the CES enzyme system in C2E5 hydrolysis. The current study suggests that the dog maybe the best for modeling human C2E5 exposure whereas the rat is uniquely useful for clarifying relative capacity of C2E5 to form more metabolites.

Intestinal metabolism plays an important role in the bioavailability of oral therapeutic ester prodrugs. The expression of intestinal CES is species-dependent. For example, the small intestine contains only enzymes from the CES2 family in humans and rats whereas CES2 expression is lacking in dog[13]. Consistent with the CES expression profile, C2E5 hydrolysis was absent following incubation in dog intestinal S9 fractions. However, C2E5 hydrolysis was minimal in human intestinal fractions whereas rat intestinal fractions almost completely hydrolyze C2E5 (Fig. 2.2B and 2.2D). The differing rates of metabolism observed in human and rat intestinal fractions may be explained, in part, by differential CES isoform expression. Humans express only one CES2 isoform, however, rats express one major CES2 (RL4) and four minor CESs in the intestine [19]. In addition to differing CES expression, it has been shown that the intestinal CES2 of rat is markedly more efficient at metabolizing ester-containing compounds

than the human CES2[13] implying the rapid disappearance of C2E5 in rat intestinal fractions is due to the greater ability to hydrolyze C2E5[13]. However, additional unidentified enzymes may be responsible for the distinct C2E5 metabolic profile identified in rat. Interestingly, in both human and rat intestinal S9 studies, C2E4 was the major metabolite. This may be due to the structure-activity relationship between C2E5 and CESs. Together, these results suggest that the intestine plays an important role in the CES-mediated first-pass metabolism of C2E5 in rats, but not in the dog and only to a small degree in human.

CES1 and CES2 are all expressed abundantly in human, dog, and rat liver [20]. The degree of C2E5 hydrolysis and the resultant metabolic profiles are vastly different between human and dog liver S9 fractions compared to rats. This could be due to different CES expression patterns in rats. The rat liver CES1 family includes 4 different isozymes, hydrolase A, hydrolase B, hydrolase C and rat egasyn and three minor CES2 isozymes (RL4, AY034877 and D50580). Among them, hydrolase A is the closest to the major human CES1 with about 78% homology [21]. Observed species-dependent CES expression profile is probably responsible for the differences in the metabolism of C2E5 identified in human and dog when compared to rat. However, a direct comparison of the full complement of human, dog and rat CES isozymes would be needed to confirm these hypotheses.

The formation of DTPA from C2E5 mediated by CES, and possibly other enzymes, appears to occur through four intermediates (C2E4, C2E3, C2E2, C2E1) as shown in Figure 1. C2E5 hydrolysis in S9 fractions suggests CES activities in the intestine and livers are insufficient for complete conversion to DTPA (Figs. 2.2 and 2.3). Thus, once C2E5, or a resulting metabolite, enters the systemic circulation, it is still susceptible to further metabolism by esterases present in plasma. Human and dog plasma have little or no detectable CES enzyme [15.]

However, in human plasma there was a moderate level of C2E5 hydrolysis even in the absence of CES activity (Fig 2.4A and 2.4B). In contrast to human liver and small intestine where greater than 90% of esterase activity is attributed to CESs [22], butyrylcholinesterase (BuChE), paraoxonase (PON), and albumin esterase, but not CESs, possess hydrolytic activity in human plasma [15]. Of the three PON isoforms (PON1, PON2, PON3), only PON 1 has hydrolytic activity [23]. Moreover, PON1 substrate specificity is restricted to organophosphate pesticides and nerve gasses [24,25], thus limiting the role that PON1 may play in the hydrolysis of C2E5. BuChE and albumin esterase, both of which contribute to the activation of prodrugs [26-29] are both likely to contribute to the hydrolysis of C2E5 in human plasma. The fact that C2E5 was rapidly hydrolyzed in rat plasma is consistent with the presence of relatively high levels of CES activity in rat plasma. This represented the most efficient cleavage of the esters resulting in the time-dependent formation of multiple metabolites.

C2E5, a lipophilic compound with a CLogP value of 4.7, was hydrolyzed by recombinant protein CES1 and CES2 [7]. Hydrolysis of C2E5 by CES1 was higher than CES2 at an enzyme concentration of 1mg/ml (Fig. 2.5). The difference in activity is most likely due to the structural and conformational differences between CES1 and CES2. Human CES2 has been shown to have a greater affinity for lipophilic substrates compared to human CES1, possibly due to greater conformational flexibility and a larger entrance to the active site [28], but human CES1 prefers substrates with smaller alcohol groups. C2E5, a lipophilic molecule with small alcohol groups, possesses attributes that make it suitable for metabolism by both enzymes. However, the metabolites of C2E5 might be expected to have an increasing preference for CES1 because of the decrease in lipophilicity associated with the cleaving each ester. Any difference in metabolism between CES1-b and CES1-c is small because the enzymes are structurally very similar. In

contrast, CES1 and CES2 share only 48% of sequence homology [31]. Bis-(4-nitrophenyl) phosphate (BNPP), an inhibitor of CES-mediated hydrolysis [32], inhibited C2E5 hydrolysis when added to samples of CES1-b, CES1-c, and human liver S9 (Fig 2.6). This result confirms that human recombinant proteins CESs are responsible for the hydrolysis of C2E5. Even though the inhibition is not one hundred percent, in all cases these results are consistent with the findings in literature on ester-based prodrug studies [32].

During the development of pharmaceutical products, drug disposition and toxicity are usually evaluated in several different animal species. For a drug such as C2E5, the FDA Animal Rule requires an in depth understanding of differences in metabolic capacities among species. In conclusion, we have shown that C2E5 metabolism is species specific due to differing CESs expression profiles. Together, the results suggest that the dog is a better predictive model for C2E5 metabolism in humans whereas the rat is important for understanding the potential toxicity of C2E5 metabolites.

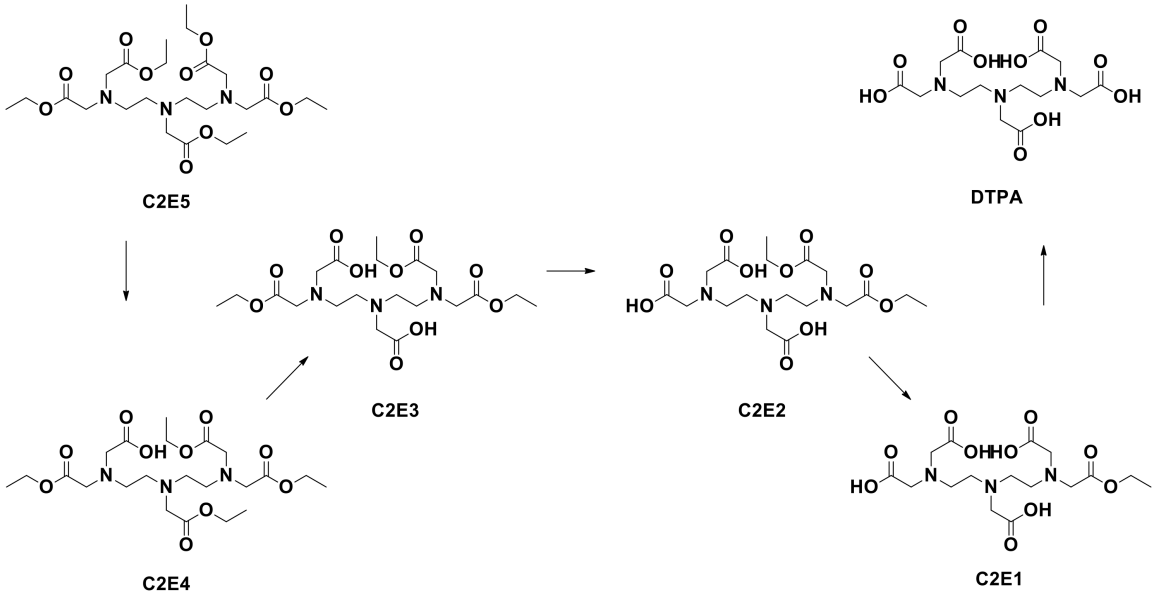

Figure 2.1. Proposed carboxylesterase-mediated metabolism of C2E5 to DPTA through four intermediates.

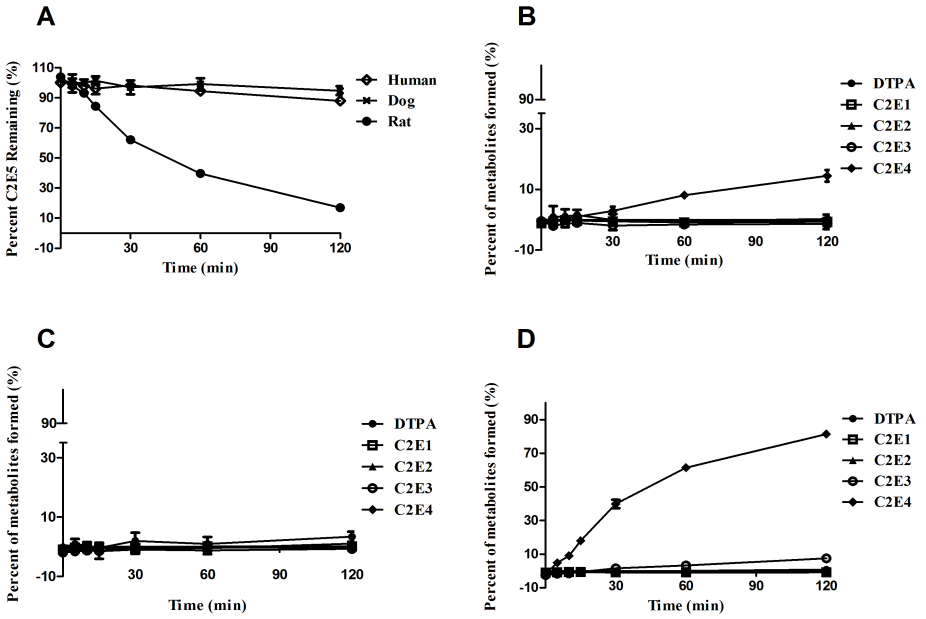

Figure 2.2. C2E5 Hydrolysis by Human, Dog, and Sprague-Dawley Rat Intestinal S9 Fractions Fifty μM [^{14}C]-C2E5 was pre-incubated in 0.1 M phosphate buffer (pH 7.4) for 5 min at 37°C. Reactions were initiated by the addition of intestinal S9 fractions (1 mg/ml final concentration) and were incubated at 37°C. The reactions were terminated at the indicated time points by addition of an equal volume of cold acetonitrile followed by centrifugation at 14,000 x g for 10 min at 4°C. The percent (A) C2E5 remaining and (B) human, (C) dog and (D) rat metabolic profiles [C2E4 (♦); C2E3 (○); C2E2 (▲); C2E1 (□); DTPA (●)] were determined by radio-HPLC. All assays were performed in triplicate and are expressed as the mean ± S.D.

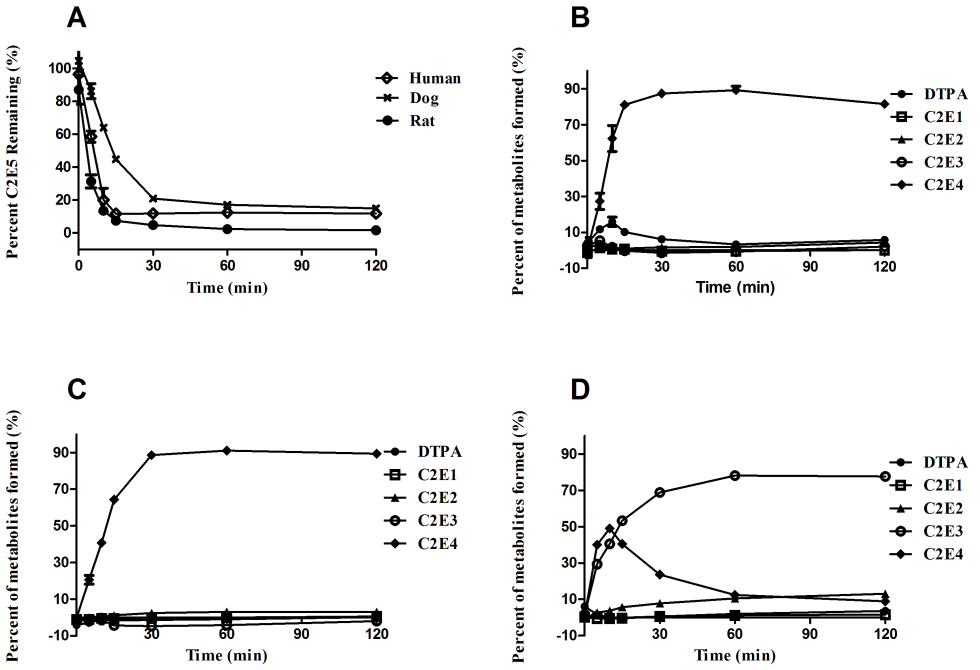

Figure 2.3. C2E5 Hydrolysis by Human, Dog, and Sprague-Dawley Rat Hepatic S9 Fractions. Fifty μM [^{14}C]-C2E5 was pre-incubated in 0.1 M phosphate buffer (pH 7.4) for 5 min at 37°C. Reactions were initiated by the addition of hepatic S9 fractions (1 mg/ml final concentration) and were incubated at 37°C. The reactions were terminated at the indicated time points by addition of an equal volume of cold acetonitrile followed by centrifugation at 14,000 x g for 10 min at 4°C. The percent (A) C2E5 remaining and (B) human, (C) dog and (D) rat metabolic profiles [C2E4 (♦); C2E3 (○); C2E2 (▲); C2E1 (□); DTPA (●)] were determined by radio-HPLC. All assays were performed in triplicate and are expressed as the mean ± S.D.

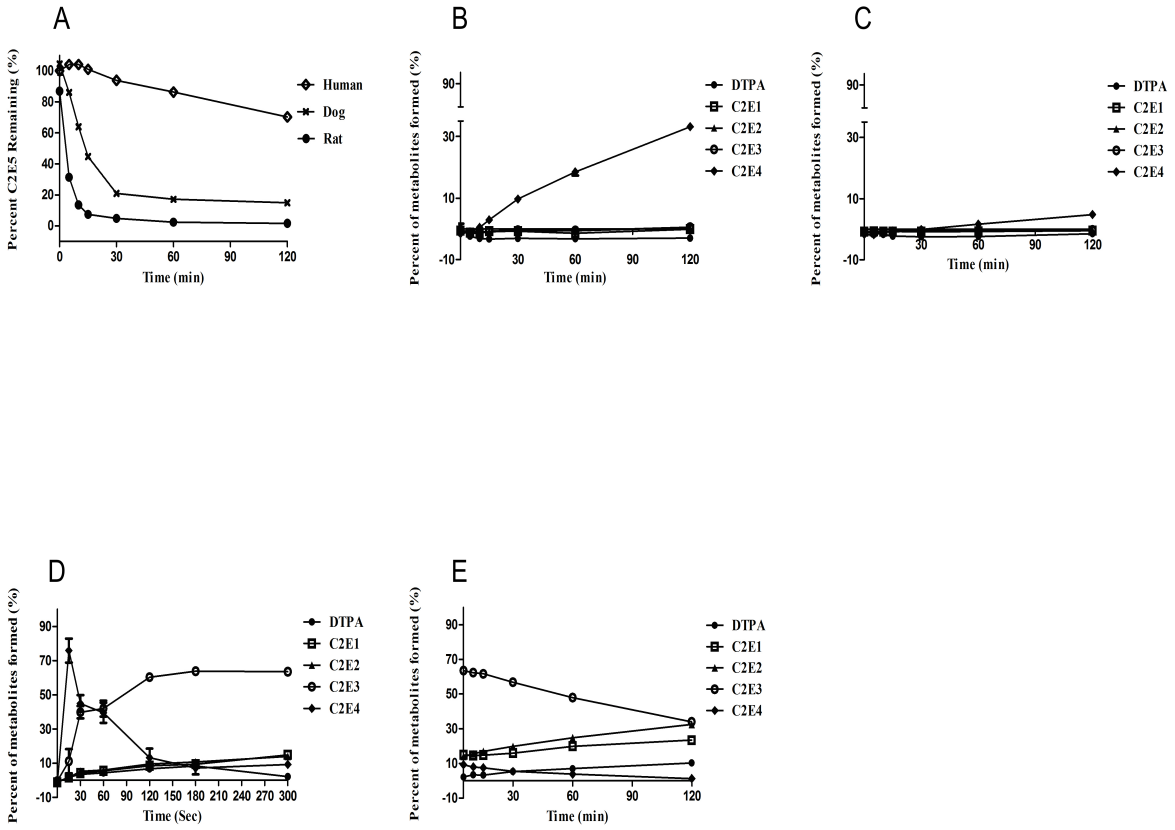

Figure 2.4. C2E5 Hydrolysis by Human, Dog, Sprague-Dawley Rat Plasma Fractions. Fifty μM [^{14}C]-C2E5 was added directly to plasma (pre-warmed for 5 min at 37°C). The reactions were terminated at the indicated time points by addition of an equal volume of cold acetonitrile followed by centrifugation (2X) at 14,000 x g for 10 min at 4°C. The percent (A) C2E5 remaining and (B) human, (C) dog and (D, E) rat metabolic profiles [C2E4 (♦); C2E3 (○); C2E2 (▲); C2E1 (□); DTPA (●)] were determined by radio-HPLC. All assays were performed in triplicate and were expressed as the mean ± S.D.

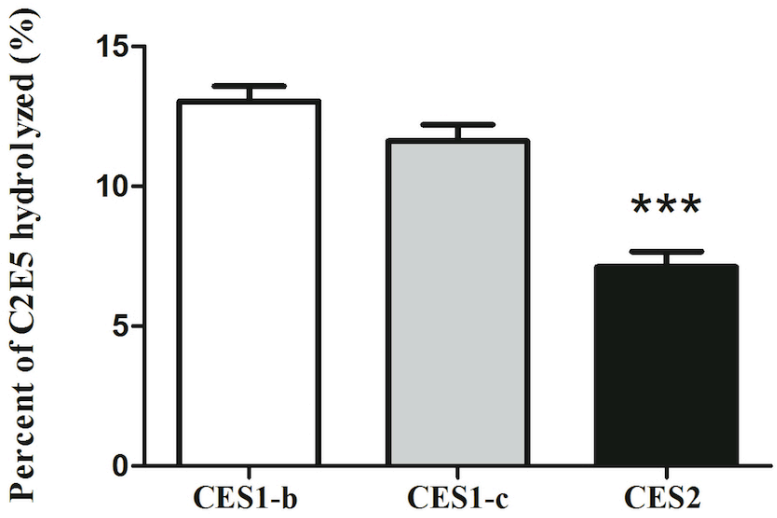

Figure 2.5. C2E5 Hydrolysis by CES1-b, CES1-c and CES2 One μM [^{14}C]-C2E5 was pre-incubated in 0.1 M phosphate buffer (pH 7.4) for 5 min at 37°C. Reactions were initiated by the addition of recombinant supersomes (1 mg/ml final concentration) and were incubated at 37°C. The reactions were terminated at the indicated time points by addition of an equal volume of cold acetonitrile followed by centrifugation at 14,000 x g for 10 min at 4°C. The disappearance of C2E5 was determined by radio-HPLC.

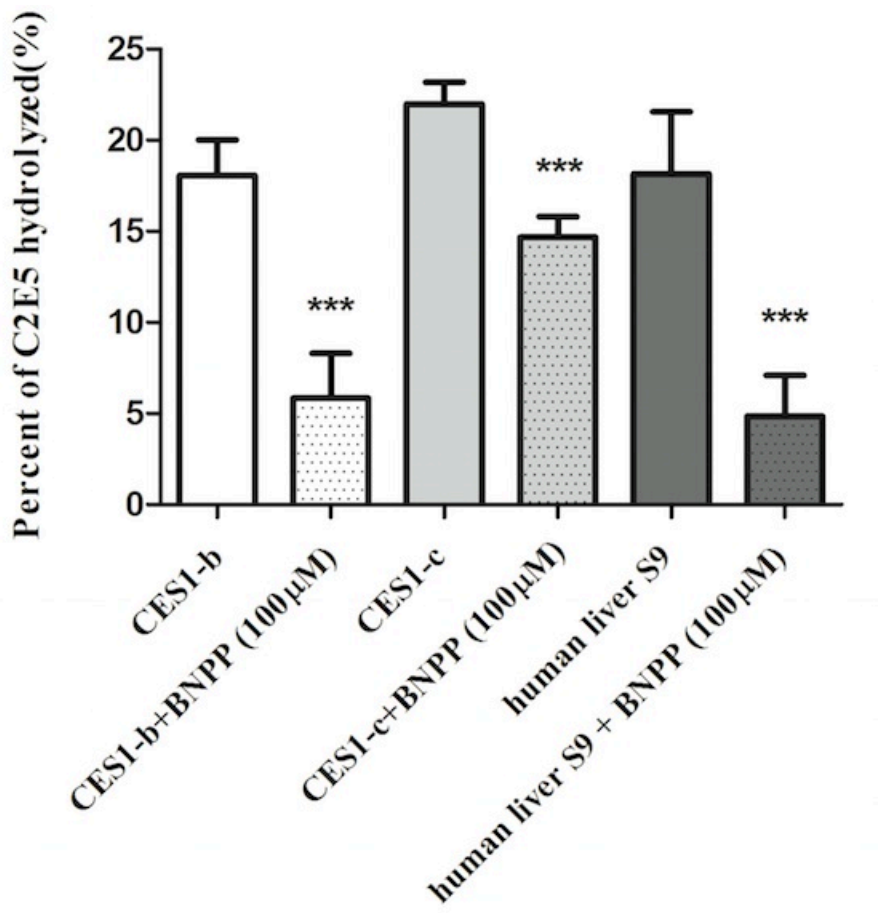

Figure 2.6. Inhibition Studies on C2E5 Hydrolysis. Fifty μM [^{14}C]-C2E5 was pre-incubated in 0.1 M phosphate buffer (pH 7.4) for 15 min at 37°C with addition of 100 uM BNPP. Reactions were initiated by the addition of recombinant supersomes (1 mg/ml final concentration) and were incubated at 37°C. The reactions were terminated at the indicated time points by addition of an equal volume of cold acetonitrile followed by centrifugation at 14,000 x g for 10 min at 4°C. The disappearance of C2E5 was determined by radio-HPLC.

REFERENCES

1. Menetrier F, Grappin L, Raynaud P, Courtay C, Wood R, Joussineau S, List V, Stradling GN, Taylor DM, Berard P, Morcillo MA, Rencova J 2005. Treatment of accidental intakes of plutonium and americium: guidance notes. Appl Radiat Isot 62:829-846.

2. Cassatt DR, Kaminski JM, Hatchett RJ, DiCarlo AL, Benjamin JM, Maidment BW 2008. Medical countermeasures against nuclear threats: radionuclide decorporation agents. Radiat Res 170:540-548.

3. FDA, 2006. Guidance for Industry Internal Radioactive Contamination - Development of Decorporation Agents. Retrieved August 6, 2015 http://www.fda.gov/downloads/drugs/guidancecomplianceregulatoryinformation/guidances/ucm071944.pdf

4. Beaumont K, Webster R, Gardner I, Dack K 2003. Design of ester prodrugs to enhance oral absorption of poorly permeable compounds: challenges to the discovery scientist. Curr Drug Metab 4:461-485.

5. Imai T 2006. Human carboxylesterase isozymes: catalytic properties and rational drug design. Drug Metab Pharmacokinet 21:173-185.

6. Nielsen NM, Bundgaard H 1988. Glycolamide esters as biolabile prodrugs of carboxylic acid agents: synthesis, stability, bioconversion, and physicochemical properties. J Pharm Sci 77:285-298.

7. Sueda K, Sadgrove MP, Huckle JE, Leed MG, Weber WM, Doyle-Eisele M, Guilmette RA, Jay M 2014. Orally administered DTPA penta-ethyl ester for the decorporation of inhaled (241) Am. J Pharm Sci 103:1563-1571.

8. Sadgrove MP, Leed M, Shapariya S, Madhura D, Jay M 2012. Evaluation of a DTPA Prodrug. C2E5 as an Orally Bioavailable Radionuclide Decorporation Agent. Drug Dev. Res 73: 243-251.

9. Zhang Y, Sadgrove M, Mumper R, Jay M 2013. Transdermal Prodrug Delivery for Radionuclide Decorporation: Nonaqueous Gel Formulation Development and In Vitro and In Vivo Assessment. Drug Dev. Res 74: 322-331.

10. Hosokawa M 2008. Structure and catalytic properties of carboxylesterase isozymes involved in metabolic activation of prodrugs. Molecules 13:412-431.

11. Satoh T, Hosokawa M 2006. Structure, function and regulation of carboxylesterases. Chem Biol Interact 162:195-211.

12. Inoue M, Morikawa M, Tsuboi M, Sugiura M 1979. Species difference and characterization of intestinal esterase on the hydrolizing activity of ester-type drugs. Jpn J Pharmacol 29:9-16.

13. Taketani M, Shii M, Ohura K, Ninomiya S, Imai T 2007. Carboxylesterase in the liver and small intestine of experimental animals and human. Life Sci 81:924-932.

14. Williams ET, Bacon JA, Bender DM, Lowinger JJ, Guo WK, Ehsani ME, Wang X, Wang H, Qian YW, Ruterbories KJ, Wrighton SA, Perkins EJ 2011. Characterization of the expression and activity of carboxylesterases 1 and 2 from the beagle dog, cynomolgus monkey, and human. Drug Metab Dispos 39:2305-2313.

15. Li B, Sedlacek M, Manoharan I, Boopathy R, Duysen EG, Masson P, Lockridge O 2005. Butyrylcholinesterase, paraoxonase, and albumin esterase, but not carboxylesterase, are present in human plasma. Biochem Pharmacol 70:1673-1684.

16. Roberts R, McCune SK 2008. Animal studies in the development of medical countermeasures. Clin Pharmacol Ther 83:918-920.

17. Snoy PJ 2010. Establishing efficacy of human products using animals: the US food and drug administration's "animal rule". Vet Pathol 47:774-778.

18. Mizen L, Burton G 1998. The use of esters as prodrugs for oral delivery of beta-lactam antibiotics. Pharm Biotechnol 11:345-365.

19. Ohura K, Tasaka K, Hashimoto M, Imai T 2014. Distinct patterns of aging effects on the expression and activity of carboxylesterases in rat liver and intestine. Drug Metab Dispos 42:264-273.

20. Satoh T, Taylor P, Bosron WF, Sanghani SP, Hosokawa M, La Du BN 2002. Current progress on esterases: from molecular structure to function. Drug Metab Dispos 30:488-493.

21. Involvement of carboxylesterase in hydrolysis of propranolol prodrug during permeation across rat skin by Teruko Imai, Yuko Takase, HarunobuIwase and Mitsuru Hashimoto.

22. Imai T, Taketani M, Shii M, Hosokawa M, Chiba K 2006. Substrate specificity of carboxylesterase isozymes and their contribution to hydrolase activity in human liver and small intestine. Drug Metab Dispos 34:1734-1741.

23. Liederer BM, Borchardt RT 2006. Enzymes involved in the bioconversion of ester-based prodrugs. J Pharm Sci 95:1177-1195.

24. Costa LG, Cole TB, Jarvik GP, Furlong CE 2003. Functional genomic of the paraoxonase (PON1) polymorphisms: effects on pesticide sensitivity, cardiovascular disease, and drug metabolism. Annu Rev Med 54:371-392.

25. Getz GS, Reardon CA 2004. Paraoxonase, a cardioprotective enzyme: continuing issues. Curr Opin Lipidol 15:261-267.

26. Jarvinen T, Poikolainen M, Suhonen P, Vepsalainen J, Alaranta S, Urtti A 1995. Comparison of enzymatic hydrolysis of pilocarpine prodrugs in human plasma, rabbit cornea, and butyrylcholinesterase solutions. J Pharm Sci 84:656-660.

27. Salvi A, Carrupt PA, Mayer JM, Testa B 1997. Esterase-like activity of human serum albumin toward prodrug esters of nicotinic acid. Drug Metab Dispos 25:395-398.

28. Udata C, Tirucherai G, Mitra AK 1999. Synthesis, stereoselective enzymatic hydrolysis, and skin permeation of diastereomeric propranolol ester prodrugs. J Pharm Sci 88:544-550.

29. Sakurai Y, Ma SF, Watanabe H, Yamaotsu N, Hirono S, Kurono Y, Kragh-Hansen U, Otagiri M 2004. Esterase-like activity of serum albumin: characterization of its structural chemistry using p-nitrophenyl esters as substrates. Pharm Res 21:285-292.

30. Redinbo MR, Potter PM 2005. Mammalian carboxylesterases: from drug targets to protein therapeutics. Drug Discov Today 10:313-325.

31. Sanghani SP, Quinney SK, Fredenburg TB, Davis WI, Murry DJ, Bosron WF 2004. Hydrolysis of irinotecan and its oxidative metabolites, 7-ethyl-10-[4-N-(5-aminopentanoic acid)-1-piperidino] carbonyloxycamptothecin and 7-ethyl-10-[4-(1-piperidino)-1-amino]-carbonyloxycamptothecin, by human carboxylesterases CES1A1, CES2, and a newly expressed carboxylesterase isoenzyme, CES3. Drug Metab Dispos 32:505-511.

32. Tabata T, Katoh M, Tokudome S, Nakajima M, Yokoi T 2004. Identification of the cytosolic carboxylesterase catalyzing the 5'-deoxy-5-fluorocytidine formation from capecitabine in human liver. Drug Metab Dispos 32:1103-1110.

CHAPTER 3

BIOTRANSFORMATION CAPACITY OF CARBOXYLESTERASE IN SKIN AND KERATINOCYTES FOR THE PENTA-ETHYL ESTER PRODRUG OF DTPA

3.1 Introduction

Transdermal drug delivery is non-invasive, can be self-administered, avoids first-pass metabolism, and is well suited to pediatric populations and specialized patient groups who have trouble swallowing [1]. In addition, transdermal products are attractive due to their sustained zero-order systemic release profile [2]. However, to reach the systemic circulation, drug molecules need to pass through the skin's multiple barriers including the hydrophobic environment of the stratum corneum, the epidermis and the dermis to reach the vascularized hypodermis. These barriers effectively limit direct transdermal drug delivery to molecules that possess aqueous solubility in physiological pH (> 1 mg/ml, pH 5-9), a low molecular weight (usually <500 Daltons), moderate lipophilicity (oil-water partition coefficient $K_{o/w}$ 10 – 1000), and those that require a moderate daily dosage (< 10 mg/day) [2, 3]. A growing number of drugs, that have many of the properties listed above, have been approved for transdermal delivery. These include estradiol, fentanyl, lidocaine and testosterone patches and ultrasonic delivery systems for analgesia [4, 5].

In addition to the physical barriers, cutaneous metabolism via local phase I and phase II metabolic enzymes can also reduce bioavailability [6, 7]. Cytochrome P450 enzymes are clearly expressed in organotypic skin models [8, 9]. In human skin, CYP families 1, 2 and 3 are

responsible for the metabolism of the majority of drugs and other xenobiotics [10]. Xenobiotic metabolizing enzymes are located in the epidermis and dermis where hair follicles and sebaceous and sweat glands are located [11, 12]. The study of dermal metabolism is complicated by significant interspecies differences in xenobiotic metabolism [13-15]. Therefore, ideally, metabolism should be investigated in human skin tissue.

Enzymatic metabolism in the skin can be utilized to bio-activate prodrug molecules and to improve dermal or transdermal delivery. For example, morphine propionate and morphine enanthate are two alkyl ester prodrugs of morphine that have been shown to enhance dermal delivery of morphine by 2 and 5 fold, respectively [16]. Many prodrugs, including these two morphine prodrugs, are formed by esterification of the active molecule. The added ester moiety can be used to alter the physicochemical properties of the molecule and improve transdermal absorption [16]. Once absorbed into the skin, enzymatic hydrolysis of the prodrug by esterases releases the active drug.

Carboxylesterases (CES1 and CES2) are involved in the metabolism of xenobiotics. For example, CES1 activates prodrugs of angiotensin-converting enzyme inhibitors and CES2 activates the anticancer prodrug CPT-11 [17, 18]. In humans, CES1 and CES2 expression is ubiquitous; however, CES1 predominates in most organs [19]. Although CESs are known to be expressed in human skin, information on their role in the metabolism of topically applied drugs and prodrugs is limited [20].

We have developed a pentaethyl ester prodrug of the chelating agent diethylene triamine pentaacetic acid (DTPA), referred to as C2E5 (Fig. 1), to enhance clearance (decorporation) of transuranic radionuclides [21]. C2E5 is metabolized by CESs [15] and the physiochemical properties of C2E5 (CLogP of 4.7, with a molecular weight of 533 Daltons) suggest that it would be a good

candidate for transdermal delivery. Evidence supporting transdermal application of C2E5 was reported in rat *in vivo* transdermal pharmacokinetics and efficacy studies [21]. Therefore, the first objective of the current work was to assess the expression of CES isoforms in four different human skin cell lines. The second objective was to determine the capacity of the CESs in each cell line to metabolize the prodrug C2E5.

3.2 Materials and methods

Materials. [^{14}C]-DTPA penta-ethyl ester ([^{14}C]-C2E5; 55 mCi/mmol, 1mCi/ml) was purchased from American Radiolabeled Chemicals, Inc. (St. Louis, MO). Ultima-Flo AP scintillation fluid was obtained from PerkinElmer Life and Analytical Sciences (Waltham, MA). Acetonitrile (ACN), 4-nitrophenyl valerate (4-NPV), *p*-nitrophenyl acetate (PNPA), Dulbecco's modified Eagle's medium, 0.25% trypsin-EDTA, and Dulbecco's phosphate buffered saline (PBS) were purchased from Sigma Aldrich (St. Louis, MO). Penicillin-streptomycin was purchased from Invitrogen Corporation (Carlsbad, CA). Fetal bovine serum was purchased from Cansera International Inc. (Rexdale, ON, Canada). Human Female skin S9 fractions were purchased from BioreclamationIVT (Hicksville, NY).

Cell Culture. HaCaT cells, immortal human keratinocytes, and A431, an immortalized epidermoid carcinoma derived, were kindly provided by Dr. Zhi Liu (Lineberger Comprehensive Cancer Center, Chapel Hill, NC). Primary neonatal human epithelial kerotinocytes (HEKn) and adult human epithelial kerotinocytes (HEKa) cells were obtained commercially (Gibco by Life Technologies, Grand Island, NY). HaCaT and A431 were maintained in 10% fetal bovine serum and Dulbecco's modified eagle medium/high glucose medium (Gibco) containing 10% fetal calf serum, penicillin (10,000 units/ml) and streptomycin (10 mg/ml) until sub-confluence was reached (after 48 h). HEKn and HEKa were cultured in EpiLife medium (Gibco), supplemented

with 1% EpiLife® defined growth supplement and 0.1% calcium chloride ($CaC1_2$) (Gibco). All incubations were conducted at 37±1°C, 95% air/5% CO_2, and saturated humidity.

Preparation of Cell Supernatant (S9 fractions). For all cell lines, cytosolic S9 fractions were prepared as cited in literature (Imai et al., 2013). Protein concentrations were determined by the Pierce™ BCA protein assay (Thermo Fisher Scientific, Waltham, MA). Human liver S9 fractions (XenoTech, Kansas City, KS), human recombinant protein (BD Biosciences, Franklin Lakes, New Jersey), and human skin S9 fractions (BioreclamationIVT, Hicksville, NY) were purchased commercially.

Determination of the Genetic Expression by real time reverse transcription-polymerase chain reaction (RT-qPCR). HEKa, HEKn, HaCaT and A431 cells were seeded and grown in 15 ml in T75 tissue culture flasks. Expression of the CESs genes were evaluated by RT-qPCR. Total RNA was extracted using the RNeasy Mini Kit (Qiagen, Cat. No.74134, Hilden, Germany) according to the manufacturer's instructions. Briefly, cell samples were lysed and homogenized using 1ml/10cm^2 cells of TRIzol (Ambion® by Life Technology) and then were isolated by QIAshredder columns (Qiagen Cat. No.79656) in a highly denaturing guanidine-thiocyanate containing buffer. Ethanol (70%) was added and the samples were applied to an RNeasy Mini Spin Column (Qiagen). RNA was bound to the membrane of the column and contaminants were washed away. Subsequently, RNA was eluted from the column using 30 µl of water. The concentration and purity of the total RNA was determined using the Nanodrop 2000 method (Thermo Scientific,Wilmington, DE). cDNAs were prepared by reverse transcription of total RNA using the iScript™ cDNA synthesis kit (Bio-Rad cat #170-8891, Hercules, CA) and stored at -20ºC until qPCR amplification. qPCR reactions were prepared using the 2X iTaq™ Universal Probes Supermix, TaqMan® CES1, CES2 and glyceraldehyde-3-

phosphate dehydrogenase (GAPDH) primers, (TaqMan® Gene Expression Assays Rack ID: 14429192. Primers: Hs00275607_m1 for CES1, Hs01077945_m1 for CES2 and Hs02758991_g1 for GAPDH) (Applied Biosystems, Foster City, CA) and nuclease-free water (Qiagen) cDNA was diluted 5-fold and qPCR was performed by the *TaqMa*n® Gene Expression Assay (Bio-Rad). The PCR amplification was conducted in a total volume of 20 µl containing universal PCR master mixture (10 µl), gene-specific *TaqMan®* assay mixture (1 µl), diluted cDNA (5 µl) and nuclease-free water (4 µl). The cycling profile was 50°C for 2 min, 95°C for 10 min, followed by 40 cycles of 15 s at 95°C and 1 min at 60°C, as recommended by the manufacturer. Amplification and quantification were done with the Applied Biosystems 7900HT Real-Time PCR System (Foster City, CA). All samples were analyzed in triplicate and the signals were normalized to GAPDH and then expressed as relative levels of mRNA. The CES1 probe recognized both CES1A1 and CES1A2; these enzymes are identical although distinct genes encoded. GAPDH was included in the study as the loading control.

Quantification of Gene Expression. Relative RNA expression levels were determined from delta Ct values using the expression of the GAPDH gene as an internal control. The real-time RT-qPCR assay was performed in triplicate for each sample. For each replicate, the CES Ct was normalized to the GAPDH Ct [$\Delta Ct = Ct_{[Target]}-Ct_{[Gapdh]}$] before the mean and SEM ΔCt was calculated.

Determination of the Protein Expression. Western blot studies were conducted to explore CES1 and CES2 expression in the different human skin cell lines. CES1 and CES2 antibodies were purchased from Abcam (Cambridge, England). Protein concentrations were determined using the Pierce™ BCA Protein Assay (Thermo Fisher Scientific). Total protein lysate (30 µg) was run on a NuPAGE™ 4–12% Bis-Tris Gel (Bio-Rad) at 120 V for 1 h.

Following electrophoresis, the proteins were transferred by blotting onto 0.45 μm polyvinyl difluoride membranes (Thermo Fisher Scientific) at 350 mA for 1.25 h in transfer buffer (Bio-Rad). The membrane was blocked in 5% skimmed milk powder in Tris-buffered saline/0.05% Tween for 1 h before overnight incubation with primary antibody: monoclonal hCES1 or hCES2 (Sigma-Aldrich) at 1:1000 dilution or GAPDH (Abcam) at 1:10,000 dilution. The membranes

were washed and incubated with a secondary antibody, horseradish peroxidase-conjugated goat anti-rabbit (Sigma-Aldrich) at 1:10000 dilution for 1 h. Finally, the membranes were incubated briefly in SuperSignal® Stable Peroxide Solution together with SuperSignal® West Pico Luminol/Enhancer Solution (Thermo Fisher Scientific) and immediately imaged. The chemiluminescent signal was registered with a FluorChem 8000 camera (Alpha Innotech Corp, San. Leandro, CA). Human liver and intestine S9 fractions served as positive controls for CES1 and CES2, respectively.

Determination of Enzyme Activity by PNPA Assay and 4-NPVAssay. Total esterase and CESs-specific enzyme activity was measured using established substrates PNPA (100μM) and 4-NPV (100μM), respectively. Hydrolysis of the freshly prepared substrates was carried out in 96 well plates with a total volume of 100 μl/well. Reactions were initiated by mixing 1 μl of substrate with diluted S9 samples (0.1 mg/ml). The rates of hydrolysis of PNPA and 4-NPV were determined spectrophotometrically by measuring reaction products at 402 nm after 10 min incubation at 37°C as previously described [22] using a UV spectrometer (BioTek, Winooski, VT). Analysis was performed using Microsoft Excel.

Determination of C2E5 Hydrolysis by High Performance Liquid Chromatography-Radiomatic Flow Scintillation Analyzers (HPLC-FSA). [^{14}C]-C2E5 (1 μM, 0.55 nCi) was pre-incubated in 0.1 M phosphate buffer (pH 7.4) for 5 min at 37°C. Reactions were initiated by the addition of S9 fractions (1 mg/ml) from different cell lines (HEKa, HEKn, HaCaT and A431) in a total volume of 100 μl; boiled S9 fractions were used as a blank to correct for non-enzymatic C2E5 degradation. The reactions were terminated by adding an equal volume of ice-cold acetonitrile (ACN), followed by centrifugation at 14,000*g* for 15 min at 4°C. The supernatant was transferred to HPLC vials for analysis as previously described [15]. Representative radiochromatograms shown in supplemental figures 1 and 2 illustrate a C2E5 peak generated from the boiled S9 fractions and C2E5 and the presences of a metabolite, C2E4, in human skin S9 fractions.

Sample Preparation for Human Skin S9 fractions-Mediated C2E5 Hydrolysis with and without Inhibitors. Experiments were designed to examine the effect of specific inhibitors on C2E5 hydrolysis in human skin S9 fractions. The following inhibitors were selected: benzil (10 μM) was chosen as a pan CES inhibitor [23], troglitazone (10 μM) as a CES1 specific inhibitor [24], loperamide (100 μM) as a CES2 specific inhibitor [25] and BNPP (1 mM) as a non-specific esterase inhibitor [26]. Inhibitors were incubated with human skin S9 fractions for 30 min at 37°C before the reaction was initiated. All reactions were initiated by the addition of S9 fractions (0.5 and 1 mg/ml) to prepared C2E5 in water to result a final C2E5 concentration of 0.5 μM at 37°C. Reactions were terminated after 120 mins by adding an equal volume of ice-cold acetonitrile with 2% of formic acid, followed by centrifugation at 14,000 *g* for 15 min at 4°C. Liver S9 fractions (1 mg/ml) were used as a positive control and boiled S9 fractions were used as negative controls. Reactions were performed in triplicate. The standards used to generate the LC/MS/MS

C2E5 calibration curve were prepared by spiking boiled S9 fractions with C2E5 and processed as described above.

LC/MS/MS Chromatographic and Spectroscopic Conditions. Chromatographic separation from matrix components was achieved using reverse-phase chromatography on an YMC ODS-AM C18 (100 x 2 mm, 3 μm) column. Gradient elution was used based on a combination of water with 0.1% formic acid (A) and acetonitrile with 0.1% formic acid (B). The mobile phase was initiated at 13% B increasing to 40% B by 1 min, to 60% B by 6 min and to 95% B by 6.2 min. The mobile phase was held at 5% A and 95% B from 6.2 min to 6.5 min when a post-run cycle that included isopropyl alcohol (C) was initiated. Between 6.5 min and 7 min solvent B (95%) was gradually replaced with solvent C (95%). The mobile phase was then held at 5% A 95% C until 7.5 min before gradually returning to initial conditions (87% A, 13% B, 0% C) after 8.5 mins, which were maintained for 1.5 mins prior to the next injection. The flow rate was 300 μl/min and the injection volume was 5 μl. The column oven temperature was set to 40 °C. C2E5 was detected on a triplequadrupole mass spectrometer (Thermo TSQ Quantum Access) using electrospray ionization (ESI) in the positive-ion mode. The ionization source and collision parameters were optimized to give maximum analyte signal intensity (Spray Voltage 3500V; Sheath and Auxiliary gas nitrogen, 10 and 25 psi, respectively; Collision gas Argon @ 1.5 mTorr; Collision energy 35 eV). The mass spectrometer was set to carry out single reaction monitoring (SRM) for the precursor → product ion transitions m/z 534 → 216 (C2E5) and m/z 506 → 188 (C2E4) at a retention times of 3.6 and 2.8 min, respectively. For C2E5 quantification, a calibration plot of analyte peak area against nominal C2E5 concentration (20 – 1000 ng/mL) was constructed from a quadratic equation with a 1/concentration^2 weighting. Representative chromatograms showed formation of C2E5 metabolite, C2E4. Representative

chromatograms shown in supplemental figures 3 and 4 illustrate a C2E5 peak generated from the boiled S9 fractions and C2E5 and the presences of a metabolite, C2E4, in human skin S9 fractions.

Data analysis. The data were processed by Graph Pad Prism 5.0, and are presented as mean ± SEM.

3.3 Results

Genetic Expression of Carboxylesterase in HEKa, HEKn HaCaT, A431 cells, and Human Skin Tissue. The mRNA expression of CES1 was primarily detected in human skin tissue. A small amount was detected in HEKa and HEKn cells, and none was detected in HaCaT and A431 cells (Fig. 3.2A). In contrast, mRNA expression of CES2 was detected in all cells. Human skin CES2 expression was about 2-fold higher than HEKa, HEKn and HaCaT and 10-fold higher than A431 expression (Fig. 3.2B). CES1 expression in the human skin was about 25-fold greater than CES2 expression. However, the human skin total RNA was obtained from only one human subject and inter-individual variability could affect these comparative results.

Protein Expression of Carboxylesterase in HEKa, HEKn, HaCaT, A431 cells and Human Skin Tissue. Human liver and intestine S9 fractions were used as positive controls. CES1 protein expression was detected in human skin S9 fractions. The band for CES1 in human skin (30 μg of skin sample) was considerably lighter than the CES1 band in human liver S9 fractions (5 μg of liver sample). There was little evidence of CES1 in HEKn, HaCaT and A431 cells (Fig. 3.3A). Meanwhile, CES2 protein expression was detected in HEKn, HaCaT, human skin and human intestine S9 fractions (Fig. 3.3B). The bands indicated that more CES2 was present in HEKn compared to HaCaT. Little evidence for CES2 in A431 was observed (Fig. 3.3B).

Hydrolysis Activity of PNPA and 4-NPV in HEKa, HEKn, HaCaT, A431 cells and Human Skin Tissue. Enzymatic activity was determined using PNPA (esterases) and 4-NPV (CES) assays with human liver S9 fractions as a control. The PNPA assay demonstrated that the S9 fractions from human skin cell lines exhibited esterase activity (Fig. 3.4A). PNPA hydrolysis activity in the cultured cells was slightly lower than in human skin S9 fractions and 5- to 10-fold

lower than in human liver S9 fractions (Table 3.1). For example, HEKn displayed approximately 20% of the esterase activity of the liver. When the amount of protein was standardized across all the samples, the catalytic rate of esterase in HEKn was the highest among all cell lines. The 4-NPV assay showed that CES activity was present in all of the tested cells; the catalytic rate of CES in HEKn cell lines was the greatest (Fig. 3.4B). 4-NPV hydrolysis activity in the cultured cells was comparable to or slightly lower than in human skin S9 fractions and 2- to 5-fold lower than in human liver S9 fractions (Table 3.2). For example, HEKn displayed approximately 60% of the CESs activity of the liver.

Hydrolytic Activity of Penta-ethyl Ester Prodrug of DTPA (C2E5) in HEKa, HEKn, HaCaT A431 Cell Lines. S9 fractions produced from HEKa, HEKn, HaCaT hydrolyzed [^{14}C]-C2E5 (1μM) to the primary metabolite, C2E4. Little hydrolysis was observed in the S9 fractions of A431 cells (Fig. 3.5A). The hydrolytic rates of C2E5 by HEKa, HEKn, HaCaT and A431 cells were 7.12, 2.63, 3.80 and 0.66 pmol/mg/min, respectively.

Inhibition of Hydrolytic Activity of Penta-ethyl Ester Prodrug of DTPA (C2E5) in Human Skin S9 Fractions. Near complete (98.6%) hydrolysis was seen in human liver S9 fractions, while human skin S9 fractions showed 62.8% loss of the parent drug (C2E5, Fig 3.6). As expected, addition of the non-specific esterase inhibitor, BNPP, totally blocked the hydrolysis of C2E5. Addition of the inhibitors benzil (pan CESs) troglitazone (CES1) and loperamide (CES2) resulted in 10.6%, 40.68%, and 77.68% loss of parent drug C2E5, respectively. These data suggest that both CES1 and CES2 hydrolyze C2E5, but the hydrolysis is primarily via CES1.

3.4 Discussion

As transdermal delivery technology becomes more common, questions remain as to how and whether ester-based prodrugs pass through the skin and whether hydrolysis during this transition effects the absorption, distribution, metabolism and excretion (ADME) of the drug. Because of interspecies differences in hydrolysis profiles, skin derived from animals may be very different from human skin [14, 27, 28]. Therefore, alternative methods to examine human specific hydrolysis are needed during drug development. Previously, we reported that CESs play an important role in the metabolism of the ester-based prodrug, C2E5, which is being investigated as a decorporation agent for contamination with transuranic elements [21]. The present study characterized CESs expression and activity in human skin tissue and different human keratinocyte cell lines and demonstrated the role of CESs in facilitating C2E5 hydrolysis in skin during transdermal delivery. In addition, the prodrug, C2E5, was hydrolyzed in all skin cell lines examined and that HEKa cells may be the most appropriate cell line to study its transdermal delivery.

CES1 and CES2 proteins were expressed in human skin S9 fractions. RT-qPCR clearly showed greater expression of CES1 mRNA compared to CES2 mRNA, which supports a previous report of greater CES1 expression in human skin microsomes [29]. As expected, measurement of total esterase activity using the PNPA assay [30] revealed much less activity in the skin compared to the liver (Fig. 3.4A). However, the 4-NPV assay, which measures CES activity [25] showed that total CESs activity was only 2-fold lower in the skin than in the liver (Fig. 3.4B), confirming the potential for human skin to contribute to the metabolism of ester compounds when applied transdermally [16].

As an alternative to human skin, we assessed different human keratinocyte cell culture models for their utility as surrogates in investigating transdermal drug metabolism. The keratinocyte tumor cell line A431 had no detectable CES1, and CES2 was expressed at barely detectable levels. Therefore, we concluded that A431 cell line is not a suitable model for investigating transdermal drug metabolism. Of the remaining keratinocyte cultures, our results demonstrated that while HEKa, HEKn and HaCaT express CES1, CES2 was more abundant across the various keratinocyte cell lines. These findings are consistent with the work of Zhu et al. who identified CES2 as the main CES in HaCaT cells [20]. Enzyme expression and activity in keratinocytes change over time in culture; cytochrome P450 enzymes are particularly vulnerable, but esterases and conjugated enzymes are also affected [22]. This observation could explain our findings that CES2 expression was slightly lower in HaCaT cells compared to HEKa or HEKn cells, and that CES1 expression was greatly reduced or absent in all the cultured cells. HEKa and HEKn are primary cultures and, as such, may retain the greater enzymatic activity observed in human skin compared to the immortalized HaCaT cell line.

CES1 and CES2 are from the same family, known as 60-kDa serine esterase. While these two isoforms have a similar molecular weight, (CES1 is 62.5 KDa and CES2 is 60.0 KDa), they are structurally quite different. The isoelectric point of CES1 is 5.8 and CES2 is 4.9 and the sequence homology between the two enzymes is only 48% [31]. These structural differences result in different substrate specificity. CES1 tends to hydrolyze molecules with a small alcohol moiety more efficiently, while CES2 is more efficient at metabolizing molecules with a larger alcohol moiety and more lipophilic molecules [25, 32]. These differences in the substrate specificity of CES1 and CES2 could lead to differences in predicting skin absorption or metabolism. In different human cell lines and skin S9 fractions, we demonstrated CESs expression by western

blot and RT-qPCR and confirmed activity with PNPA and 4-NPV assays; subsequently, we examined the metabolism of C2E5, a prodrug developed for transdermal delivery.

C2E5 is the penta-ethyl ester of DTPA, administered intravenously to treat plutonium, americium, and curium (Pu, Am and Cm) contamination. In vivo studies, in rats, report de-esterification of C2E5 mainly into the tri- and di-ethyl esters, C2E3 and C2E2, with some DTPA also present [21]. In vitro binding experiments, using human, rat and dog plasma, suggest that C2E2 is an effective chelator of Am [33], and this hypothesis is supported by efficacy study following oral administration of C2E2 in beagle dogs [34]. Thus, to be effective, when applied transdermally, C2E5 needs to be metabolized to C2E2 in the body. Sustained plasma concentrations of C2E2 are observed in rats following transdermal application of C2E5 in a non-aqueous gel [21] and this is associated with effective Am decorporation [35], suggesting that transdermal delivery of C2E5 to the active C2E2 is possible. In the present study, we used the S9 fractions model to assess the potential translation of these preclinical observations to human tissues.

Previously, we used a human recombinant protein system to examine human CES1 and CES2 mediated C2E5 hydrolysis; the results demonstrated that both CES1 and CES2 were reponsible for C2E5 hydrolysis. However, CES1 hydrolyzed C2E5 to a greater extent compared to CES2 [15]. The results in the current study agree with our previous findings (Fig. 3.5 and 3.6). Although complete metabolism to an active drug, C2E2, was not observed in human skin in the current study, once in the systemic circulation, further hydrolysis of C2E5's metabolites can occur in the liver, mainly by CES 1, and in plasma, possibly by paraoxonase and butrylcholinesterase as CES1 and 2 are not present [36]. Additionally, the metabolism of C2E5 by

CESs in keratinocytes, which we report here, results in metabolites that are more hydrophilic than C2E5 and could potentially more readily enter the systemic circulation.

The differences in enzyme activity and expression among cell lines and skin tissue has important implications for future studies examining transdermal metabolism of ester-based prodrugs. HEKa, HEKn and HaCaT cell cultures have the potential for examining the metabolism of compounds that are substrates for CES2. However, of the human cell lines we examined, only HEKa cells have the potential for establishing the metabolism of compounds that are substrates for CES1.

In summary, this is the first study to characterize the expression of CES isoforms in multiple human skin cell lines and human skin tissue with a view to using native phase 1 enzymes in skin to enhance transdermal delivery of C2E5. The differences in enzyme activity and expression among cell lines and skin tissue has important implications for future studies examining transdermal metabolism of ester-based prodrugs. We confirmed that CES activity is present in skin, albeit at lower levels compared to the liver, and that CES2 activity, but not CES1 activity, in HEKa, HEKn and HaCaT cells is comparable to that of human skin. Consequently, human skin cell cultures may be useful in quantifying CES2-mediated drug metabolism. Of the human cell lines we examined, HEKa cells have the potential for establishing the metabolism of compounds that are substrates for CES1. However, caution should be used when human skin cells lines are used as alternative models for human cutaneous metabolism in transdermal drug delivery. Since the CES1 specific inhibitor reduced human skin S9 fractions-mediated hydrolysis of C2E5, CES1 appears to be crucial for C2E5 metabolism; as a result, the HEKa cell line could be an appropriate model for metabolism of C2E5.

Table 3.1. Esterase activity in human skin cell cultures, human skin S9 fractions and human liver S9 fractions

Cell Type	Hydrolytic activity (nmol/min/mg)
HEKa	20.2 ± 1.82
HEKn	31.6 ± 3.76
HaCaT	26.2 ± 1.97
A431	16.7 ± 1.11
Human skin	39.0 ± 11.54
Human Liver	167.2 ± 5.50

Data are the Mean ± SEM. N = 3.

Table 3.2. Carboxylesterase activity in human skin cell cultures, human skin S9 fractions and human liver S9 fractions

Cell Type	Hydrolytic activity (nmol/min/mg)
HEKa	40.9 ± 8.87
HEKn	125.8 ± 5.87
HaCaT	103.0 ± 9.65
A431	57.3 ± 7.56
Human skin	114.3 ± 5.60
Human Liver	217.7 ± 13.83

Data are the Mean ± SEM. N = 3.

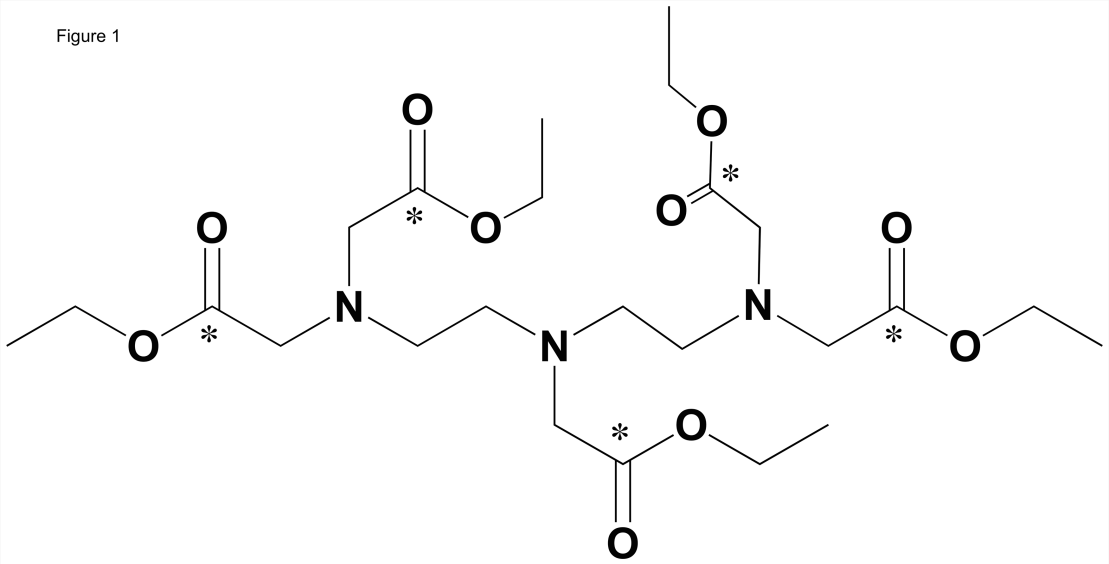

Figure 3.1. Structure of penta-ethyl ester DTPA prodrug (C2E5). ^{14}C-radiolabel positions are indicated by asterisks.

Figure 2

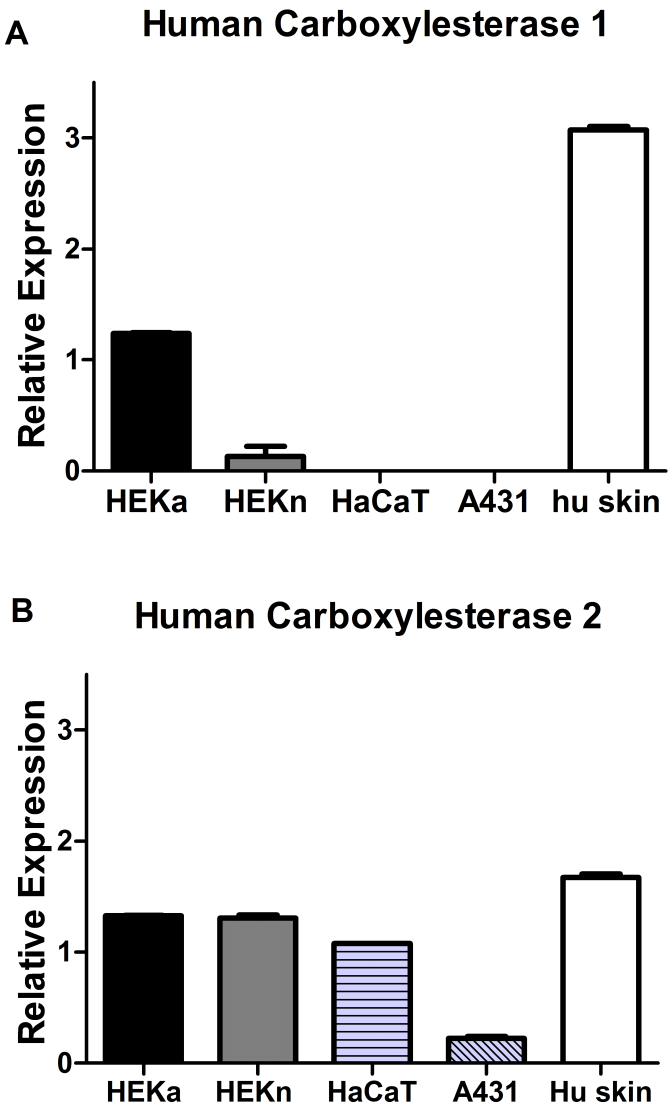

Figure 3.2. Log of relative expression of CES1 and CES2 mRNA in human epidermal keratinocyte HEKa, HEKn, HaCaT, A431 cells and human skin by RT-qPCR analysis. [A] CES1 expression. [B] CES2 expression. Values represent mean ± SEM (n=3).

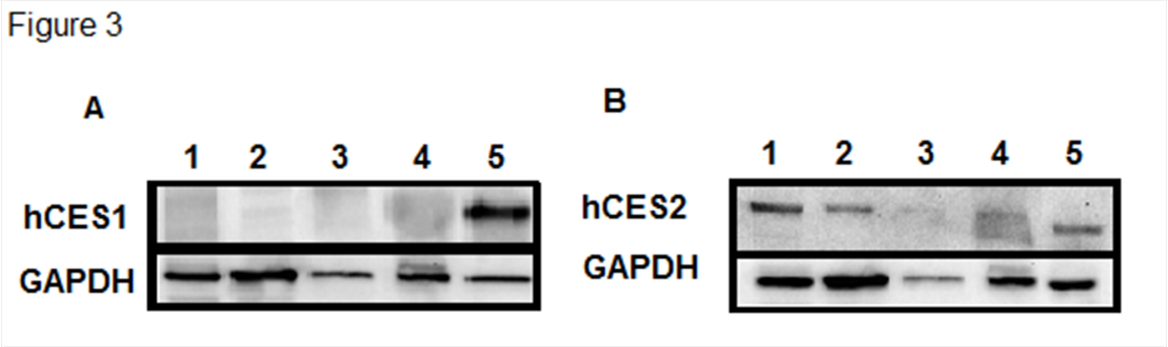

Figure 3.3. Western blot analysis of human epidermal keratinocyte HEKn, HaCaT and A431 cells and human tissue. Each band was detected with CES1 and CES2 antibodies. [A] CES1 expression. [B] CES2 expression. Lane 1 = HEKn, 2 = HaCaT, 3 = A431, 4 = human skin, 5A = human liver, and 5B = human intestine.

Figure 4.

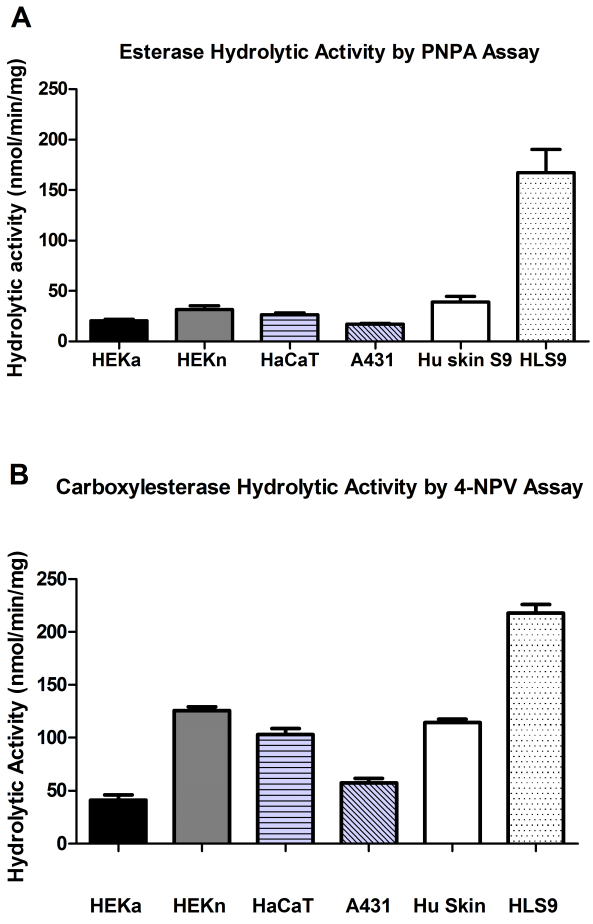

Figure 3.4. Esterase and carboxylesterase activities in human epidermal keratinocyte HEKa, HEKn, HaCaT, A431 cells and human skin tissue measured with a PNPA and 4-NPV assay. [A] PNPA assay in the presence of S9 fractions of HEKa, HEKn, HaCaT, A431 cells and human skin. [B] 4-NPV assay in the presence of S9 fractions of HEKa, HEKn, HaCaT, A431 cells and human skin. The hydrolysis of the freshly prepared substrates was carried out in 96 well plates with a total volume of 100 μl/well. Reactions were initiated by mixing 1 μl of substrate with diluted S9 samples (0.1 mg/ml). The rates of hydrolysis of PNPA and 4-NPV were determined spectrophotometrically by measuring reaction products at 402 nm after 10 min incubation at 37°C using a UV spectrometer. Values represent mean ± SEM. (n=3).

Figure 5

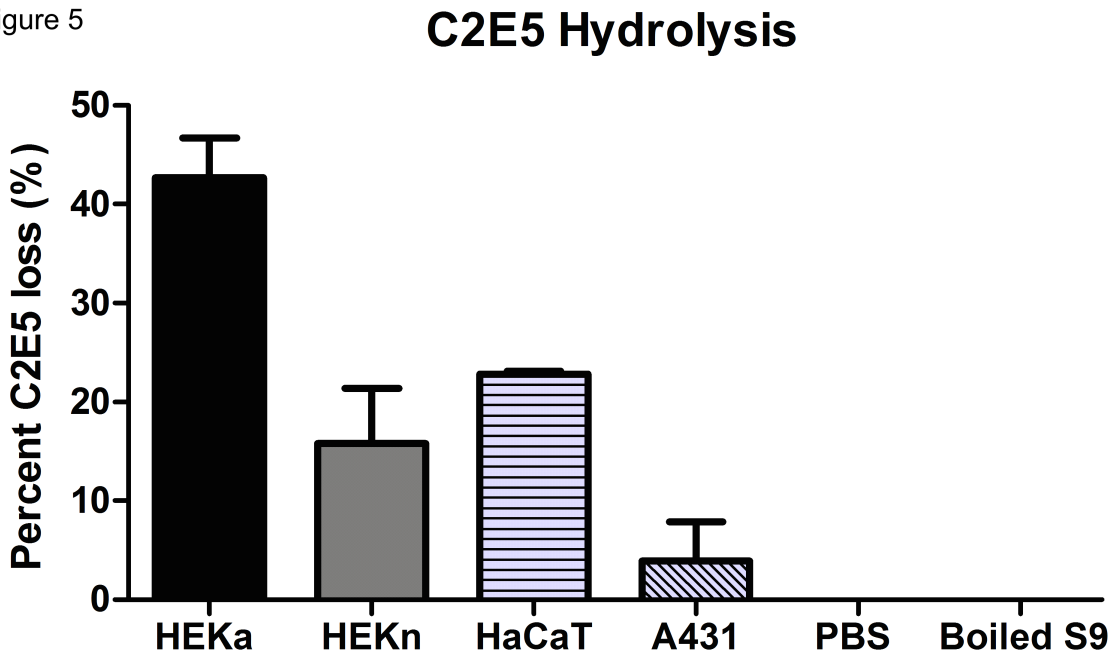

Figure 3.5. C2E5 hydrolysis in human epidermal keratinocyte HEKa, HEKn, HaCaT, A431 cells. Loss of parent drug was measured by detecting changes in radioactivity of C2E5 at HPLC elution peak (7.3 min) during a 60 mins incubation of 1μM [^{14}C]-C2E5 with HEKa, HEKn, HaCaT and A431 cells. Values represent mean ± SEM (n=3).

Figure 6

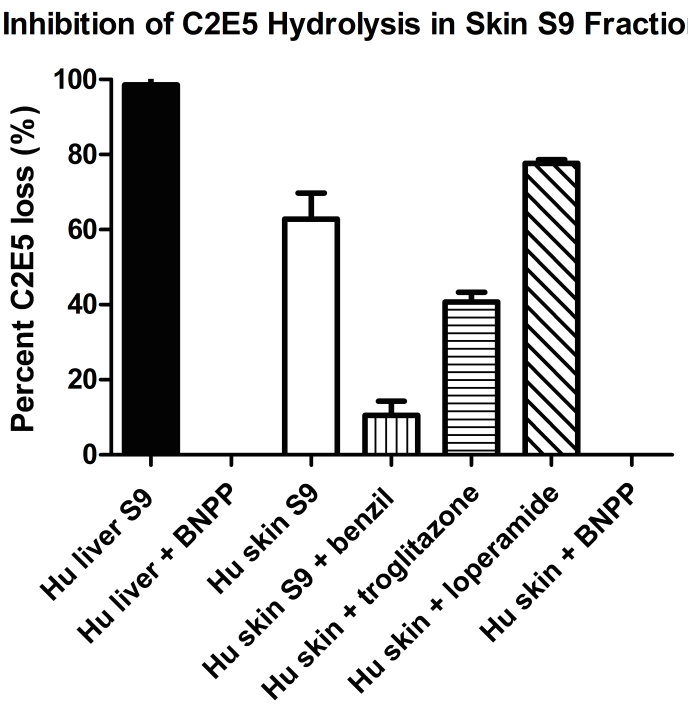

Figure 3.6. C2E5 hydrolysis in human skin S9 fractions and inhibition studies on C2E5 hydrolysis. Inhibitors, benzil, trogliazone, loperamide, and BNPP were incubated with human skin S9 fractions for 30 min at 37°C before the reaction was initiated. Loss of parent drug was measured by detecting changes in spectromatogram at the LC/MS/MS analyte peak (3.6 min) after 120 mins incubation of 0.5 μM C2E5 with human skin S9 fractions with and without inhibitors. Liver S9 fractions (1 mg/ml) were used as a positive control and boiled S9 fractions were used as negative controls. Values represent mean ± SEM (n=3).

REFERENCES

1. Zempsky WT 1998. Alternative routes of drug administration--advantages and disadvantages (subject review). Pediatrics 101:730-731.

2. Naik A, Kalia YN, Guy RH 2000. Transdermal drug delivery: overcoming the skin's barrier function. Pharm Sci Technolo Today 3:318-326.

3. Perumal O, Murthy SN, Kalia YN 2013. Turning theory into practice: the development of modern transdermal drug delivery systems and future trends. Skin Pharmacol Physiol 26:331-342.

4. Nitti VW 2003. Transdermal therapy for overactive bladder: present and future. Rev Urol 5 Suppl 8:S31-6.

5. Prausnitz MR, Langer R 2008. Transdermal drug delivery. Nat Biotechnol 26:1261-1268.

6. Esser C, Gotz C 2013. Filling the gaps: need for research on cell-specific xenobiotic metabolism in the skin. Arch Toxicol 87:1873-1875.

7. Zhang Q, Grice JE, Wang G, Roberts MS 2009. Cutaneous metabolism in transdermal drug delivery. Curr Drug Metab 10:227-235.

8. Saeki M, Saito Y, Nagano M, Teshima R, Ozawa S, Sawada J 2002. mRNA expression of multiple cytochrome p450 isozymes in four types of cultured skin cells. Int Arch Allergy Immunol 127:333-336.

9. Swanson HI 2004. Cytochrome P450 expression in human keratinocytes: an aryl hydrocarbon receptor perspective. Chem Biol Interact 149:69-79.

10. Du L, Hoffman SM, Keeney DS 2004. Epidermal CYP2 family cytochromes P450. Toxicol Appl Pharmacol 195:278-287.

11. Sugibayashi K, Hayashi T, Morimoto Y 1999. Simultaneous transport and metabolism of ethyl nicotinate in hairless rat skin after its topical application: the effect of enzyme distribution in skin. J Control Release 62:201-208.

12. Scheuplein RJ, Blank IH 1971. Permeability of the skin. Physiol Rev 51:702-747.

13. Inoue M, Morikawa M, Tsuboi M, Ito Y, Sugiura M 1980. Comparative study of human intestinal and hepatic esterases as related to enzymatic properties and hydrolizing activity for ester-type drugs. Jpn J Pharmacol 30:529-535.

14. Prusakiewicz JJ, Ackermann C, Voorman R 2006. Comparison of skin esterase activities from different species. Pharm Res 23:1517-1524.

15. Fu J, Pacyniak E, Leed MG, Sadgrove MP, Marson L, Jay M 2015. Interspecies Differences in the Metabolism of a Multiester Prodrug by Carboxylesterases. J Pharm Sci .

16. Wang JJ, Sung KC, Huang JF, Yeh CH, Fang JY 2007. Ester prodrugs of morphine improve transdermal drug delivery: a mechanistic study. J Pharm Pharmacol 59:917-925.

17. Bencharit S, Morton CL, Howard-Williams EL, Danks MK, Potter PM, Redinbo MR 2002. Structural insights into CPT-11 activation by mammalian carboxylesterases. Nat Struct Biol 9:337-342.

18. Thomsen R, Rasmussen HB, Linnet K, INDICES Consortium 2014. In vitro drug metabolism by human carboxylesterase 1: focus on angiotensin-converting enzyme inhibitors. Drug Metab Dispos 42:126-133.

19. Satoh T, Taylor P, Bosron WF, Sanghani SP, Hosokawa M, La Du BN 2002. Current progress on esterases: from molecular structure to function. Drug Metab Dispos 30:488-493.

20. Zhu QG, Hu JH, Liu JY, Lu SW, Liu YX, Wang J 2007. Stereoselective characteristics and mechanisms of epidermal carboxylesterase metabolism observed in HaCaT keratinocytes. Biol Pharm Bull 30:532-536.

21. Zhang Y, Sadgrove MP, Sueda K, Yang YT, Pacyniak EK, Kagel JR, Braun BA, Zamboni WC, Mumper RJ, Jay M 2013. Nonaqueous gel for the transdermal delivery of a DTPA penta-ethyl ester prodrug. AAPS J 15:523-532.

22. Williams FM 2008. Potential for metabolism locally in the skin of dermally absorbed compounds. Hum Exp Toxicol 27:277-280.

23. Wadkins RM, Hyatt JL, Wei X, Yoon KJ, Wierdl M, Edwards CC, Morton CL, Obenauer JC, Damodaran K, Beroza P, Danks MK, Potter PM 2005. Identification and characterization of novel benzil (diphenylethane-1,2-dione) analogues as inhibitors of mammalian carboxylesterases. J Med Chem 48:2906-2915.

24. Fukami T, Takahashi S, Nakagawa N, Maruichi T, Nakajima M, Yokoi T 2010. In vitro evaluation of inhibitory effects of antidiabetic and antihyperlipidemic drugs on human carboxylesterase activities. Drug Metab Dispos 38:2173-2178.

25. Williams ET, Bacon JA, Bender DM, Lowinger JJ, Guo WK, Ehsani ME, Wang X, Wang H, Qian YW, Ruterbories KJ, Wrighton SA, Perkins EJ 2011. Characterization of the expression and activity of carboxylesterases 1 and 2 from the beagle dog, cynomolgus monkey, and human. Drug Metab Dispos 39:2305-2313.

26. Li P, Callery PS, Gan LS, Balani SK 2007. Esterase inhibition by grapefruit juice flavonoids leading to a new drug interaction. Drug Metab Dispos 35:1203-1208.

27. Tauber, U. R and Rost KL 1987. Esterase activity of the skin including species variations. Pharmacology and the Skin .

28. Hewitt NJ, Buhring KU, Dasenbrock J, Haunschild J, Ladstetter B, Utesch D 2001. Studies comparing in vivo:in vitro metabolism of three pharmaceutical compounds in rat, dog, monkey, and human using cryopreserved hepatocytes, microsomes, and collagen gel immobilized hepatocyte cultures. Drug Metab Dispos 29:1042-1050.

29. Jewell C, Prusakiewicz JJ, Ackermann C, Payne NA, Fate G, Williams FM 2007. The distribution of esterases in the skin of the minipig. Toxicol Lett 173:118-123.

30. Imai T, Takase Y, Iwase H, Hashimoto M 2013. Involvement of Carboxylesterase in Hydrolysis of Propranolol Prodrug during Permeation across Rat Skin. Pharmaceutics 5:371-384.

31. Pindel EV, Kedishvili NY, Abraham TL, Brzezinski MR, Zhang J, Dean RA, Bosron WF 1997. Purification and cloning of a broad substrate specificity human liver carboxylesterase that catalyzes the hydrolysis of cocaine and heroin. J Biol Chem 272:14769-14775.

32. Brzezinski MR, Abraham TL, Stone CL, Dean RA, Bosron WF 1994. Purification and characterization of a human liver cocaine carboxylesterase that catalyzes the production of benzoylecgonine and the formation of cocaethylene from alcohol and cocaine. Biochem Pharmacol 48:1747-1755.

33. Huckle JE, Sadgrove MP, Mumper RJ, Jay M 2015. Species-dependent chelation of (241)Am by DTPA Di-ethyl ester. Health Phys 108:443-450.

34. Huckle JE, Sadgrove MP, Pacyniak E, Leed MG, Weber WM, Doyle-Eisele M, Guilmette RA, Agha BJ, Susick RL, Mumper RJ, Jay M 2015. Orally administered DTPA di-ethyl ester for decorporation of (241)Am in dogs: Assessment of safety and efficacy in an inhalation-contamination model. Int J Radiat Biol 91:568-575.

35. Zhang Y, Sadgrove MP, Mumper RJ, Jay M 2013. Radionuclide decorporation: matching the biokinetics of actinides by transdermal delivery of pro-chelators. AAPS J 15:1180-1188.

36. Bahar FG, Imai T 2013. Aspirin hydrolysis in human and experimental animal plasma and the effect of metal cations on hydrolase activities. Drug Metab Dispos 41:1450-1456.

CHAPTER 4

THE EFFECT OF EXCIPIENTS ON CARBOXYLESTERASE-MEDIATED HYDROLYSIS OF A DTPA PRODRUG FOR TRANSDERMAL DELIVERY

4.1 Introduction

Pharmaceutical excipients are substances that preserve and support active drugs to retain their optimal biopharmaceutical activities during treatment. Excipients can serve in a variety of ways, including as manufacturing aids, stability enhancing agents and as coloring, taste masking and coating agents. Traditionally, excipients are inactive, exerting no effect on active drugs. However, an increasing number of reports have demonstrated that some excipient affect the ADME properties of active drug or increase the potential for patients to develop toxicities at higher excipient doses. For instance, Tween 80, an excipient in some amiodarone formulations, has been reported to cause hepatotoxicity and reduce the level of phase II metabolic enzyme, glutathione S-transferases [1]. Hydroxypropyl-beta-cyclodextrin causes transaminase to increase in rodents [2] . High doses of propylene glycol have been reported to cause cardiovascular abnormalities, renal failure and CNS changes [3]. Solubilizing agents appear to alter intestinal membrane barrier functions and cause damage to the intestinal epithelium, for example, sodium taurocholate (NaTC), Gelucire 44/14 and Cremophor EL [4]. Meanwhile, there is an increased interest in evaluating the effect of excipients on metabolic enzymes and drug transporters. Labrasol at low concentrations inhibits the function of the efflux transporter P-gp in the intestine and thus increases the intestinal absorption of P-gp substrates [5]. Polyethylene glycol (PEG) 400, HP-beta-CD, Solutol HS 15 (SOL), and Cremophor EL (EL 35) alter OATP biopharmaceutical

functionality [6]. Polyoxyl 35 castor oil, Tween 80, PEG400, and EL 35 can affect the activity of cytochrome P450 enzymes [7].

Interest in the development of transdermal drug delivery has been increasing because it is non-invasive, can be self-administered, avoids first-pass metabolism, and is well suited to special populations. Many drugs that are delivered via transdermal and topical routes require a specific category of excipients due to the unique anatomical structure of skin. Generally, excipients used in transdermal delivery are non-ionic or oil-based in order to make them easily miscible with formulations containing active pharmaceutical ingredients with oil/water partition coefficients between 10 and 1000. Excipients found in transdermal formulations include sodium dodecyl sulfate (SDS), Tweens, Spans, polyethylene glycol, povidone and others. Ester-based and amide-based drugs delivered by transdermal route are designed to be metabolized to the active drug by CESs, which are ubiquitous Phase I metabolic enzymes. CESs play a vital role in determining the metabolic paths for both xenobiotic and endogenous compounds. Currently, little is known about the effect of excipients used in transdermal delivery formulation on the activities of CESs in human.

We have developed a penta-ethyl ester prodrug of the chelating agent diethylene triamine penta-acetic acid (DTPA), referred to as C2E5 (Fig. 1), to enhance decorporation of transuranic radionuclides [8]. C2E5 is metabolized by CESs [9] and the physiochemical properties of C2E5 (CLogP of 4.7, 533 Da) suggest that it would be a good candidate for transdermal delivery. Evidence supporting transdermal application of C2E5 was reported in *in vivo* transdermal pharmacokinetics and efficacy studies [8]. Therefore, the objective of current work is to assess the effect of common excipients, on skin CES-mediated hydrolysis of C2E5.

Table 4.1. List of 12 excipients used in transdermal delivery.

	Application	**Name**
1	Nonaqueous gel for the transdermal delivery of a DTPA penta-ethyl ester prodrug [10]	Miglyol 840
2	The effect of Miglyol 812 oil on the oral absorption of propranolol in the rat [11]	Miglyol 812
3	Transdermal delivery of propranolol using mixed grades of Eudragit: design and in vitro and in vivo evaluation [12]	Eudragit RL PO
4		Eudragit RS PO
5	Effect of ethanolamine salts and enhancers on the percutaneous absorption of piroxicam from a pressure sensitive adhesive matrix[74]	Crodamol EO-LQ-(MH)
6	Formulation and evaluation of microemulsion system for transdermal delivery of nimodipine [13]	Capmul MCM
7	Ultra-fine self nanoemulsifying drug delivery system for transdermal delivery of meloxicam: dependency on the type of surfactants [14]	Capmul MCM EP

8	Novel nanoemulsion as vehicles for transdermal delivery of clozapine: in vitro and in vivo studies [15]	Captex 355
9	Development of a microemulsion formulation for antimicrobial SecA inhibitors [16]	Polyoxyethylene tridecyl ether
10	Effect of surfactants on the characteristics of fluconazole niosomes for enhanced cutaneous delivery [17]	Brij 72
11	The effect of excipients on the permeability of BCS Class III compounds and implications for biowaivers [18]	Sodium lauryl sulfate (SLS)
12	Status of surfactants as penetration enhancers in transdermal drug delivery [19]	Tween 20

4.2 Materials and Methods

Chemicals Diethylenetriaminepentaacetic acid pentaethyl ester (C2E5) was prepared using the Fischer esterification method by reacting DTPA with ethanol under reflux in the presence of a hydrochloric acid catalyst [20] Human skin S9 fractions were purchased from Celsis *In Vitro* Technologies (Baltimore, MD). Human liver S9 fractions were purchased from Xenotech LLC (Lenexa, KS). Absolute ethanol and acetonitrile were purchased from Acros Organics (NJ). Miglyol 840 and 812, (Sasol, Hamburg, Germany), Eudragit RL PO and Eudragit RS PO (Evonik-*Degussa* GmbH, Darmstadt, Germany), Crodamol EO-LQ-(MH) (Croda Inc, Edison, NJ), Capmul MCM, Capmul MCM EP, Captex 355(Abitec Corporation, Columbus, Ohio, US), Polyoxyethylene tridecyl ether (Sigma-Aldrich, St. Louis, Missouri), SLS (Fisher scientific, NJ) and Tween 20 (Sigma-Aldrich, St. Louis, Missouri) were purchased.

Sample Preparation for Human Skin S9 fractions-Mediated C2E5 Hydrolysis with and without excipients. Experiments were designed to examine the effect of excipients on C2E5 hydrolysis in human skin S9 fractions. The excipients analyzed are listed in the Table1. Excipients at various concentrations (0, 0.1, 1, 10 and 100 μg/ml) were incubated with human skin S9 fractions for 30 min at 37°C before the reaction was initiated. All reactions were initiated by the addition of S9 fractions (0.5 and 1 mg/ml) to prepared aqueous solutions of C2E5 with a final C2E5 concentration of 0.5 μM at 37°C. Reactions were terminated after 120 min by adding an equal volume of ice-cold acetonitrile with 2% of formic acid, followed by centrifugation at 14,000 *g* for 15 min at 4°C. Liver S9 fractions (1 mg/ml) were used as a positive control; boiled S9 fractions were used as negative controls. All reactions were performed in triplicate. The

standards used to generate the LC/MS/MS C2E5 calibration curve were prepared by spiking boiled S9 fractions with C2E5 and processing as described above.

LC/MS/MS Chromatographic and Spectroscopic Conditions. Chromatographic separation from matrix components was achieved using reverse-phase chromatography on an YMC ODS-AM C18 (100 x 2 mm, 3 μm) column. Gradient elution was used based on a combination of water with 0.1% formic acid (A) and acetonitrile with 0.1% formic acid (B). The mobile phase was initiated at 13% B increasing to 40% B by 1 min, to 60% B by 6 min and to 95% B by 6.2 min. The mobile phase was held at 5% A and 95% B from 6.2 min to 6.5 min when a post-run cycle that included isopropyl alcohol (C) was initiated. Between 6.5 min and 7 min solvent B (95%) was gradually replaced with solvent C (95%). The mobile phase was then held at 5% A 95% C until 7.5 min before gradually returning to initial conditions (87% A, 13% B, 0% C) after 8.5 min, which were maintained for 1.5 min prior to the next injection. The flow rate was 300 μl/min and the injection volume was 5 μl. The column oven temperature was set to 40°C. C2E5 was detected on a triplequadrupole mass spectrometer (Thermo TSQ Quantum Access) using electrospray ionization (ESI) in the positive-ion mode. The ionization source and collision parameters were optimized to give maximum analyte signal intensity (Spray Voltage 3500V; Sheath and Auxiliary gas nitrogen, 10 and 25 psi, respectively; Collision gas Argon @ 1.5 mTorr; Collision energy 35 eV). The mass spectrometer was set to carry out single reaction monitoring (SRM) for the precursor → product ion transitions m/z 534 → 216 (C2E5) and m/z 506 → 188 (C2E4) at a retention times of 3.6 and 2.8 min, respectively. For C2E5 quantification, a calibration plot of analyte peak area against nominal C2E5 concentration (20 – 1000 ng/ml) was constructed from a quadratic equation with a $1/\text{concentration}^2$ weighting.

Data analysis. The data were processed by Graph Pad Prism 5.0, and are presented as mean ± SEM.

4.3 Results

To compare the inhibitory effects of the excipients on human skin S9 fraction-mediated hydrolysis of C2E5, the loss of parent drug C2E5 was assessed by LC/MS/MS analysis (Fig. 4.1-4.7). The evaluated concentrations of the test excipients were 0.1, 1, 10, and 100 μg/ml. The data produced from human skin S9 fraction-mediated C2E5 hydrolysis without the presence of any excipients were used as negative controls and they were set as 100%. Therefore, any samples generated with the pre-incubation of the excipients were measured and compared with this control.

SLS and Tween 20 were reported to have inhibitory effect on CESs by PNPA assays [21], therefore, we used 100 μg/ml of SLS and Tween 20 as positive control for this study. This means that it is expected to see reduction in percent of loss of C2E5 (hydrolysis) from the samples that were pre-incubated with SLS and Tween 20. Preferably, those inhibition patterns from SLS and Tween 20 should exhibit in a concentration-dependent manner.

Inhibition of C2E5 metabolisms were measured and quantified. The data displayed (Fig 4.1-4.7) were produced by normalization of the relative reduction of the hydrolyzed C2E5 to negative controls that were defined in the first paragraph. The samples with pre-incubation of Miglyol 840 (100 μg/ml), Eudragit RLPO (100 μg/ml), Crodamol EO-LQ-(MH) (100 μg/ml) and Brij 72 (100 μg/ml) as well as SLS (100 μg/ml) and Tween (100 μg/ml) indicated remarkable inhibitions of C2E5 hydrolysis. For example, only 49.12% of the loss of C2E5 occurred in sample that was pre-incubated with Miglyol 840 (100 μg/ml) in contrast to 100% of

the loss of C2E5 occurred in samples without pre-incubation of Miglyol 840. However, Miglyol 840 (0.1-10 μg/ml) did not exhibit significant inhibitory effect. Miglyol 812 (100 μg/ml) inhibited the enzyme-mediated hydrolysis moderately (Fig 4.2). Among all the excipients, SLS and Tween 20 inhibited the C2E5 hydrolysis the most (Fig 4.7). Eudragit RLPO (0.1-100 μg/ml) showed slightly inhibitory effects on C2E5 hydrolysis. On the contrary, Eudragit RSPO (0.1-100 μg/ml) stimulated C2E5 hydrolysis by 2.5-fold to controls (without excipients). The remaining excipients had a negligible effect.

4.4 Discussion

This study focused on the effects of individual excipients on human skin S9 fraction-mediated C2E5 hydrolysis. An LC/MS/MS method was developed and validated to measure human skin S9 fraction-mediated prodrug C2E5 hydrolysis in the absence and presence of excipients. This approach allowed for rapid and sensitive assessment to both controls and test samples. The effects of all excipients were measured *in vitro* using human skin S9 fractions.

The findings provide initial safety information of excipients used in the transdermal delivery formulations, particularly for multiester-based prodrugs. Miglyol 840 and 812 are used not only in transdermal delivery, but also in topical and intramuscular formulations [10]. The fact that they exert inhibitory effects on ester hydrolysis at concentrations of 100 μg/ml might help to explain the compromised drug actions of ester-based prodrugs. From this study, it is suggested that, among the excipients analyzed, Capmul MCM, Capmul MCM EP, Captex 335 and polyoxyethylene tridecyl ether are appropriate excipients for transdermal formulations of multiester-based prodrug. The others can be used for transdermal formulation at concentration less than 100 μg/ml.

The inhibitions of skin metabolic enzymes caused by these excipients are not necessarily concentration-dependent inhibitions. This might be attributed to the denaturation and precipitation of the proteins or enzymes in human skin S9 fractions. This caused them to lose their 3-dimensional structures and become incapable of metabolizing C2E5.

In contrast to all the other test excipients, Eudragit RSPO increased the hydrolysis of C2E5. Usually multiple excipients are employed in transdermal formulations. However, this

study did not investigate the synergistic effects of combinations of excipients, therefore, the studies on these effects could become the future directions.

Currently, studies on cutaneous metabolism are limited to the knowledge on using the appropriate model for evaluating biotransformation in transdermal delivery. Usually, pig skin or rat skin is used to evaluate the permeability, metabolism and absorption of drugs [22, 23]. However, it is also known that species-differences do exist among those models [24]. The data generated from those animal models should be extrapolated carefully to human. Therefore, the use of human skin S9 fractions is a rational approach to assess drug metabolism in human skin. Previous chapters of this dissertation describe the characterization of CES-mediated hydrolysis of C2E5 in human skin S9 fractions. However, certain limitations of using human skin S9 fractions still need to be addressed, such as batch-to-batch differences in human S9 fractions, collected from different patients and genetic polymorphisms that could alter the activity of CESs in the skin, which could lead to differences in the skin S9 fraction-mediated hydrolysis.

Broadly speaking, these findings also have important clinical implications. Individuals with CESs polymorphisms that produce a poor CESs phenotype may be at increased risk of experiencing drug interactions that involve with CESs substrates and inhibitors. However, when this is applied to C2E5 transdermal delivery, it is unlikely to cause drug-drug interactions as long as the co-administered drugs do not pass through skin. Miglyol 840, Miglyol 812, Eudragit RLPO, and Crodamol EO-LQ- (MH) affect ester-based prodrug hydrolysis in the skin because of their delivery sites, suggesting that they do not affect the ADME properties of co-administered drugs from other routes.

In summary, the effect of twelve excipients used in transdermal formulations on the hydrolysis of C2E5 was investigated. Human skin S9 fractions were used to study cutaneous metabolism. Within the tested concentration range, Miglyol 840, Eudragit RLPO, Cromdamol EO-LQ- (MH), Brij 72 showed inhibitory effect at 100 µg/ml. Zhang's reported that SLS and Tween 20 can inhibit CESs activity, evaluated by PNPA assay [21]. In our study, SLS and Tween 20 also inhibit CES-mediated prodrug C2E5 hydrolysis at a concentration of 100 µg/ml. In contrast, Eudragit RSPO (0.1-100 µg/ml) increased the C2E5 hydrolysis. The remaining excipients had smallest effect. This study initiates the safety concerns for excipients used in transdermal delivery and emphasizes the importance of selecting appropriate surfactants for multiester-based prodrugs.

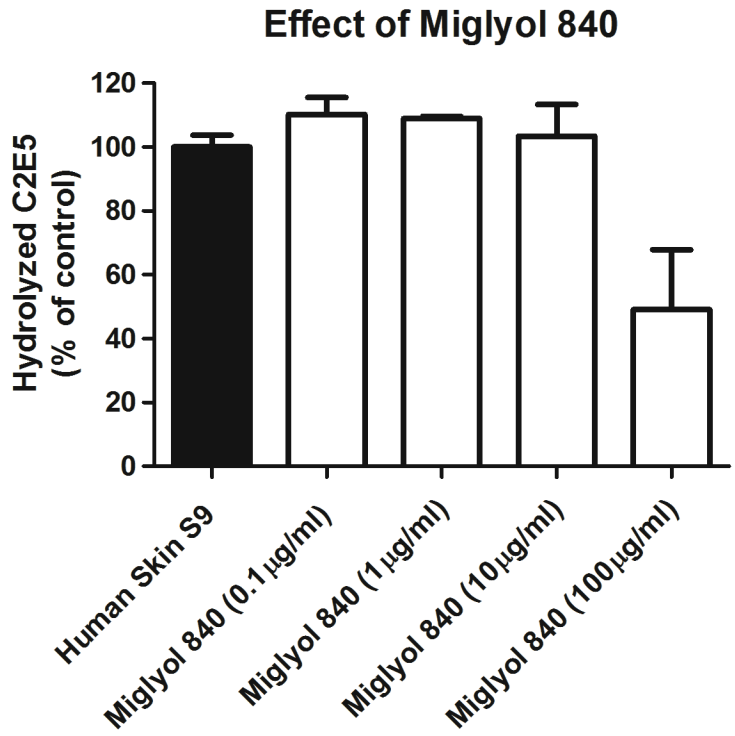

Figure 4.1. The effects of Miglyol 840 at various concentrations (0, 0.1, 1, 10 and 100 µg/ml) on the hydrolysis of C2E5 in human skin S9 fractions. Miglyol 840 were incubated with human skin S9 fractions for 30 min at 37°C before the reaction was initiated. Loss of parent drug was measured by detecting changes in spectromatogram at the LC/MS/MS analyte peak (3.6 min) after 120 mins incubation of 0.5 µM C2E5 with human skin S9 fractions with and without Miglyol 840. Values represent mean ± SEM (n=3).

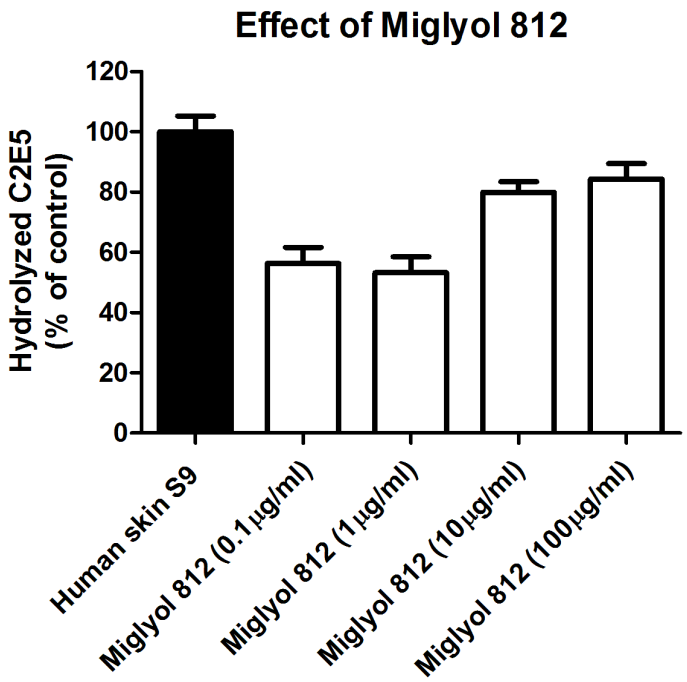

Figure 4.2. The effects of Miglyol 812 at various concentrations (0, 0.1, 1, 10 and 100 μg/ml) on the hydrolysis of C2E5 in human skin S9 fractions. Miglyol 812 were incubated with human skin S9 fractions for 30 min at 37°C before the reaction was initiated. Loss of parent drug was measured by detecting changes in spectromatogram at the LC/MS/MS analyte peak (3.6 min) after 120 mins incubation of 0.5 μM C2E5 with human skin S9 fractions with and without Miglyol 812. Values represent mean ± SEM (n=3).

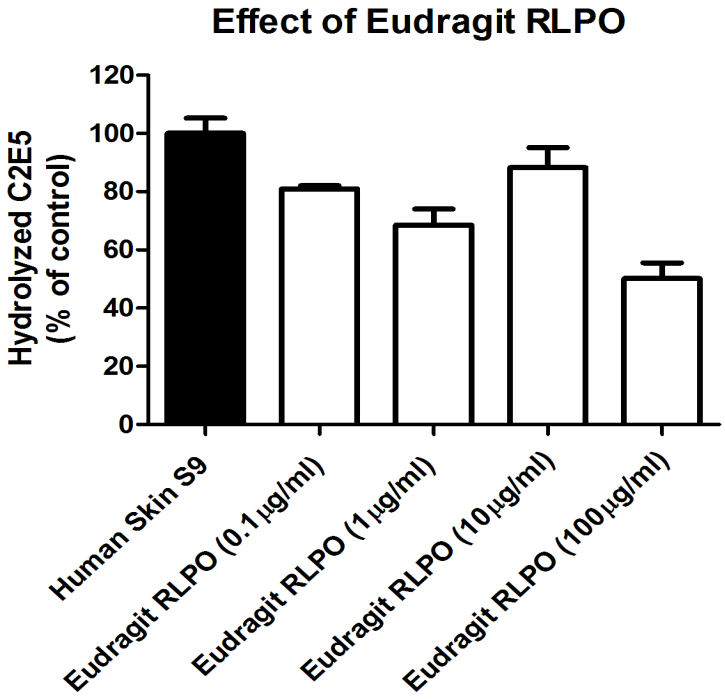

Figure 4.3. The effects of Eudragit RLPO at various concentrations (0, 0.1, 1, 10 and 100 μg/ml) on the hydrolysis of C2E5 in human skin S9 fractions. Endragit RLPO were incubated with human skin S9 fractions for 30 min at 37°C before the reaction was initiated. Loss of parent drug was measured by detecting changes in spectromatogram at the LC/MS/MS analyte peak (3.6 min) after 120 mins incubation of 0.5 μM C2E5 with human skin S9 fractions with and without Eudragit RLPO. Values represent mean ± SEM (n=3).

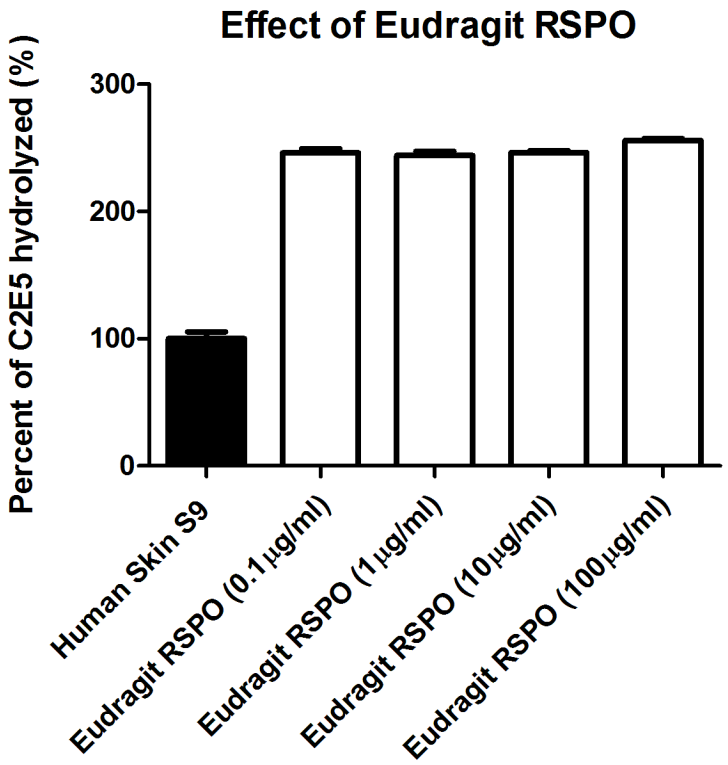

Figure 4.4. The effects of Eudragit RSPO at various concentrations (0, 0.1, 1, 10 and 100 µg/ml) on the hydrolysis of C2E5 in human skin S9 fractions. Endragit RSPO were incubated with human skin S9 fractions for 30 min at 37°C before the reaction was initiated. Loss of parent drug was measured by detecting changes in spectromatogram at the LC/MS/MS analyte peak (3.6 min) after 120 mins incubation of 0.5 µM C2E5 with human skin S9 fractions with and without Eudragit RSPO. Values represent mean ± SEM (n=3).

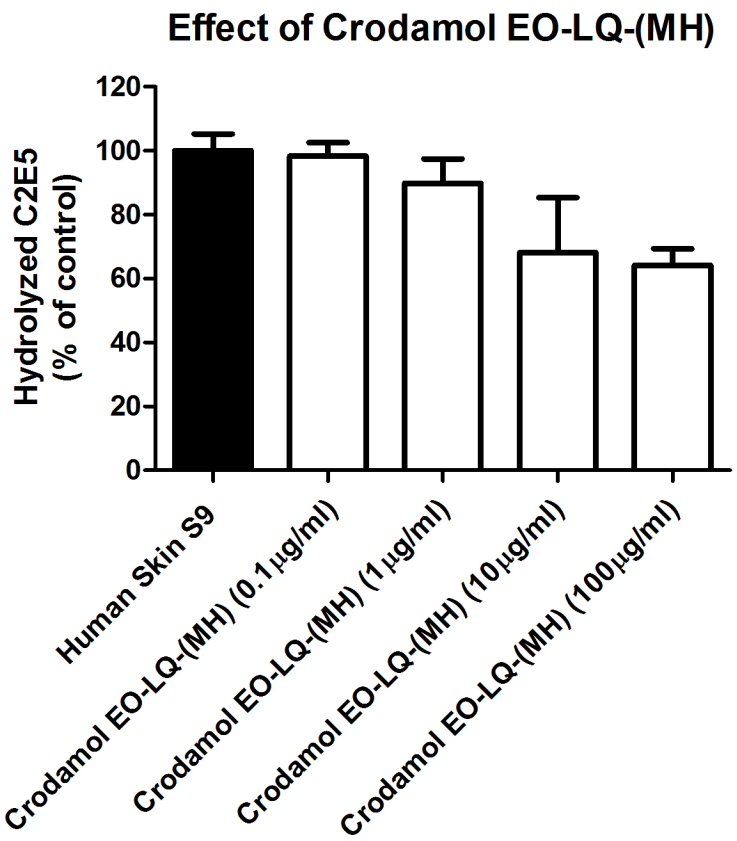

Figure 4.5. The effects of Crodamol EO-LQ-(MH) at various concentrations (0, 0.1, 1, 10 and 100 µg/ml) on the hydrolysis of C2E5 in human skin S9 fractions. Crodamol EO-LQ-(MH) were incubated with human skin S9 fractions for 30 min at 37°C before the reaction was initiated. Loss of parent drug was measured by detecting changes in spectromatogram at the LC/MS/MS analyte peak (3.6 min) after 120 mins incubation of 0.5 µM C2E5 with human skin S9 fractions with and without Crodamol EO-LQ-(MH). Values represent mean ± SEM (n=3).

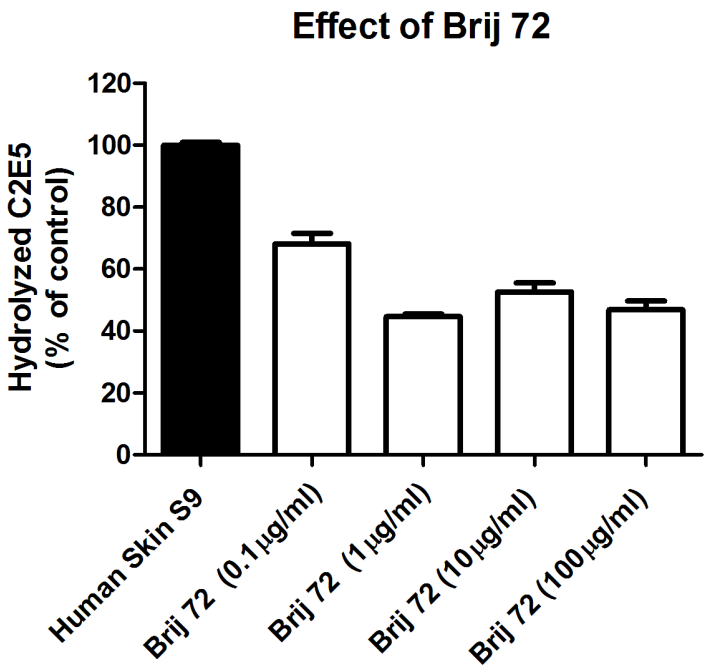

Figure 4.6. The effects of Brij 72 at various concentrations (0, 0.1, 1, 10 and 100 μg/ml) on the hydrolysis of C2E5 in human skin S9 fractions. Brij 72 were incubated with human skin S9 fractions for 30 min at 37°C before the reaction was initiated. Loss of parent drug was measured by detecting changes in spectromatogram at the LC/MS/MS analyte peak (3.6 min) after 120 mins incubation of 0.5 μM C2E5 with human skin S9 fractions with and without Brij 72. Values represent mean ± SEM (n=3).

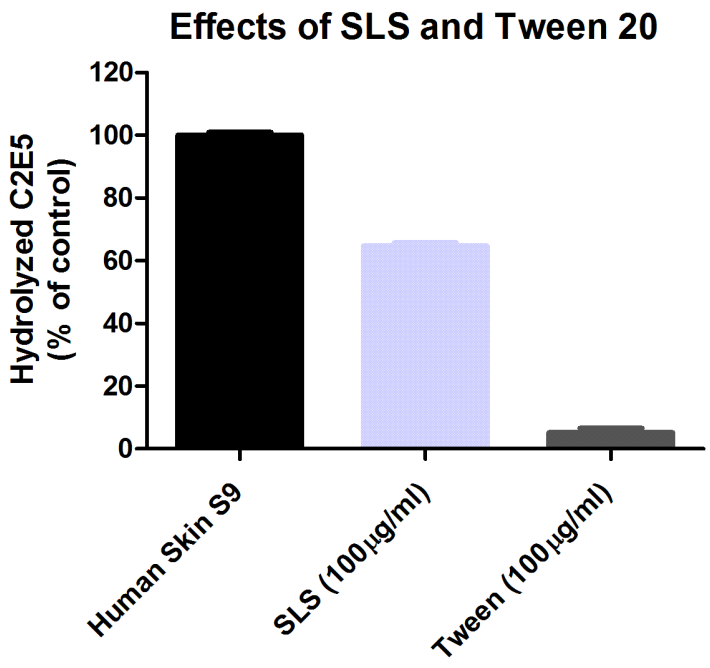

Figure 4.7. The effects of SLS and Tween 20 at various concentrations (100 µg/ml) on the hydrolysis of C2E5 in human skin S9 fractions. SLS and Tween 20 were incubated with human skin S9 fractions for 30 min at 37°C before the reaction was initiated, respectively. Loss of parent drug was measured by detecting changes in spectromatogram at the LC/MS/MS analyte peak (3.6 min) after 120 mins incubation of 0.5 µM C2E5 with human skin S9 fractions with and without SLS or Tween 20. Values represent mean ± SEM (n=3).

REFERENCES

1. Hirama S, Tatsuishi T, Iwase K, Nakao H, Umebayashi C, Nishizaki Y, Kobayashi M, Ishida S, Okano Y, Oyama Y 2004. Flow-cytometric analysis on adverse effects of polysorbate 80 in rat thymocytes. Toxicology 199:137-143.

2. Thackaberry EA, Kopytek S, Sherratt P, Trouba K, McIntyre B 2010. Comprehensive investigation of hydroxypropyl methylcellulose, propylene glycol, polysorbate 80, and hydroxypropyl-beta-cyclodextrin for use in general toxicology studies. Toxicol Sci 117:485-492.

3. Nahata MC 2009. Safety of "inert" additives or excipients in paediatric medicines. Arch Dis Child Fetal Neonatal Ed 94:F392-3.

4. Hamid KA, Katsumi H, Sakane T, Yamamoto A 2009. The effects of common solubilizing agents on the intestinal membrane barrier functions and membrane toxicity in rats. Int J Pharm 379:100-108.

5. Lin Y, Shen Q, Katsumi H, Okada N, Fujita T, Jiang X, Yamamoto A 2007. Effects of Labrasol and other pharmaceutical excipients on the intestinal transport and absorption of rhodamine123, a P-glycoprotein substrate, in rats. Biol Pharm Bull 30:1301-1307.

6. Engel A, Oswald S, Siegmund W, Keiser M 2012. Pharmaceutical excipients influence the function of human uptake transporting proteins. Mol Pharm 9:2577-2581.

7. Ren X, Mao X, Cao L, Xue K, Si L, Qiu J, Schimmer AD, Li G 2009. Nonionic surfactants are strong inhibitors of cytochrome P450 3A biotransformation activity in vitro and in vivo. Eur J Pharm Sci 36:401-411.

8. Zhang Y, Sadgrove MP, Mumper RJ, Jay M 2013. Radionuclide decorporation: matching the biokinetics of actinides by transdermal delivery of pro-chelators. AAPS J 15:1180-1188.

9. Fu J, Pacyniak E, Leed MG, Sadgrove MP, Marson L, Jay M 2015. Interspecies Differences in the Metabolism of a Multiester Prodrug by Carboxylesterases. J Pharm Sci .

10. Zhang Y, Sadgrove MP, Sueda K, Yang YT, Pacyniak EK, Kagel JR, Braun BA, Zamboni WC, Mumper RJ, Jay M 2013. Nonaqueous gel for the transdermal delivery of a DTPA penta-ethyl ester prodrug. AAPS J 15:523-532.

11. Woolfrey SG, Palin KJ, Davis SS 1989. The effect of Miglycol 812 oil on the oral absorption of propranolol in the rat. J Pharm Pharmacol 41:579-581.

12. Verma PR, Iyer SS 2000. Transdermal delivery of propranolol using mixed grades of Eudragit: design and in vitro and in vivo evaluation. Drug Dev Ind Pharm 26:471-476.

13. Prashant Khade, Ganesh Chailang, Gurauraj Shahabade, Sujit Kakade, Sachin kotwal 2014. Formulation and evaluation of microemulsion system for transdermal delivery of nimodipine. World Journal of Pharmaceutical Sciences 2:988-996.

14. Mohamed M. Badrana, b, Ehab I. Tahaa, b, Moustafa M. Tayela, Saleh A. Al-Suwayeh 2014. Ultra-fine self nanoemulsifying drug delivery system for transdermal delivery of meloxicam: Dependency on the type of surfactants. Journal of Molecular Liquids 190:16-22.

15. Kausar Shafaat , Brajesh Kumar , Sreemoy Kanti das , Rizwan ul hasa s. k. Pajapati 2013. Novel nanoemulsion as vehicles for transdermal delivery of clozapine: in vitro and in vivo studies. International Journal of Pharmacy and Pharmaceutical Sciences 5.

16. Hu J, Akula N, Wang N 2016. Development of a Microemulsion Formulation for Antimicrobial SecA Inhibitors. PLoS One 11:e0150433.

17. Gupta M, Vaidya B, Mishra N, Vyas SP 2011. Effect of surfactants on the characteristics of fluconazole niosomes for enhanced cutaneous delivery. Artif Cells Blood Substit Immobil Biotechnol 39:376-384.

18. Parr A, Hidalgo IJ, Bode C, Brown W, Yazdanian M, Gonzalez MA, Sagawa K, Miller K, Jiang W, Stippler ES 2016. The Effect of Excipients on the Permeability of BCS Class III Compounds and Implications for Biowaivers. Pharm Res 33:167-176.

19. Som I, Bhatia K, Yasir M 2012. Status of surfactants as penetration enhancers in transdermal drug delivery. J Pharm Bioallied Sci 4:2-9.

20. Sueda K, Sadgrove MP, Fitzsimmons JM, Jay M 2012. Physicochemical characterization of a prodrug of a radionuclide decorporation agent for oral delivery. J Pharm Sci 101:2844-2853.

21. Zhang C, Xu Y, Zhong Q, Li X, Gao P, Feng C, Chu Q, Chen Y, Liu D 2014. In vitro evaluation of the inhibitory potential of pharmaceutical excipients on human carboxylesterase 1A and 2. PLoS One 9:e93819.

22. Jewell C, Prusakiewicz JJ, Ackermann C, Payne NA, Fate G, Williams FM 2007. The distribution of esterases in the skin of the minipig. Toxicol Lett 173:118-123.

23. Barbero AM, Frasch HF 2009. Pig and guinea pig skin as surrogates for human in vitro penetration studies: a quantitative review. Toxicol In Vitro 23:1-13.

24. Martignoni M, Groothuis GM, de Kanter R 2006. Species differences between mouse, rat, dog, monkey and human CYP-mediated drug metabolism, inhibition and induction. Expert Opin Drug Metab Toxicol 2:875-894.

CHAPTER 5

GENERAL DISCUSSIONS AND CONCLUSIONS

The studies undertaken in this dissertation project have focused on deciphering the role of CESs in the metabolism of C2E5, a penta-ethyl ester prodrug for DTPA, to provide information for the development of C2E5 as a formulation for oral and transdermal deliveries. The findings on the metabolic mechanism of C2E5 provide important insights into prodrug formulation strategies, and establish a model for future possible multi-ester or amide-based prodrug development.

Studies reported in chapter 2 demonstrated that C2E5 is hydrolyzed in the liver, intestine, and plasma of humans, dog and rat, and that the metabolic profiles of C2E5 are different among humans, dog and rat. The major metabolites of prodrug C2E5 in humans and dog are C2E4 as opposed to C2E2 in rat. Differences in the expression of CESs isoforms among the three species contribute to differences in C2E5 metabolism. Dog is a better predictive model for C2E5 metabolism in humans, whereas the rat is important for understanding the potential toxicity of C2E5 metabolites. These findings clearly suggest that laboratory animal models (*e.g.*, rodents, dogs) may not always be suitable for prediction of ADME profiles of prodrugs in humans. This information led us to confine further analysis of C2E5 metabolism to only human tissues.

In humans, C2E5 was metabolized to the greatest extent in the liver, with a greater contribution by CES1 to C2E5 metabolism, compared to CES2. Therefore, it is

likely that the rapid conversion of C2E5 to its metabolites in the liver is due to higher hepatic CES1 expression. Based on the chemical structure of C2E5 and the high expression of hepatic CESs, it was expected that C2E5 would be extensively metabolized to DTPA in the liver, indicating that oral delivery would be advantageous to C2E5 prodrug formulation strategy. Moreover, the fact that C2E5 was converted to C2E2, an active chelator, provides evidence of an effective prodrug design.

CESs play an important role in metabolizing endogenous and xenobiotic compounds for detoxification. CES isoforms 1b, 1c and 2, expressed in the liver and intestine, are responsible for C2E5 hydrolysis. Both CES1 and CES 2 are important for metabolism of the prodrug C2E5, and CES1 metabolizes C2E5 slightly more readily than CES2. This is likely due to the fact that the smaller and shorter chain of ethyl-esters in C2E5 cause it to preferably fit the cavity of the CES1 enzyme.

The data from chapter 3 reports the characterization of gene and protein expression of CES isoforms in multiple human skin cell lines and human skin tissue. This study confirmed that CESs are present as metabolic enzymes in the keratinocytes. Although these enzymes are expressed at lower levels in the skin than in the liver, specifically CES2 compared to CES1, the capacities of CESs for xenobiotic metabolism in the keratinocyte cell lines analyzed in this study are substantial. Because these keratinocyte cell lines are comparable to that of human skin, they can be used as alternative models for cutaneous metabolism studies in transdermal drug delivery. Overall, the data presented in chapter 3 provide evidence that metabolic enzymes in the skin enhanced transdermal delivery of C2E5 *in vitro.*

Studies reported in chapter 3 demonstrated that CES1 in human skin S9 fractions readily metabolizes C2E5, and corroborate data in chapter 2 that demonstrated that C2E5 is a preferable substrate for the human recombinant CES1.

Since biotransformation of C2E5 in transdermal delivery would commence as soon as it enters skin cells, patients affected by idiosyncratic alterations in CES1 cutaneous expression may demonstrate variability in the absorption of C2E5. The higher expression of CES1 in human skin would result in a faster conversion of C2E5 into C2E4, a charged molecule, which potentially diffuses into the systemic circulation more readily than C2E5 due to its physiochemical properties. Once C2E4 and unchanged C2E5 reach the system circulation, a majority of the C2E5 would be metabolized in the liver, and to some extent in the intestine; this pathway is supported by results reported in Chapter 2. Studies described in chapters 2 and 3 collectively demonstrated this C2E5 transdermal delivery metabolic pathway (Fig 5.1). Compared to the hepatic and intestinal metabolism of C2E5, human skin metabolism of this prodrug is less efficient. However, since the transdermal delivery route would bypass first-pass metabolism, it suggests that the skin would be the first metabolic organ, as well as a reservoir that controls drug release, and therefore, would affect the absorption and subsequent fate of the drug.

Although this is not the first study to characterize CESs in human skin, it is the first study to relate gene expression, protein expression and enzyme activities in each of the four human keratinocyte cell lines and skin tissue. The relatively higher gene expression of CES2 compared to CES1 in the different cell lines is consistent with protein expression. Nevertheless, certain factors such as cell passage number; cell culture conditions and the origin of the donor cells could influence the expression and activities of CESs.

Chapter 3 provides evidence that CESs in human skin are advantageous to C2E5 transdermal delivery; therefore, it is important to study the effect of excipients commonly used in transdermal formulations on C2E5 hydrolysis (reported in chapter 4). Since different CESs isoforms show differences in substrate recognition that can lead to dramatic interspecies differences in enzyme activity in the skin, the effect of the transdermal excipients evaluated in human skin S9 fractions would more accurately relate to their *in vivo* behavior in humans. Results from this experiment clearly show that some of the transdermal excipients act as modulators of enzyme-excipient interactions, which is likely due to excipient-induced conformational change in the metabolic enzymes in human skin S9 fractions.

CESs, the most important members of the esterase family, work to catalyze reactions with their Ser-His-Glu triads (catalytic domain) [1]. The hydrophobic chains form non-ionic excipients that could interfere with the catalytic domains of the CESs, thus impeding CES-mediated hydrolysis of C2E5.

The effect of excipients on CES-mediated hydrolysis of C2E5 in human skin S9 fractions (reported in chapter 4) could also be determined using an alternative approach that evaluates excipient-drug interactions *in silico*. Evidence from protein formulation research showed that protein-excipient interactions affect the stability of protein medicine or other macromolecule drug [2]. It proposed that key mechanisms of protein-excipient interactions are related to electrostatic interactions, preferential hydration, dispersive forces, and hydrogen bonding in the context of different physical states of the formulation.

On the other hand, current research by other investigators also employs *in silico* molecular simulation of excipients, in combination with drugs, to predict the selection of the most suitable excipients for transdermal drug delivery [3].For example, human skin in Franz

Diffusion cell system [4] was used to predict the effect of impurities in topical formulations. The study results have ranked the impurity risk priority of 20 excipients. The mathematical quantifications are a rapid tool to provide a general concept of excipient safety, which is mandated by Good Manufacturing Practice (GMP) guidelines for dermal excipients. However, those types of approaches have their own advantages and limitations compared to our *in vitro* methods. Although computational studies quantitatively estimate the mechanism of excipient-protein interactions, those theoretical data cannot fully describe the biological environment at the cellular level. On the contrary, human keratinocyte cell lines are derived from human skin and are representative of human skin tissue; therefore, data obtained from using human skin cell lines provide valuable insights into CES-mediated metabolism of drugs delivered transdermally in humans. A combination of our experimental results with computational modeling to elucidate excipient and enzyme interactions would be a good strategy.

Most transdermal delivery excipients are surfactants that are generally used in protein formulations to inhibit protein aggregation caused by agitation or shaking. However, studies have shown that non-ion surfactants could directly interact with hydrophobic regions in protein-based drugs, which raises the concern that the excipients could act as competitive inhibitors of protein adsorption or protein surface denaturation which could occur in a concentration-dependent manner [5, 6]. Some excipients could contain peroxides, which can oxidize proteins, while others could be degraded by either oxidation or hydrolysis, which affects protein or enzyme stability.

In summary, this dissertation highlights the interspecies differences in CES isoforms that catalyze penta-ethyl ester prodrug, resulting in differences in the pharmacokinetics of C2E5. It also provides an explanation for how differences in the structure and activities of CES1 and

CES2 contribute to dissimilarities in their metabolism of DTPA prodrugs. This information is useful for future DTPA prochelator drug design. This work also describes the metabolic path involved in the sustained release of C2E5 by non-aqueous gel transdermal delivery. As the first investigation of CES expression in human keratinocyte cell lines and skin tissue, it also clearly demonstrates that CES1 in the skin metabolizes transdermally delivered C2E5. Lastly, the common excipients used in transdermal delivery had varying effects on CES-mediated C2E5 hydrolysis, underscoring the importance of selecting appropriate excipients in future formulations.

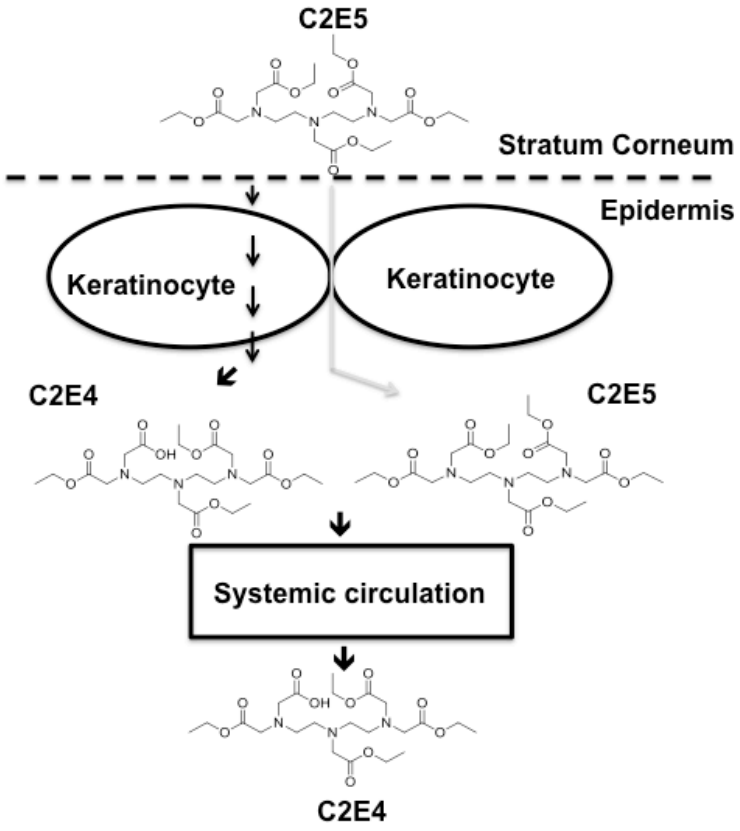

Figure 5.1. Proposed biotransformation pathway for C2E5 during transdermal delivery. C2E5 crosses the stratum corneum, and can passively diffuse into keratinocytes. Metabolism of C2E5 by CESs in keratinocytes results in the formation of metabolite C2E4 that are more hydrophilic than C2E5. Meanwhile, it is unlikely that C2E5 will go through the paracellular route because it is large in size to pass through the intercellular space. Metabolites and unchanged C2E5 eventually reach the systemic circulation and are totally converted to C2E4 in the liver and other metabolizing tissues.

REFERENCES

1. Bencharit S, Morton CL, Xue Y, Potter PM, Redinbo MR 2003. Structural basis of heroin and cocaine metabolism by a promiscuous human drug-processing enzyme. Nat Struct Biol 10:349-356.

2. Kamerzell TJ, Esfandiary R, Joshi SB, Middaugh CR, Volkin DB 2011. Protein-excipient interactions: mechanisms and biophysical characterization applied to protein formulation development. Adv Drug Deliv Rev 63:1118-1159.

3. Martinez L, Betz G, Villalobos R, Melgoza L, Young PM 2013. Correlation between compactibility values and excipient cluster size using an in silico approach. Drug Dev Ind Pharm 39:374-381.

4. Baert B, Boonen J, Burvenich C, Roche N, Stillaert F, Blondeel P, Van Boxclaer J, De Spiegeleer B 2010. A new discriminative criterion for the development of Franz diffusion tests for transdermal pharmaceuticals. J Pharm Pharm Sci 13:218-230.

5. Deechongkit S, Wen J, Narhi LO, Jiang Y, Park SS, Kim J, Kerwin BA 2009. Physical and biophysical effects of polysorbate 20 and 80 on darbepoetin alfa. J Pharm Sci 98:3200-3217.

6. Randolph TW, Jones LS 2002. Surfactant-protein interactions. Pharm Biotechnol 13:159-175.

CHAPTER 6

FUTURE DIRECTIONS

In this study, we found that the interspecies differences in prodrug C2E5 metabolism are likely due to differences in CES isoform expression profiles among different species. However, currently, knowledge on CES characterization in different species is limited. Although studies have suggested similarities in rat and pig CES to that of humans, some of the protein crystal structures of CES isoforms in the different species have not been crystalized. Protein crystal structures provide important information that is useful for simulations and docking experiments. In studies reported in the following appendices, we attempted to dock human CES1 with C2E5 metabolites by selecting human CES crystal structure published in the National Center for Biotechnology Institute database. However, these studies (in the appendices) only generated results that describe how human CES interacts with C2E5. Therefore, a future direction would be to explore interspecies differences at the molecular level by docking human, rat and dog CESs with C2E5 to examine enzyme-drug interactions and elucidate mechanisms of interspecies differences.

In addition, we also have found that human skin cell lines could be used as alternative models for elucidating cutaneous metabolism of drugs that are transdermally delivered in humans. Although we utilized keratinocytes isolated from the complex anatomy of the skin to characterize its cellular metabolic function, other epidermal cell types, such as fibroblasts, were not included in these studies, as this was beyond the scope of this dissertation project.

Although cell lines are simple tools for assessing cutaneous metabolism, they cannot demonstrate the effect of physiological features of skin tissue on drug metabolism and absorption. For example, the abundance of blood vessels, types of appendages such as hair follicles and sebaceous glands, and Langerhans cells could alter the absorption pathway of drugs by transdermal delivery. Therefore, a 3-dimensional cell model could be utilized to assess the impact of physiological factors on C2E5 hydrolysis.

The effect of excipients on prodrug C2E5 hydrolysis, determined in this study using an *in vitro* model, emphasizes safety issues associated with excipients used in transdermal delivery. The *in vitro* study serves as a rapid tool to assess excipient-enzyme interactions; however, data obtained from these *in vitro* experiments cannot be easily extrapolated to the whole body. Therefore, a possible study in the future would be to conduct clinical studies to investigate the combined effect of multiple excipients used in transdermal formulations.

APPENDIX A: HUMAN CARBOXYLESTERASES TRANSFECTION

Introduction

Bacterial transformation is the process of introducing foreign DNA into the competent bacteria. Foreign DNA usually is incorporated by a plasmid vector, which can introduce a gene fragment to the host bacteria easily. Plasmid DNA is usually short, easily replicated, and have an independent circular chromosome with an origin of replications. Replication origin is a particular sequence in a genome at which replication is initiated. As a result, they are used widely as gene vectors. Plasmid chromosome replicates independently from the bacteria chromosome, and can be easily separated from the bacteria chromosome. Plasmid vector carriers a negative charge and the surfaces of the bacteria membrane also are negatively charged, therefore, plasmid vector and bacteria cells repulse each other under natural conditions. In order to insert the plasmid vector to the bacterial cells, calcium phosphate methods, electroporation, and heat shock methods could be applied.

In order to test the transfection efficiency, certain reporter protein can be co-transfected as an indicator. It is also well known that green fluorescent protein (GFP) can be used for co-transfection. Therefore, it is necessary to know the properties of GFP. GFP is found in jellyfish, which consists of 238 amino acids with a size of 27 KDa [1] . The green fluorescent protein (GFP) has a chromophore creating the fluorescent; its autocatalytic activity is generated by protein conformation, yielding an interaction between arginine and tyrosine residues. This chromophore absorbs UV light and fluoresces green signals. GFP has a structure of "11 Betastrands forming a

hollow cylinder through which is treaded a helix bearing the chromophore"[2]. Because GFP is a vital tool in several subfields of biology and biochemistry, it is widely used in protein localization studies, regulation and expression studies, cell sorting and other analytical techniques.

Currently, the penta-ethyl ester prodrug of the chelating agent diethylene triamine pentaacetic acid (DTPA), referred to as C2E5, is being developed for radionuclide decorporation. Carboxylesterases (CESs) are important contributors to the metabolic pathways of xenobiotics, including prodrugs. It is necessary to use genetic engineering methods to produce purified human recombinant protein to examine which isoform of carboxylesterases, if any, is most vital for C2E5 hydrolysis. Therefore, The objective of this study was to utilize competent *E. coli* (DH5alpha) bacteria to replicate a specific human CES plasmid DNA. The second objective was to apply genetic engineering technology to incorporate the GFP gene as a reporter to exam the hCES1 and hCES2 transfection efficiency in HEK293 cells for scaling up the quantity of the hCES1 and hCES2. Those transfected cells can be easily visualized under fluorescent microscopy as so the percent of the transfected cells can be estimated. The third objective was to measure the activities of the produced human recombinant CESs.

Materials and Methods

Chemicals.

Competent Cells (DH5-ALPHA) and S.O.C media were purchased from Invitrogen. Plasmid DNA, pEGFP-N1 was obtained from Dr. Ming Xin at UNC-CH and positive control plasmid DNA pUC19, were purchased from OriGene. Petri dish 60mm (+LB, +50µg/µl kanamycin) and petri dish, 60mm (+LB, +100µg/µl Ampicillin) were purchased from tissue culture facility of UNC and were manufactured by CellTreat™ (Shirley, MA). The complete DMEM (10% FBS, 1% Pen/Strep) growth medium was obtained from TCF as well. TurboFect ™ transfection reagent was purchased from thermo fisher scientific. RT-qPCR materials with cyber green (SYBR) were purchased form Bio-Rad.

Transfection of human carboxylesterases to HEK293 cells.

HEK293 cells were transfected with plasmid DNA which carries hCES1, hCES2. Meanwhile, empty vector was transfected as negative control, and pEGFP plasmid was transfected as a positive control. Plasmid DNA samples were produced from *E. coli* bacterial transformation. The growth of the transformed bacteria colony took place in LB culture media. The transformant was produced in a large quantity and plasmid DNA was isolate by mini prep (Qiagen).

Transfection efficiency measured by GFP reporter.

In a six-well cell culture plate, HEK293 cells were seeded 24 h prior to transfection. (Confluency for adherent cells on the day of transfection is 60-80%.) Then hCES1 (2 µg) plasmid DNA and GFP plasmid DNA (2 µg) were added to pre-warmed DMEM medium (400 µl). TurboFect™ reagent (6 µl) was subsequently added to this mixture. The same procedure applied to hCES2 plasmid DNA. TurboFect™ (6 µl) reagent was added to the previous made

mixture as the mock vector. DNA and transfection reagent mixture was incubated for 15-20 minutes at room temperature. Then the TurboFect^{TM}/DNA mixture was added to cells and incubated for 48 h. Transfection efficiency was observed by fluorescent microscopy.

S9 fractions prepared from transfected cells.

Supernatant (S9) fractions were prepared from HEK293 cells expressing human CES 1 (NM_001266.4) or CES 2 (NM_00369.4). The method was described in chapter 2 and chapter 3. For all cell lines, cytosolic S9 fractions were prepared as described as follows. Briefly, cells were washed with ice-cold PBS and then removed from the culture dish with a cell scraper, suspended in PBS and homogenized in a Potter-Elvehjem glass homogenizer with a Teflon pestle under ice-cold condition. After centrifugation of the cell homogenate at 9000g for 15 min at 4°C, then the S9 fractions were obtained. Protein concentrations were determined by the Bradford method with bovine serum albumin used as the standard.

CESs expression confirmed by RT-PCR

The relative RNA expression levels were determined by the delta Ct method. The amount of target gene expression was calculated using the expression of the GAPDH gene as an internal control. The CESs mRNA levels were given as ratios to the GAPDH mRNA levels. Triplicate real-time RT-PCR assays were carried out for each sample. Regarding sample analysis, it was normalized to the GAPDH comparative CT (ΔΔCT) [$\Delta Ct = Ct_{[Target]}-Ct_{[Gapdh]}$], and samples were analyzed in triplicate [Standard Deviation Error Bar = -FOLD + FOLD x ($2^{Ct\ Dev.}$)].

Functional studies by PNPA and 4-NPV

The enzyme activity of esterase and CESs were measured using established substrates para-nitrophenyl acetate (PNPA) and 4-nitrophenyl valerate (4-NPV), respectively. The hydrolysis of the freshly prepared substrates was carried out in 96 well plates with a total volume

of 100 μl/well. Bis(p-nitrophenyl) phosphate (BNPP), a CESs inhibitor was used to confirm the presence of carboxylesterase. Loperamide, a CES2 specific inhibitor, further was used to confirm the presence of CES2. Inhibitors were added to the human recombinant protein S9 fractions for 30 minutes, following, the reactions were initiated by mixing 1 μl of substrate (PNPA or 4-NPV). The hydrolysis of PNPA and 4-NPV were determined spectrophotometrically by measuring reaction products at 402 nm after 1 min incubation at 37°C. The data generated from the plates were read by a UV spectrophotometer (BioTek, VT). All the data was measured in triplicate.

Results

Transfection of human carboxylesterases.

Newly generated hCES1 plasmid DNA sample is 0.8708 μg/μl, hCES2 plasmid DNA sample is 0.4734 μg/μl, GFP plasmid DNA sample is 1.591 μg/μl, and renilla plasmid DNA sample is 0.8231 μg/μl. Those entire prepared plasmid DNA sample has an A260/A280 ratio greater than 1.8, which indicates that the prepared DNA samples has a decent quality. Among them, hCES1, hCES2 and GFP plasmid DNA will be used for transfection steps in the following studies. The data of plasmid concentrations were summarized in Table A.1.

Transfection efficiency measured by GFP reporter.

GFP reporter gene was transformed in competent *E. coli* bacterial cells, and was isolated and purified from the bacteria genome, then was transfected with hCES1 and hCES2 plasmid DNA to HEK293 cells through cationic polymer transfection agent, TurboFect^{TM} (Fig A.2). The results from transfection study were monitored by fluorescence microscopy. Gross observations of the green fluorescence can be used to estimate the amount of transfected cells. After 24 h of transfection, only 10% of cells were transfected, however, after 48h of transfection, about 50% of the cells were transfected, on the other hand, certain cytotoxicity was observed after 48 h of transfection.

CES expression confirmed by RT-qPCR.

Genetic expression of CES1 and CES2 were both detected in cells that were transfected with CES1. Genetic expression of CES2 was both detected in cells that were transfected with CES2.

Functional studies by PNPA and 4-NPV.

Functional studies using the esterase specific substrate p-nitrophenylacetate (PNPA) and carboxylesterase-specific substrate 4-nitrophenyl valerate (NPV) confirmed the esterase activity of these S9 fractions. On the other hand, bis(p-nitrophenyl) phosphate (BNPP), significantly inhibited CESs-mediated PNPA and 4-NPV hydrolysis. On the other hand, loperamide, a CES2 specific inhibitor, significantly inhibited the activities of CES2 in S9 fractions generated from transfected HEK293 cells, confirming the presence of CES2.

Discussions

CESs are important contributors to the metabolic pathways of xenobiotic. Many prodrugs are designed to be converted into active drugs by CESs. Genetic engineering and recombinant protein technology have been established for decades. With those techniques, pharmaceutical scientists can isolate a single protein or enzyme from the complex biological systems and then use purified protein or enzyme for drug development, for example, protein formulations. In this study, competent *E. coli* (DH5alpha) bacteria were used to replicate a specific human CES gene what was inserted to pCMV6-XL4 mammalian expression vectors (Origene). The data from table1 showed that the production of plasmid DNAs from bacteria were successful. These plasmid DNAs can be used for transfection in mammalian cell lines.

The gene from GFP protein was used as a reporter to examine the hCES1 and hCES2 transfection efficiency in HEK293cells for scaling up the quantity of the hCES1 and hCES2. The percent of the transfected cells was estimated. While optimizing the condition for transfection, several factors could affect the transfection of mammalian gene, for example, transfection time, serum or serum free media, and pDNA/transfect agent ratio. This study showed that the transfection time played as an important role in determining transfection efficiency. According to the observation, the number of cells that express transfected GFP protein increased from 40% in 24h to 70% in 48h. At the same condition, cells that were treated with serum-rich media or serum-free media were compared and the result showed that cells expressed more GFP protein in serum-free media. Following, the samples transfected with 4 μg of pDNA and 6 μg of pDNA were compared, and the results showed that the one transfected with 6μg of pDNA produced better GFP protein expression.

PCR result (Fig A.3) did show that CES were expressed in human HEK293 cells. However, there is slightly higher CES2 that are also expressed in the cells transfected with CES1. This could be a noise from the assay. Other common methods used to examine if the correct pDNA is transfected are DNA gel electrophoresis or DNA sequencing. Gel electrophoresis can be used to identify qualitatively if the gene of interest is present. In contrast, DNA sequencings are used for checking the entire sequences of the nucleic acids.

BNPP is an inhibitor for both esterase and cholinesterase. Loperamide is commonly used as CES2 specific inhibitor. This study has shown that they can inhibit the esterases and CES2 activities in human recombinant protein S9 fractions (Fig A.4 and A.5). However, this inhibition was short-term.

In conclusion, a human recombinant CESs expression system was established. The recombinant CESs S9 fractions were isolated and the activities of CESs were characterized.

Figure A.1

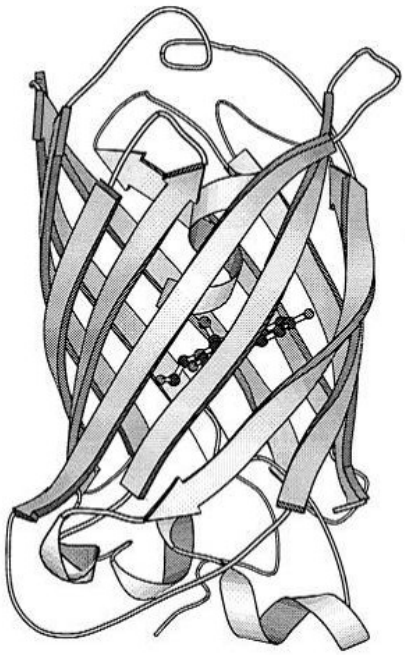

Figure A.1. GFP protein three-dimensional structure

Table A.1. Plasmid DNA (hCES1, hCES2, GFP, and Renilla plasmid DNA) concentrations were measured prior to the transfection in HEK293 cell lines.

Plasmid DNA Concentration Determination						
Plasmid	**Trial 1**	**Trial 2**	**Trial 3**	**Average (ng/µl)**	**STDEV (ng/µl)**	**Percent of variation (%)**
hCES1	870.63	869.06	872.59	870.76	1.768587	0.20
hCES2	472.78	472.98	474.41	473.39	0.888988	0.19
GFP	1600.95	1593.83	1578.87	1591.217	11.26959	0.70

Figure A.2.

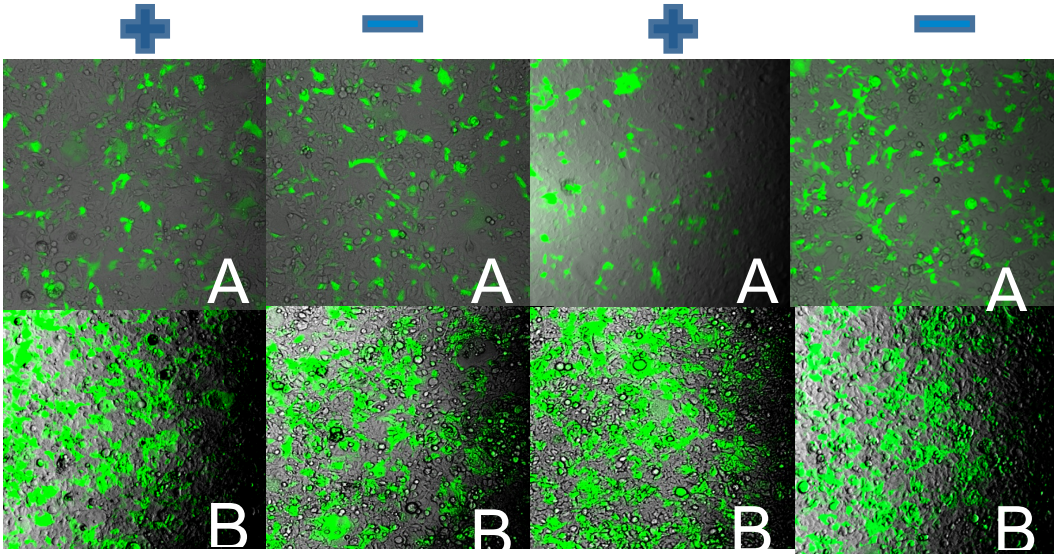

Figure A.2. HEK 293 cells were transfected with pEGFP to establish the optimal transfection condition for human CESs plasmid DNA. Group A shows transfection at 24 h, and group B shows transfection at 48hr. "+"=serum media, "-"=serum free media

Figure A.3

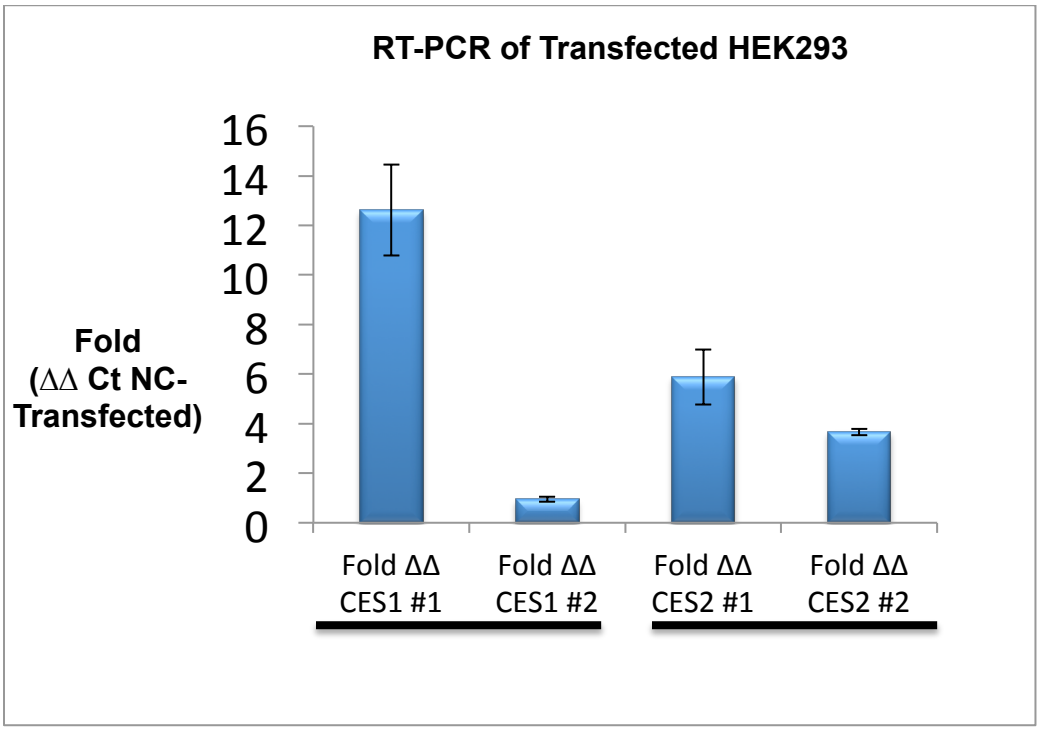

Figure A.3. The evaluation of human CES1 and CES2 genetic expression in transfected HEK293 cells by RT-qPCR.

Figure A.4

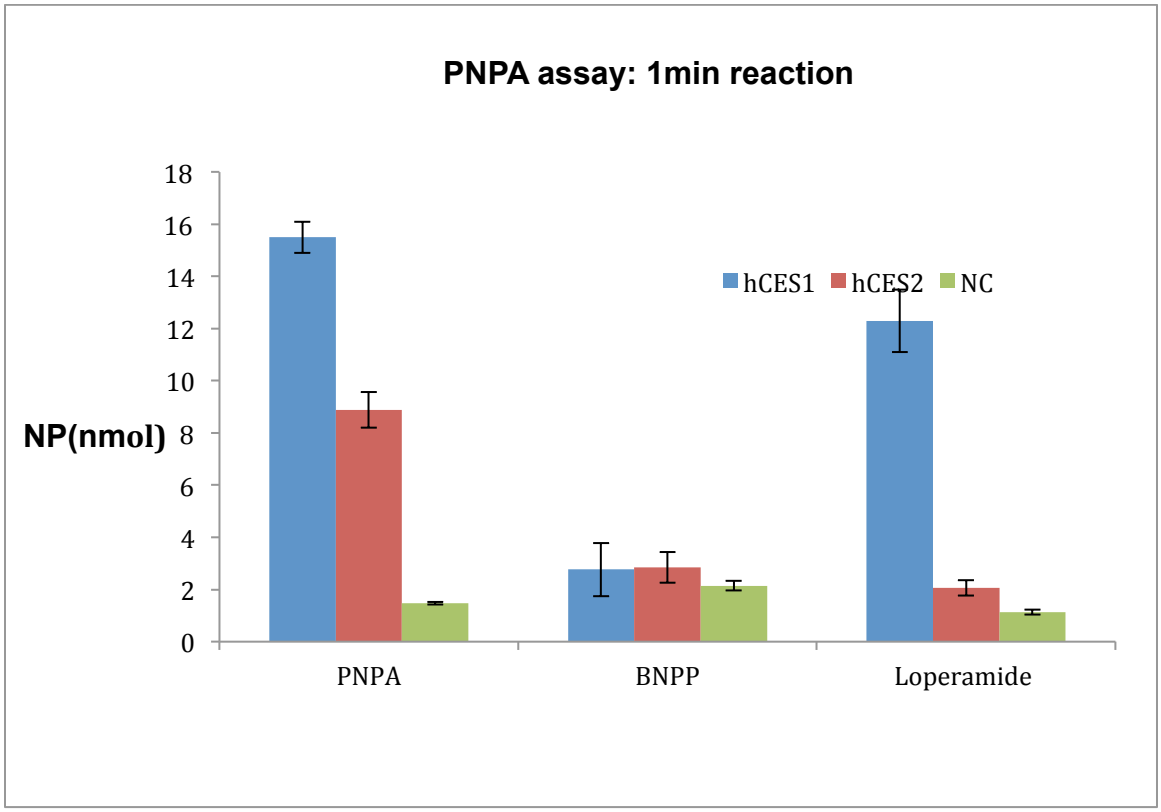

Figure A.4. Recombinant protein S9 fraction-mediated hydrolysis was measured by PNPA assays. Esterases inhibitors (BNPP) and carboxylesterase inhibitor (loperamide) were used to inhibit CESs activities to demonstrate that esterase and CES2 are present in human recombined protein. Inhibitors were added to the human recombinant protein S9 fractions for 30 minutes, following, the reactions were initiated by mixing 1µl of substrate (PNPA). The hydrolysis of PNPA and 4-NPV were determined spectrophotometrically by measuring reaction products at 402 nm after 1 minute incubation at 37°C.

Figure A. 5

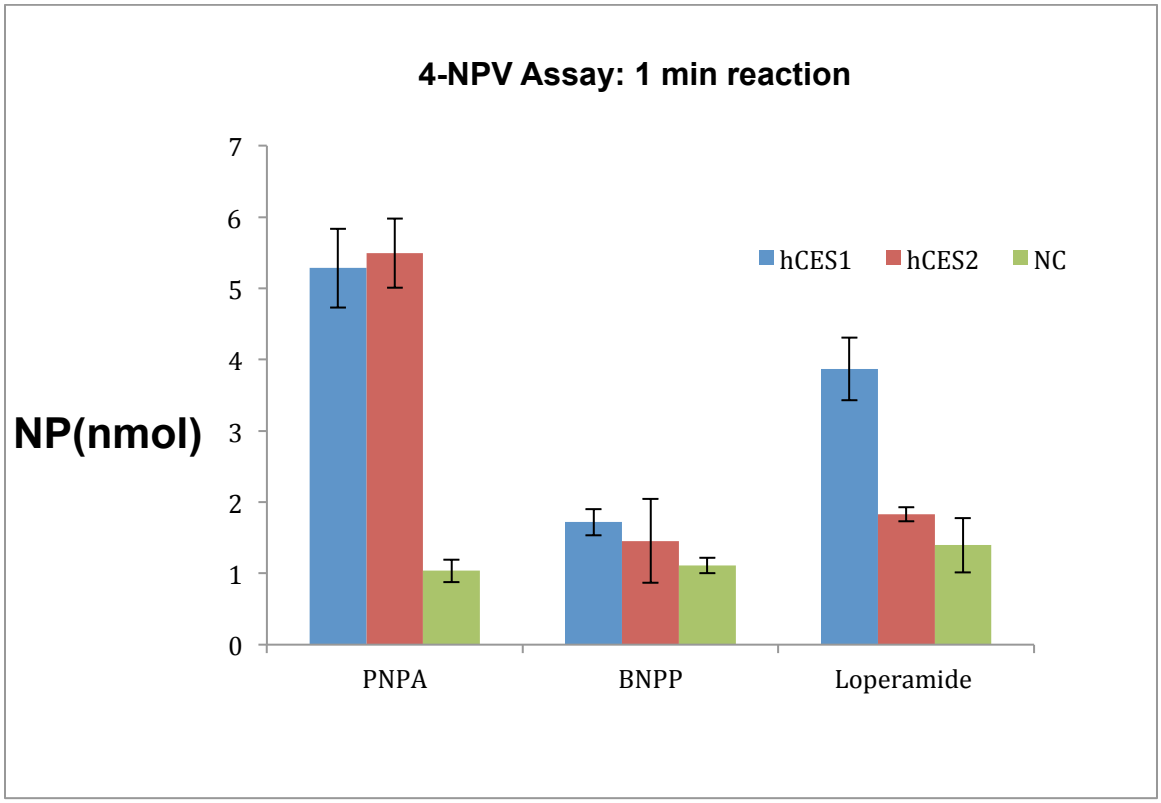

Figure A.5. Recombinant protein S9 fraction-mediated hydrolysis was measured by 4-NPV assays. Esterases inhibitors (BNPP) and carboxyl esterase inhibitor (loperamide) were used to inhibit CESs activities to demonstrate that esterase and CES2 are present in human recombinant protein. Inhibitors were added to the human recombinant protein S9 fractions for 30 minutes, following, the reactions were initiated by mixing 1µl of substrate (4-NPV). The hydrolysis of PNPA and 4-NPV were determined spectrophotometrically by measuring reaction products at 402 nm after 1 min incubation at 37°C.

REFERENCES

1. Sample V, Newman RH, Zhang J 2009. The structure and function of fluorescent proteins. Chem Soc Rev 38:2852-2864.

2. Tsien RY 1998. The green fluorescent protein. Annu Rev Biochem 67:509-544.

APPENDIX B: A COMPARISON OF SKIN METABOLISM IN ADULT AND JUVENILE RATS

Introduction

Previously, we have determined that CESs play an important role in C2E5 hydrolysis. The penta-ethyl ester prodrug of the chelating agent DTPA, referred to as C2E5, effectively decorporates transuranic radionuclides after transdermal delivery, an attractive route of administration for treating contaminated pediatric populations. Previous study showed that C2E5 can be hydrolyzed by adult rat skin S9 fractions. However, whether the skin S9 fractions of juvenile rats have the same metabolic capacity to biotransform prodrug C2E5 remains unknown. Therefore, the objectives of the current work is to compare the esterases activity in the skin of adults rat with that of juvenile rats and assess the C2E5 hydrolysis in juvenile rats skin S9 fractions.

Methods

CESs activities in rats skin measured by ρNPA

The enzyme activity of esterase was measured using established substrates para-nitrophenyl acetate (ρNPA). The hydrolysis of the freshly prepared substrates was carried out in 96 well plates with a total volume of 100 μl/well. Following, the reactions were initiated by mixing 1 μl of substrate (ρNPA) to the adult and juvenile rat skin S9 fractions. The hydrolysis of ρNPA were determined spectrophotometrically by measuring the formation of products at 402 nm at 1-10 mins at 37°C. The results generated from the plates were read by a UV spectrophotometer (BioTek, VT). All the data were measured in triplicate.

Juvenile rat skin S9 fraction-mediated C2E5 hydrolysis measured by HPLC

[^{14}C]-C2E5 (50 μM) was incubated in juvenile rat (postnatal 30-60 days) skin S9 fractions for 0, 5, 15, 30, 60, 120, 360, and 1440 minutes at 37ºC. Following, the reactions were terminated at the indicated time points by the addition of an equal volume of cold ACN followed by centrifugation at 14,000g for 10 min at 4ºC. The disappearance of C2E5 was determined by radio-HPLC.

Results

Comparison of CESs activities by juvenile and adult rat skin S9 fractions

ρNPA assay was used to measure and compare the esterase activities from the juvenile (P30-60 days) and adult rat (> P60) skin S9 fractions. It showed that there are differences in rat skin S9 fractions-mediated ρNPA hydrolysis at the first minute. However, this difference starts to minimize as time of the reaction goes and eventually reached the same level at 10 minutes. Figure B.1 shows the esterase activities in adult rat skin and juvenile rat skin over the time course of 10 minutes. Figure B.2 shows the comparison of the esterase activities in adult rat skin and juvenile rat skin at time of 10 minutes.

C2E5 metabolism by juvenile rat skin S9 fraction

Juvenile rat skin hydrolysis was quantified by HPLC-FSA. [^{14}C]-C2E5 is hydrolyzed significantly over time course from 0-1440 minutes. It was seen that most of the C2E5 was converted into C2E4 at 30 mins. Then C2E4 reaches its maximum at 30 minutes, followed by slow conversion to C2E3 from 30 mins to 1440 mins.

Discussion

The comparison of adult and juvenile animal studies may be useful to predict the potential differences in pediatric drug product development. Juvenile and adult rat skin S9 fractions displayed similar esterase activities. The data also showed that the juvenile rat skin S9 fractions metabolized C2E5. This implies the potential application of the non-aqueous gel formulation delivery of C2E5 to younger populations. In the future, human pediatric skin samples could be collected and used for human age-dependent metabolism investigations. Per the FDA pediatric product development guidance, juvenile animal studies may be extrapolated to human pediatric populations.

Figure B.1

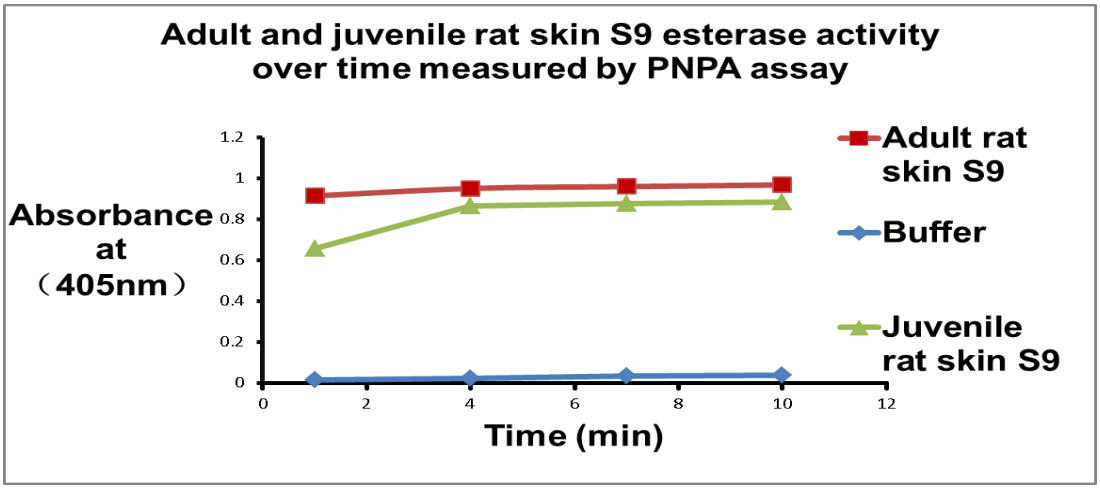

Figure B.1. The activities of esterases in adult and juvenile rat skin S9 fractions were measured by ρNPA assay at reaction time of 1, 4, 7, and 10 mins. The hydrolysis of ρNPA was determined spectrophotometrically by measuring reaction products at 402 nm at each time point at 37°C.

Figure B.2

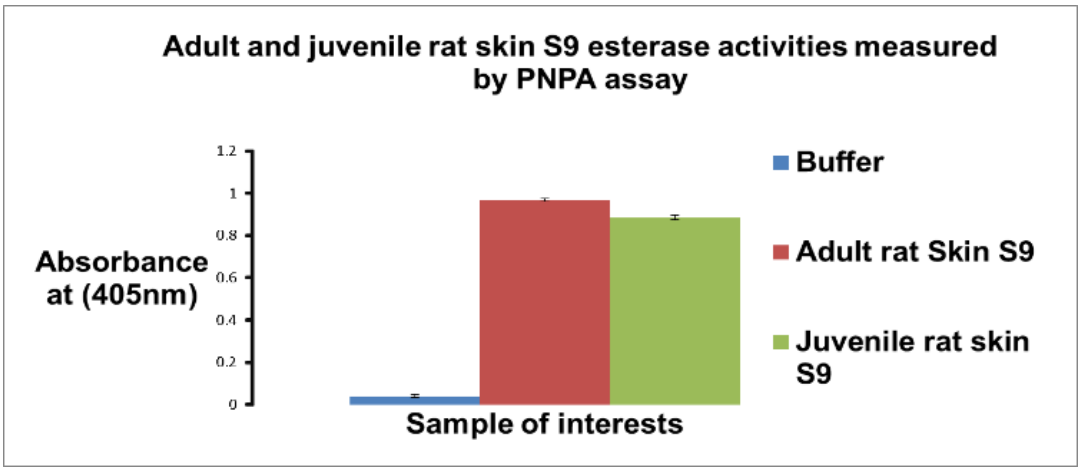

Figure B.2. A comparison of esterases activities in adult and juvenile rat skin S9 fractions were measured by ρNPA assay at reaction time of 10 mins. The hydrolysis of ρNPA was determined spectrophotometrically by measuring reaction products at 402 nm at each time point at 37°C.

Figure B.3

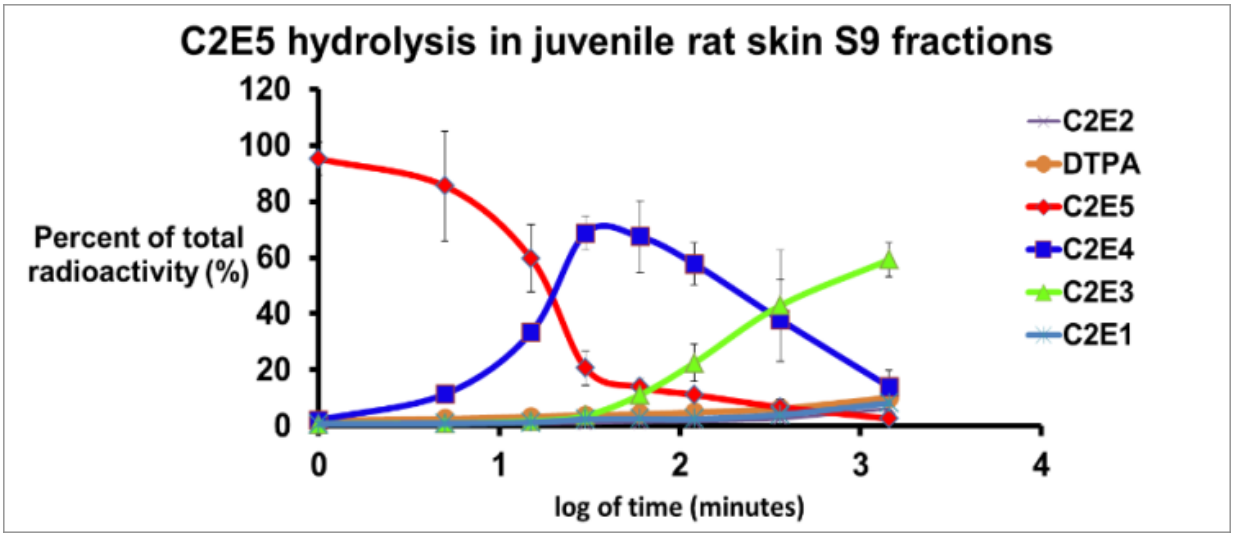

Figure B.3. C2E5 hydrolysis by juvenile Spraguee Dawley rat skin S9 fractions. [^{14}C]-C2E5 (50 µM) was added directly to rat skin S9 fractions (pre-warmed for 5 min at 37ºC). The reactions were terminated at the indicated time points (0, 5, 15, 30, 60, 120, 360, and 1440 mins) by addition of an equal volume of cold ACN followed by centrifugation at 14,000g for 10 min at 4ºC. All the reactions were determined by radio-HPLC. All assays were performed in triplicate and were expressed as the mean ± SD.

APPENDIX C: MOLECULAR SIMULATIONS OF C2E5/C2EX BINDING TO HUMAN CARBOXYLESTERASE

Introduction

Maestro® is a powerful, all-purpose molecular modeling tool; it provides the unified interface for all Schrodinger software. It has powerful selection of analysis ability and has been well known for its user-friendly characters. The chemical simulation software of Maestro is mostly used in pharmaceutical, biotechnology, and materials science research. Maestro is written in Java language and it can be performed in many platforms, such as Microsoft, Windows, Macintosh, Solaris, Linux and Irix. The companion datasets can be obtained from Maestro headquarters.

In molecular modeling, docking is a useful method to predict the best orientation of one ligand to another to form a stable complex. The calculation in the preferential orientation of the molecular complex can be used to predict the strength of the association. The relative orientation of the two interactive molecules also can tell the information about the type of signal produced. It is a tool mostly used for predicting the binding orientation of small molecule drug candidates to their protein targets so as to predict the affinity and activity of the small molecule. Docking can be used to predict biological and pharmaceutical properties of small molecules.

GlideScore is an empirical scoring function that approximates the ligand binding free energy. It has many terms, including force field (electrostatic, van der Waals) contributions and terms rewarding or penalizing interactions known to influence ligand

binding. It has been optimized for docking accuracy, database enrichment, and binding affinity prediction. GlideScore should be used to rank poses of different ligands, for example in virtual screening. While the XP GlideScore shares many terms with the SP and HTVS GlideScore, they do have significant differences and have been optimized separately; as a result, these two GlideScores cannot be compared directly. (Schrodinger, 2011)

Previously, the penta-ethyl ester of DTPA (C2E5) is expected to be metabolized in stepwise fashion to DTPA by the action of carboxylesterases, however, after both oral and transdermal administrations, the primary metabolites detected in plasma were the tri-ethyl (C2E3) and di-ethyl (C2E2) esters of DTPA. In this study, the investigation is to determine why this is happening. It is possible that this happens due to the increasing negative charge with each subsequent removal of an ethyl group. In order to test this theory, DTPA prodrugs C2Ex and CxE2 can be docked with carboxylesterase crystal structures using the Maestro program. Molecular modelling is used to predict the position and orientation of the ligand when it is bound to a protein receptor or enzyme. The preferential bond energy, binding constant and affinity energy will be calculated based on the hydrodynamic of the molecule against with the enzyme. Considering the measureable enzymatic parameters, the interactions between ligands and protein, the information derived from docking would be able to explain metabolism obstacles of C2E5 to DTPA. Therefore, the objective is to develop docking system of human carboxylesterase complexed with C2E5 and its metabolites C2E4, C2E3, C2E2 and C2E1 to interpret the barrier in DTPA prodrug metabolism.

Methods

Molecular Modeling of CES

Simulation of selected CES isoform with C2E5, C2E4, C2E3, C2E2, and C2E1 in the docking program to generate docking scores. Modeling program, maestro version 9.3, was used for simulation. Methods included the preparation of the protein of CES1, grid generation, ligand preparation, and docking steps.

Model Validation and Refinement

Installing the structure of interested protein, CESs from Protein Data Bank (PDB) to Schrodinger Maestro 9.3 program. Human CES crystal (1MX5) was optimized and refined. The calculation methods used was simple gradient method and nonlinear conjugate gradient method.

Ligand Design, Protein and Ligand Preparation

The 2-D sketcher utility of Maestro 9.3 was used to design the structures of ligand molecules in two-dimensions, which were then converted into three-dimensional structures. Before proceeding with the docking studies, water and other hetero-atom groups from the protein structure were removed using protein preparation application of Maestro. Ligands were refined with the help of LigPrep to define their charged state and their stereo-isomers.

Modeling Enzyme-ligand Interactions

C2E5 and its 10 metabolites were docked in the CES binding site cavity of the prepared CES. A grid was made by selecting the amino acids at active site (residues) involved with the binding of the substrates. Flexible ligand docking was carried out using

the standard precision option. Ligands were chosen by Confgen to generate 10000 poses per docking run, but write out at most 10 poses per ligand.

Results

The preferential bond energy, binding constant and affinity energy were calculated based on the hydrodynamics of the enzyme interactions with the molecules. Considering the measureable enzymatic parameters, the interactions between ligands and protein, the information derived from docking would be able to explain the binding of C2E5 to DTPA. C2E1A ligands with top energy preferred structures binding to the active sites of 1MX5 (Fig C.1). In contrast, in order to display the molecular interactions between ligands and enzyme, the hydrogen bond was added to the scheme. As a result, the top five structures of C2E1 docked with 1MX5 crystal with hydrogen bond interactions labeled in-between ligand and metabolic enzyme (Fig C. 2). Table1 summarizes the number of poses produced from program for each of the metabolites. Finally, figure 3 displays the G-score ranking from high to low: C2E3B, C2E4A, C2E2B, C2E2A, DTPA, C2E1A, C2E5, C2E3A, C2E4B, C2E3C, C2E2C, and C2E1B, respectively. C2E4A has a preferred gliding score, which makes it a preferred metabolite formed during the stepwise hydrolysis in humans.

Discussion

It has reported that similar *in silico* models used to predict CYP450 and transferases metabolism have been established. Some other molecular dynamic methods were involved with using simulation to predict the binding of CES substrate to enzyme. This study comprises of three major sections. The first one is to choose the proper CES crystal structure for docking. Currently, more than 13 experimental structures of hCES1 are available in PDB data bank. 1MX5 was chosen in this study as the investigated carboxylesterase crystal structure because it has the closest chemical properties in binding with small molecule as C2E5. The modeling program calculated the optimized geometry, in another words, the minimum energy in the conformation, which is the integrations of equilibrium bond lengths, bond angles, dihedral (torsional) angles, dipole moment and enthalpy of formation.

C2E3B has lowest gliding score, which means the interaction of C2E3B to the enzyme CES costs the lowest bonding energy. However, this is not the case for other metabolites. This makes it a preferred metabolite that is formed during the stepwise hydrolysis in human. This explains why C2E5 was readily hydrolyzed to C2E4 and C2E3 in human S9 fractions from liver, intestine and plasma. However, it did not transform further into other metabolites. In this study, we did not use rat and dog CES as the model enzymes for study the species differences. Therefore, this result is limited to human.

In the future explorations, additional parameters can be added to calculation of scoring system to account for hydrophobic and electrostatic interactions between substrates and contributing residues. We could have calculated MLPins score (Molecular

Lipophilicity Potential Interaction Score.) in the docking analysis. The application of mutual hydrophobic contacts between substrate and enzyme and physicochemical properties of each metabolite, for example, solubility and permeability. By accounting for those properties, we could generate a more precise estimation in the scoring systems. Hence, molecule modeling does have certain limitations to take into considerations; the results cannot be used to replace the real experimental results. However, it can reduce redundant experiments and give more insight into the theoretical implications of ester-based prodrug development.

Figure C.1

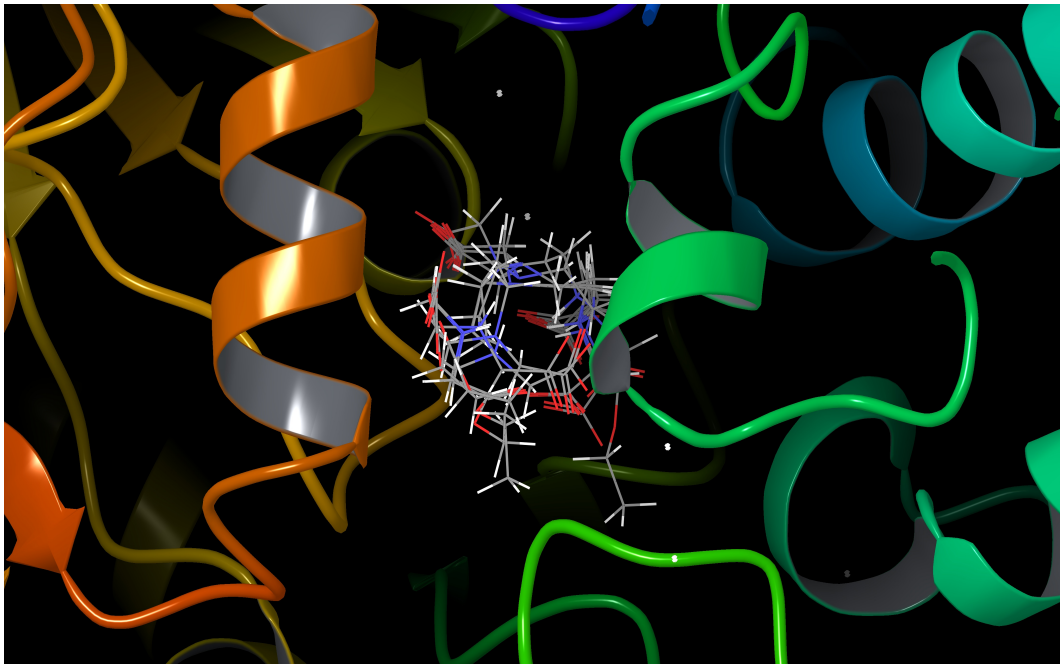

Figure C.1. Top five poses of C2E1A ligands (lowest energy) binding to the active sites of human CES crystal (1MX5).

Figure C.2

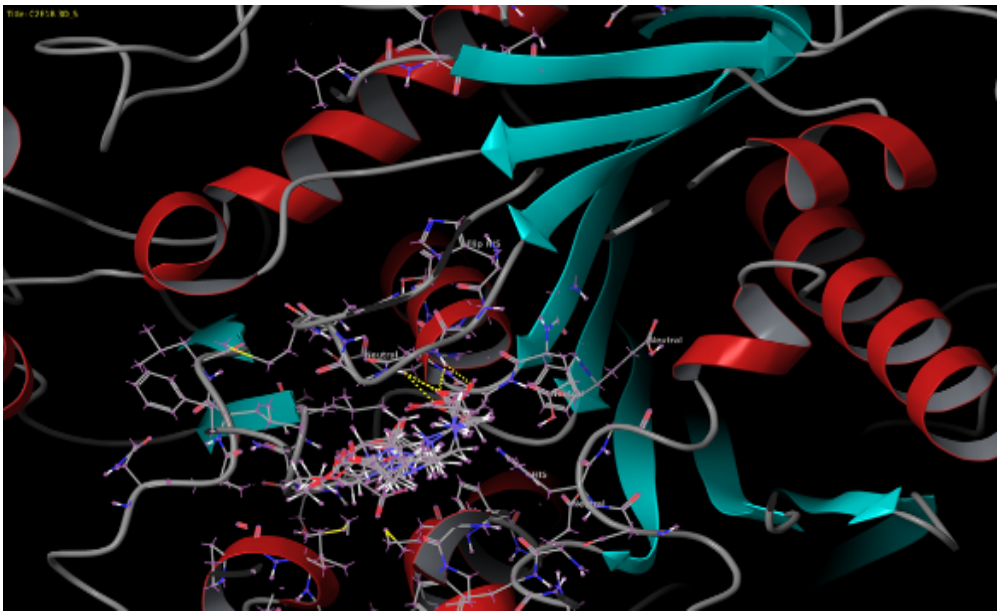

Figure C.2. The interactions of the top five poses of C2E1A with human CES crystal (1MX5). THE yellow lines represent the hydrogen bonds formed between compound and amino acids.

Table C.1. The number of poses of each C2E5 metabolites calculated from Confgen.

Name	Number of poses
C2E1 A3D	313
C2E1 B 3D	390
C2E2 A 3D	1821
C2E2 B 3D	1552
C2E2 C 3D	271
C2E3 A 3D	105
C2E3 B 3D	1236
C2E3 C 3D	392
C2E4 A 3D	233
C2E4 B 3D	105
C2E5	29
DTPA	425

Figure C.3

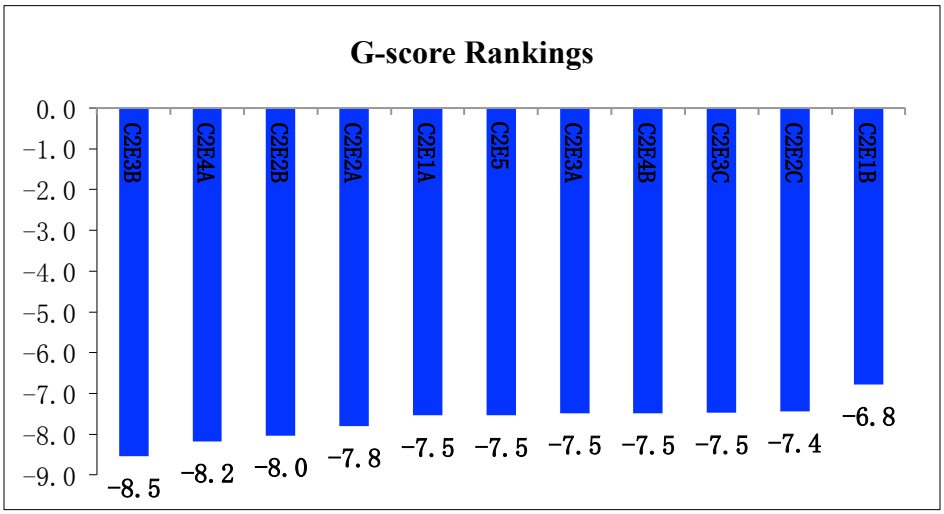

Figure C.3. The ranking of G-score indicates the relative affinities of C2E5 metabolites to the human CES1.